Alma Mater Studiorum - Università di Bologna

DOTTORATO DI RICERCA IN

ONCOLOGIA, EMATOLOGIA E PATOLOGIA

Ciclo 34

Settore Concorsuale: 06/F4 - MALATTIE APPARATO LOCOMOTORE E MEDICINA FISICA E RIABILITATIVA

Settore Scientifico Disciplinare: MED/33 - MALATTIE APPARATO LOCOMOTORE

DISSECTING THE ROLE OF IGF2BP3 IN THE STRESS-ADAPTIVE RESPONSE AND IN INTERCELLULAR COMMUNICATION IN EWING SARCOMA.

Presentata da: Giulia Caldoni

Coordinatore Dottorato

Prof.ssa Manuela Ferracin

Supervisore

Prof.ssa Katia Scotlandi

Co-supervisore

Prof. Davide Maria Donati

Esame finale anno 2022

TABLE OF CONTENT

ABSTRACT

Tumor microenvironment has emerged as key factor influencing tumor progression and metastatization. In this context, small vesicles produced by cancer cells can influence the fate of their surroundings via the horizontal transfer of specific molecular cargos. Ewing Sarcoma, the second most common bone tumor in young patients, presents early metastasis associated to worse prognosis. The RNA binding protein Insulin-like Growth Factor 2 mRNA Binding Protein 3 (IGF2BP3) exerts a pro-oncogenic role associated with metastasis formation and worse prognosis in Ewing Sarcoma. Our aim was to investigate the still unexplored role of IGF2BP3 in the stress-adaptive response to tumor microenvironment and in the interactions between Ewing Sarcoma cells.

Hypoxia is a major feature of Ewing Sarcoma microenvironment and we demonstrated that IGF2BP3 can direct the CXCR4-mediated migratory response to CXCL12 in Ewing Sarcoma cells subjected to oxygen deprivation. We also discovered that the interaction between IGF2BP3 and CXCR4 is regulated through CD164 and which colocalize at plasma membrane level, upon CXCL12 exposure. Interestingly, high IGF2BP3 levels in Ewing Sarcoma metastatic lesions positively correlated with the expression of both CD164 and CXCR4, indicating the IGF2BP3/CD164/CXCR4 oncogenic axis as a critical modulator of Ewing Sarcoma metastatic progression. We demonstrated for the first time that IGF2BP3 is loaded into Ewing Sarcoma derived exosomes, accordingly to its cellular levels. We discovered that IGF2BP3+ exosomes carry high levels of IGF2BP3-client mRNAs involved in cellular migration, CD164 and IGF1R, and, by transferring this cargo, sustain the migratory abilities of receiving cells, induce a sharp up-regulation of CD164, CXCR4 and IGF1R and enhance the activation of AKT/mTOR and ERK down-stream signalling pathways. We demostrated that the pro-tumorigenic role of IGF2BP3 is not only exerted at cellular level, but that intercellular communication is crucial in the context of Ewing Sarcoma microenvironment.

1 INTRODUCTION

1.1 EWING SARCOMA

Sarcomas, which could be classified in bone sarcomas and soft tissue sarcomas, are rare tumors of mesenchymal origin, accounting for approximately 1% of all malignancies (Ferrari et al, 2016). The duplicity of the classification accounts for the heterogeneity of localization, hystotype, pattern of incidence that characterize these subtypes. Primary bone sarcomas actually represent less than 0,2% of all malignancies (Strauss et al, 2018): among them, Osteosarcoma and Ewing Sarcoma show a peak of incidence during childhood and adolescence (Casali et al, 2018) while Chondrosarcoma, on the other hand, is the most frequent bone sarcoma of adulthood (Whelan et al, 2012).

Ewing Sarcoma (EWS, ES) is an highly aggressive small round cell sarcoma occurring predominantly in bone localizations, mainly pelvis, femur, tibia and ribs, but also, yet less frequently, in soft-tissues. (Grunewald et al, 2018; Riggi et al, 2021)

Ewing Sarcoma was firstly described in 1921, by James Ewing, as a diffuse hemangioendothelioma of bone (Ewing, 1921). Historically, Ewing Sarcoma has been grouped, based on morphological and immunophenotypical features and on the presence of chromosomal translocations, with peripheral primitive neuroectodermal tumors (PNET) and Askin tumors in the macro-group designated as "Ewing Sarcoma Family of Tumors" (ESFT) (Kovar, 1998). Since 2013, though, the WHO classification of sarcomas identified as "Ewing Sarcoma" those tumors presenting the pathognomonic FET-ETS gene fusion, while classifying as 'Ewing-like sarcomas' small round cell sarcomas presenting morphologycal resemblance to Ewing Sarcoma but yet characterized by different fusion genes and different clinico-pathological features (Doyle, 2014).

In Ewing Sarcoma, the FET/ETS balanced chromosomal translocation, most commonly in the form of EWSR1/FLI1 fusion gene (85% of cases), represents the major oncogenic feature, since this chimeric product drives pathogenesis and tumor progression (Arvand and Denny, 2001) in the proper context of adjuvant factors, such as an active insulin-like growth factor (IGF) system (Scotlandi et al, 1996; Scotlandi et al, 2002) and the presence of the membrane glycoprotein CD99 (Ambros et al. 1991; Llombart-Bosch et al. 2009). In parallel, large-scale genomic sequencing studies demonstrated that Ewing Sarcoma has one of the lowest mutation rates amongst all cancers, with significant mutation rates only for STAG2 and TP53 genes (Crompton et al, 2014). The stability of Ewing Sarcoma genome represents a limit for the identification of "druggable" alteration while it reinforces the need to study post-transcriptional mechanisms cooperating with EWSR1/FLI1 in the malignancy of this tumor.

1.1.1 CLINICAL FEATURES, DIAGNOSIS AND THERAPY

Malignant bone tumors account for 5% of all cancers occurring among children and adolescents. Following Osteosarcoma, Ewing Sarcoma is the second most frequent primary bone tumorof young patience, with an incidence peak around the age of 15 years (Stiller et al, 2001).

The most frequent localization of Ewing Sarcoma is the bone tissue, with a prevalence of pelvic and axial primary tumors in older patients (20-24 years) than in young children (0-9 years) (Rochefort et al, 2017). Still, 25% of Ewing Sarcoma tumors develope in soft tissues, such as thoracic wall, gluteal muscle, pleural cavities and cervical muscles (Ou et al, 2017), specially in older patients. (Rochefort et al, 2017). Ewing Sarcoma is moderately more frequent in male than in female patients (ratio 3:2) (Kovar, 1998). It is predominantly observed in population of European descent, while lower incidence rates can be detected when considering populations of Asian and American descent. This remark suggests that Ewing Sarcoma risk could be influenced by genetic variants specific to European ancestry. (Jawad et al, 2009; Worch et al, 2011).

Almost 25% of patients present with metastases at diagnosis, which represent the most adverse prognostic factor in Ewing Sarcoma. The most common localization for metastases in Ewing Sarcoma patients is represented by the lungs (50%), followed by bone and bone marrow. (Esiashvili et al, 2008.). Patients with localized primary tumors show a 5-year overall survival (OS) of almost 70-80% while the OS of metastatic patients is dramatically reduced to <30%. Yet the presence of isolated pulmonary metastases correlates with an OS of approximately 50%. (Gaspar et al, 2015.).

The median time of diagnosis for Ewing Sarcoma ranges between 3 and 9 months. Patients usually present with tumor-related symptoms, such as localized pain, often accompanied by a detectable mass. The diagnostic process encompasses different procedures, including imaging modalities and molecular techniques. Employing imaging techniques, such as MRI, CT, FDG, PET-CT, for Ewing Sarcoma diagnosis allows to properly evaluate the extent of the primary disease and to detect the presence of possible metastases. Laboratory techniques, carried out on biopsy-derived samples, are thus needed to confirm the primary diagnosis. Immunohistochemistry is the technique of election to evaluate the expression of different markers, such as CD99, FLI1 and caveolin 1 (CAV1), all commonly expressed in Ewing Sarcoma (Grunewald et al, 2018). CD99 is a membrane associated glycoprotein contributing to tumorigenesis in ES and its diffuse membranous staining is evident by IHC in approximately 95% of cases (Perlman et al, 1994). The detection of FLI1, though, is more specific for this tumor type due to the presence of the characteristic pathognomonic gene fusion, while CAV1 is a useful marker in CD99-negative cells. (Llombart-Bosch et al. 2009).

Molecular techniques, such as FISH, RT-PCR (Reverse Transcription PCR) and more recently NGS (Next Generation Sequencing), are employed to finally confirm the Ewing Sarcoma diagnosis (Machado et al, 2009; Chen et al, 2016.).

1.1.2 MORPHOLOGICAL FEATURES

From an histological point of view, Ewing Sarcoma lesions are highly cellular and present little intercellular space. Necrotic areas are usually present and can be extensively represented (Kim et al, 2016.). Ewing Sarcoma is composed of undifferentiated small round or oval cells, usually defined as"blue" due to their high basophilic staining: this characteristic is correalated to the tipically moderate amount of cytoplasm, which is frequently vacuolated. The nuclei are generally centrally located and present smooth contours, rare nucleoli and dispersed chromatin, summarizing the features of a primitive ucommitted cell (Folpe et al, 2005; Sbaraglia et al, 2020). Ewing Sarcoma cell morphology gives little hints about the cellular origin of this tumor type. The developmental origin of Ewing Sarcoma is still unclear and this lack of knowledge is a barrier in the identification of an appropriate model to study the development of this disease (Tirode et al, 2007; Sheffield et al, 2017). Historically, the expression of EWSR1/FLI1 in the NIH3T3 mouse fibroblast cell line was observed to induce cell transformation and was thought to ricapitulate the Ewing Sarcoma characteristics (May et al, 1993). Recent analyses questioned this hypotesis by demostrating a complexive poor correlation in gene expression patterns between the NIH3T3 model and primary Ewing Sarcoma and, moreover, some targets of the fusion protein (i.e., NKX2.2 or NR0B1) happen to play an oncogenic role in patient-derived ES cell lines but are not induced in NIH3T3 cells (Riggi et al, 2008; Embree et al, 2009; Franzetti et al, 2017).

The main localization of Ewing Sarcoma, arising in bone in the majority of cases, pushes towards the hypotesis that candidate tumor progenitors reside in the bone mesenchyme (Lipinski et al, 1987; Staege et al, 2004.). Konockdown of EWSR1/FLI1 in Ewing Sarcoma cells FLI1 drives towards an acquired mesenchymal stem cell (MSC) gene expression profile (Tirode et al, 2007). Moreover, he hypothesis that Ewing Sarcoma could originate from a neural-crest derived stem cell is sustained by the observation that Ewing Sarcoma cells express cell surface antigens associated with the neuroectodermal lineage, besides presenting high transcription levels of genes involved in neuronal differentiation (Staege et al, 2004). Experimental evidences obtained by the study of the bone marrow of developing sustain the idea that the two previously proposed origins may not be mutually exclusive and that Ewing Sarcoma might arise from a neural crest stem cell harbouring mesenchymal potential or from a neural- crest derived stem cell (Riggi et al 2009; Coste et al, 2017).

1.1.3 MOLECULAR FEATURES

1.1.3.1 EWS/ETS fusion

Genomic instability is now widely recognized as one of the driving forces implicated in tumorigenesis. A total of 358 gene fusions, involving 337 different genes, are known at present and have been described in all the main subtypes of human neoplasia, both in solid and haematological malignancies (Mertens et al, 2015). The first tumor-specific translocation to ever be described was the reciprocal translocation t(9;22)(q34;q11), which origins the Philadelphia chromosome in chronic myelogenous leukemia (CML) (Eden et al, 2021). Specific chimeric genes happen to be associated with specific tumor types, which makes them not only a powerful diagnostic tool but also a potential target for therapy.

All tumors classified in the Ewing Sarcomas Family of Tumors (EFTs) are characterized by the presence of a fusion gene (Watson et al. 2018). Ewing sarcoma cells specifically present the *FET*/*ETS* balanced chromosomal translocation as a major oncogenic feature. The most common (85% of cases) form of this chimeric product is the t(11;22)(q24;q12) traslocation, exiting in the *EWSR1/FLI1* fusion which features the amino terminus of the EWSR1 gene and the carboxy terminus of the FLI1 gene. *EWSR1* gene, located on chromosome 22, encodes for a widely expressed and highly conserved RNA-binding protein belonging to the TET/FET family and involved in transcriptional regulation and RNA processing *FLI1* gene is located instead on chromosome 11 and encodes for a usually nuclear protein, a transcription factor of the ETS (E26 transformation-specific) family which binding to promoter and/or enhancer elements of target genes to promote transcriptional activation or repression. ETS proteins are characterized by the presence of structurally related site-specific DNA-binding-domains (Delattre et al, 1992).

Different subtypes of EWSR1/FLI1 transcripts have been described, depending on the position of the breakpoints occurring in the two genes: most commonly, they are located in exon 7 of EWSR1 and exon 6 of FLI1 but different exons can be incorporated into the fusion genes and are thought to have prognostic value (de Alava et al, 1998; Kovar et al. 2009).

EWSR1 is the most common member of the FET gene family (FUS, EWSR1, TAF15) involved in the Ewing Sarcoma pathognomonic gene fusion, followed by its paralogue FUS (Sankar and Lessnick, 2011). Beyond the most common fusion partner FLI1, different members of the ETS family have been reported to be involved in the chimaeric product, such as ERG, ETV1, ETV4 (Sorensen et al, 1994; Jeon et al, 1995; Urano et al, 1997). The second most common fusion protein observed in ES is reportedly EWSR1/ERG, likely occurring in half of those patients not presenting the canonical fusion (Shing et al, 2003). These alternative fusions actually replace ESWSR1/FLI1 in the tumorigenesis of Ewing Sarcoma, exerting the same oncogenic role (Ginsberg et al, 1999).

The chimaeric protein acts as a dominant oncoprotein (May et al, 1993) and the overexpression of EWS/FLI1 promoted Ewing Sarcoma -like transformation in murine fibroblasts, which acquired anchorage-independent growth capabilities and ES morphology (May et al, 1993). The fusion protein can bind DNA, taking advantage of FLI1 specific DNA-binding domain, and then act, via EWS role as a transcriptional activation domain, as an aberrant transcription factor, thus regulating a series of genes involved in many aspects of tumor progression, such as transcription regulation (NKX2.2, GLI1), tumor growth (BCL11B, PARP1), resistance to chemotherapy (GSTM4) and more (Beauchamp et al, 2009; Joo et al, 2009; Owen, et al, 2008; Wiles et al, 2013, Balestra et al, 2021).
EWS/FLI1 transcriptional targets are characterized by the presence of the specific binding motifs that are usually targeted by ETS family members. Specifically, they are located in the promoter region or its proximities and are characterized by the presence of GGAA elements, which can be present in tandem repeats forming a microsatellite sequence. Higher numbers of consecutive GGAA motifs are proven to increase the enhancer activity (Gangwal et al, 2010). Moreover, the EWSR1 portion of the fusion protein can regulate transcription by enhancing promoter selectivity, via the interaction with hsRPB7, a subunit of RNA polymerase II (Petermann et al, 1998; Todorova et al, 2009). It is also reported the interaction between EWSR1/FLI1 and the RNA helicase A (RHA): the two proteins can form a complex that can bind to promoters of EWSR1/FLI1 target genes, thus regulating their transcription (Erkizan et al, 2009).
Ewing-like Sarcomas (ELSs) are a heterogeneous group of small round cells sarcomas sharing almost identical histologyc and immunohistochemical features with ES but tipically lacking the key FET/ETS gene fusion. Instead, they harbour other recurrent specific gene fusions or rearrangements, such as the CIC-fusion (CIC-DUX4, CIC-FOXO4) or the BCOR-rearrangement (BCOR-CCNB3, BCOR-MAML3), leading to distinct gene expression profiles and different patterns of secondary aberrations (Gambarotti et al, 2016; Antonescu et al. 2017; Carrabotta et al, 2021; Kao et al, 2017).

1.1.3.2 Additional genetic alterations

Pediatric tumors are usually characterized by a nearly stable genome, presenting few recurring somatic mutations. Ewing Sarcoma, as well, exhibits a very stable genome showing few recurrent mutations (Grunewald et al, 2018).
STAG2 and TP53 mutations can be observed at diagnosis in 15-20% and 5-7% of cases respectively. STAG2 (cohesin subunit SA2) encodes for a member of the cohesin complex holding sister chromatids together during the mitotic process a protein which is also involved in chromatine remodelling (van der Lelij et al, 2017),. STAG2 locus is reportedly affected by loss of function mutations, such as single-nucleotide variants (SNV) or indels (Solomon et al, 2011).

It has been demonstrated that STAG2 loss is associated with disease dissemination in Ewing Sarcoma, as a study reported that 88% of patients presenting STAG2 mutations also presented with metastases at diagnosis (Tirode et al, 2014). TP53 is a transcription factor which plays an oncogenic role in a wide variety of human cancers. In Ewing Sarcoma, TP53 mutations are more often observed in samples collected from patients who already experienced treatment, suggesting a putative role for TP53 mutation in treatment resistance (Crompton et al, 2014). STAG2 and TP53 mutations can occurr simultaneously, identifying a group of patients with particularly poor outcome (Tirode et al, 2014). Rare, recurrent mutations in other genes have been reported in genes such as BCOR, ZMYM3, CDKN2A and EZH2 (Tirode et al, 2014).

Chromosomal abnormalities identified in Ewing Sarcoma, besides the balanced translocation generating the pathognomonic gene fusion, include chromosome deletions, usually involving chromosome 9p, and chromosome gains which occurr more frequntly in chromosome 8, 2, 1q and 20. An unbalanced translocation can result in the gain of chromosome 1q with the loss of chromosome 16q, a condition usually associated with poor clinical outcome (Crompton et al, 2014).

Besides genetic and chromosomal alterations, the Ewing Sarcoma molecular landscape is characterized by the aberrant expression and/or activation of specific proteins and pathways.

CD99 (cluster of differentiation 99), encoded by the gene MIC2, is a transmembrane glycoprotein which is expressed by almost 100% of Ewing Sarcomas in the cytoplasmic membrane. CD99 overexpression is thightly connected to Ewing Sarcoma tumorigenesis, as tumor cells deprived of this protein show inhibited growth and reduced metastatic capabilities (Ambros et al. 1991; Llombart-Bosch et al. 2009). The high CD99 expression levels reportedly contribute to Ewing Sarcoma progression by interfering with MAPK and PI3K/AKT signalling pathways. This important oncogenic role identifies this protein as a valid therapeutic target (Scotlandi et al, 2000; Guerzoni et al, 2015.).

The activation of the insulin-like growth factor (IGF) pathway is of major relevance in Ewing Sarcoma tumorigenesis. The IGF system phisiologically exerts a role in normal tissues but is also involved in tumor progression in different cancer types (Kim et al, 2009.). It comprises different IGF-receptors (IGF-1R, IGF2-R, IR), their ligands (IGF1, IGF2,insulin) and a group of proteins, named insulin-like growth factor binding proteins (IGFBPs) regulating the bio-availability of the ligands (Adams et al, 2000). In Ewing Sarcoma, EWSR1/FLI1 reportedly binds IGF-1R promoter, thus sustaining the receptor expression (Herrero-Martin et al, 2009). Moreover, an autocrine loop exists betweer IGF-1R and IGF1: the ligand produced by the tumoral cell binds its receptor which, thanks to its tyrosin-kinasic activity, can convey anti-apoptotic signals and support the tumor prorgession and survival. (Scotlandi et al, 1996; Scotlandi et al, 1998; Scotlandi et al, 2002).

1.1.3.3 Epigenetic alterations

The high stability of Ewing Sarcoma genome evokes epigenetic or mRNA translational reprogramming, rather than the mutational changes and clonal selection observed in epithelial tumors, as mechanisms involved in tumor progression.

Epigenetic modifications consist in heritable changes in gene expression that do not cause permanent alteration of the underlying DNA sequences, regulating the DNA accessibility for transcription factors and polymerases (Portela and Esteller, 2010; Vedeld et al, 2017).

The EWSR1/FLI1 chimaera plays a prevalent role in epigenetic reprogramming by affecting the expression of downstream genes whose enhancers contain GGAA microsatellites elements. Through this mechanism, new Ewing-specific enhancers can be induced while others, normally active in many cell types, are repressed. The binding of the fusion protein to its specific target motifs seems to increase DNA accessibility to other transcriptor factors, which can associate into chromatin remodelling complexes (Guillon et al, 2009). Histone methyltransferation and deacetylation are two epigenetic remodelation processes which are upregulated by the binding of EWSR1/FLI1 to the promoter of EZH2 (enhancer of zeste homolog 2) and Sirtuin 1 (SIRT1), further increasing the role played by the fusion transcript in the epigenetic remodeling (Kailayangiri et al, 2019). The presence of methylated CpG islands in Ewing Sarcoma genomes is only partially studied, but a low percentage of hypermetilated genes was observed and a correlation between poor outcome and increased methylation of CpG islands is reported (Sheffield, et al. 2017).

Ewing Sarcoma tumorigenesis, according to recent sudies, is also driven by post-transcriptional regulation mechanisms like non-coding RNAs (micro-RNAs or long non-coding RNAs) or RNA-binding proteins (RBPs). Micro-RNAs are small non-coding RNAs with regulatory roles, targeting more than 60% of the human genes by mainly binding target sequences located at the 3'UTR of the mRNA. Depending on their targets, micro-RNAs can support or hamper tumor progression by affecting different crucial pathways. Many different micro-RNAs are reportedly up- or down-regulated in Ewing Sarcoma, influencing chromatine remodeling, DNA damage repair, IGF signaling. Expression of non-coding RNAs, including micro-RNAs, can be affected by EWSR1/FLI1 (McKinsey et al, 2011; Dylla et al, 2013). MiR-145 is predicted to bind CD99 3'UTR and its expression, leading to the interruption of cellular growth, increases in EWSR1/FLI1 deprived cells (Ban et al, 2011). Moreover, the fusion protein directly binds to the let-7a promoter, blocking its transcription, and leading to Ewing Sarcoma progression via HMGA2, a DNA-binding protein involved in the activity of many transcription factors (De Vito et al, 2011.).

RBPs are emerging as chritical regulators of posttranscriptional mechanisms in Ewing Sarcoma, affecting tumor aggressiveness and outcome. Y-box-binding protein 1 (YB-1) is an RNA binding protein which can both promote or inhibit translation depending on the mRNA availability. In Ewing Sarcoma, this RBP plays a role in metastatic development by promoting the translation of its target HIF-1α, a protein involved in tumoral adaptation and survival in hypoxic conditions (El-Naggar et al, 2015).). In addition, recent studies evidenced a role for Insulin-like growth factor 2 mRNA binding protein 3 (IGF2BP3) in Ewing Sarcoma tumorigenesis. IGF2BP3 belongs to a family of oncofetal RBPs and its expressed de novo in different cancers, acting as an oncogene (Mancarella and Scotlandi, 2020). In Ewing Sarcoma, this protein sustaining cell growth and migration both *in vitro* e *in vivo*, and correlating with the most adverse outcomes of the patients (Mancarella et al, 2018; Mancarella et al, 2018; Mancarella et al, 2020).

1.1.4 THERAPEUTIC APPROACHES

Patients with newly diagnosed localized standard-risk Ewing Sarcoma are treated with a combination of multi-agent cytotoxic chemotherapy and local control measures, such as surgery and/or radiotherapy. The use of chemotherapy has greatly improved survival rates for patients with localized primary tumors, from 10% to 70-80%, but the intense cytotoxic drug regimens adopted are associated to late secondary effects while no remarkable prognostic progress can be seen in metastatic patients (Stahl et al, 2011).

Intense induction chemotherapy is administered to standard risk patients before local treatment, to reduce the size of the primary tumor. Modern protocols consist of a combination of vinca alkaloids, alkylating agents and anthracyclines, commonly consisting in vincristine, ifosfamide, doxorubicin and etoposide (VIDE) or vincristine, doxorubicin, cyclophosphamide, ifosfamide and etoposide (VDC-IE) (Juergens et al, 2006). Consolidation chemotherapy in manteinance phase for these patients can consist both in cyclophosphamide or ifosfamide, combined with vincristine and dactinomycin (VAC vs VAI) (Yock et al, 2006) Typically, long consolidation chemotherapy is an important element in the treatment of Ewing Sarcoma to destroy slowly proliferating remaining tumor cells (Grunewald et al, 2018). Ewing Sarcoma is considered a radiosensitive tumor since its first description in 1921 (Ewing, 1921), yet historically the benefits for patients whose primary tumors were treated with radiation alone were overcome by the high incidence of local recurrence and increased risk of late effects, such as the onset of second malignant tumors, specially taking into account the early age of the patients (DuBois et al, 2015).Thus, orthopaedic surgery was introduced as local treatment and patients whose primary tumors are excised might survive more often, despite the prognostic influences of site and size (Schuck et al, 2003).

Tumor resection can be followed or not by reconstruction, as this procedure might not be possible or not necessary depending on the localization of the tumor(Germain et al, 2007). Patients presenting with metastatic disease, who represent the main challenge in Ewing Sarcoma treatment, either undergo the standard therapeutic regimens utilized with patients with localized disease or are inserted in randomized clinical trials seeking to improve outcomes for this group of patients (Paulussen et al. 1998).

The aggressiveness of the disease and the serious treatment-related toxicity, despite the use of multidrug treatments combined with local control strategies, contribute to determine the particularly poor prognosis of Ewing Sarcoma patients, especially for those presenting with metastatic disease. Moreover, conventional cytotoxic chemotherapy is ineffective in a quarter of patients with localised tumors, and in three-quarters of patients with metastases (Scotlandi et al, 2009). Thus it is fundamental to identify new therapeutic strategies to improve survival rates for these patients.

Novel insights regarding Ewing Sarcoma biology seem to offer a series of new potential therapeutic targets, beginning with the EWS-FLI1 signature gene fusion. Attempts of targeting the expression of the fusion protein have been carried out via drug-based approaches (i.e. administering cytarabine to inhibit the tumor growth (DuBois et al, 2015), with poor positive outcomes mainly due to its lack of enzymatic activity (Herrero-Martin et al, 2011). The application of a RNA interference approach, though showing promising results in decresasing the invasiveness and proliferation of Ewing Sarcoma cells *in vitro*, is still clinically unfeasible due to the lack of useful siRNA delivery systems (Chansky et al, 2004). Targeting EWS-FLI1 transcript partner proteins, such as the RNA helicase A (RHA), shows a significant therapeutic potential (Erkizan et al, 2009) by reducing proliferation of ES cells. Still, the identification via genetic approaches of EWS-FLI1 downstream pathways for potential drug-mediated inhibition of key downstream partners seems to unlock more therapeutic potential targets (Sonnemann et al. 2007; Theisen et al, 2016; Sonnemann et al, 2007).

The IGF (Insulin-like Growing Factor) system activation is a feature of Ewing Sarcoma (Scotlandi et al, 1996), as tumor cells express IGF-1R and produce IGF-1, causing autocrine stimulation. Ligand binding to the type 1 IGF receptor (IGF-1R) activates an intracellular tyrosin kinase domain and leads to the activation of the MAPK pathways, inducing cell proliferation, invasion, metastases (Scotlandi et al, 1996.; Scotlandi et al, 1998; Scotlandi et al, 2002). The fusion protein EWS-FLI1 plays a role in this autocrine loop by downregulating IGFBP3 (IGF-binding protein 3) and thus ensuring a larger availability of biologically-active IGF-1 to sustain tumor progression (Prieur et al, 2004).

The use of monoclonal antibodies targeting IGF-1R and inhibiting the binding with its ligand has been evaluated, with or without combination with cytotoxic chemotherapy, in different trials (Benini et al, 2001; Manara et al, 2007; Kurzrock et al, 2010; Olmos et al, 2010; Juergens et al, 2011; Pappo et al, 2011; Pappo et al, 2014) with various but promising results.

Another potential therapeutic target connected to EWS-FLI1 role in Ewing Sarcoma is the poly (ADP-ribose) polymerase 1 (PARP1). This enzyme is involved in single-strand DNA repair and acts as a cofactor for EWS-FLI1 DNA binding (Brenner et al, 2012). PARP1 inhibitors, alone or in combination with temozolomide, not only showed therapeutic potential in Ewing Sarcoma models but are also already employed in clinical trials (Gorthi et al, 2018).

When considering the biological features of Ewing Sarcoma in order to identify potential therapeutic targets, the role and importance of CD99 can't be overlooked. The approach using anti-CD99 monoclonal antibodies has already showed effective results, targeting and eliminating tumor cells, both when used with or without combination therapy with other agents (Guerzoni et al, 2015; Scotlandi et al, 2000). Other therapeutic strategies directed to suppress the activity of CD99, such as the application of RNA silencing sia siRNA or miRNA approaches, are being evaluated (Kim et al, 2016).

The activity of RANK and its ligand RANKL it is typical of Ewing Sarcoma and other bone tumors, governing the characteristic combination of tumor growth and osteolysis (Wittrant et al, 2004). RANK expression can be inhibited by zoledronic acid, a potent inhibitor of bone resorption and osteoclastogenesis. Thus, zoledronic acid is being associated to classical chemotherapy agents in different clinical trials (Odri et al, 2012). *In vivo*, zoledronic acid alone happens to be active only against bone Ewing Sarcoma tumor, while an effect on the extraosseous component has been observed after the combination of zoledronic acid with ifosfamide (Odri et al, 2012).

The ganglioside GD2, a neuroectodermic marker occasionally expressed in Ewing Sarcoma (Kailayangiri et al.. 2012), has been identified as a putative target for anti-GD2 antibodies or chimeric antigen receptor T cells (CAR T cells). Though the immune infiltration in ES microenvironment is known to be poor (Chen and Mellman, 2017), CD8+ T cell infiltration correlates with better outcome and the employment of CAR T cells against Ewing Sarcoma *in vitro* showed potent GD2-specific cytolitic response (Thiel et al, 2017), providing positive evidence sustaining their application in clinical trials.

1..2 INSULIN-LIKE GROWTH FACTOR-2 mRNA BINDING PROTEINS

1.2.1 GENERAL CHARACTERISTICS

Insulin-like Growth Factor-2 mRNA Binding Proteins (IGF2BPs) constitute a highly conserved family of proteins, comprising IGF2BP1, IGF2BP2 and IGF2BP3. IGF2BPs can recognize and bind specific target RNAs, thus influencing their cellular fate. Together with other RNA binding proteins (RBPs) and non-coding RNAs, IGF2BPs play a role in the post-transcriptional regulation of gene expression, modulating various cellular functions including morphology, metabolism, proliferation, migration, and differentiation (Bell et al, 2013). Physiologically, the three IGF2BPs are expressed only during embryonic development and only IGF2BP2 is present in adult tissues, where it plays a metabolic role. Instead, *de novo* expression of IGF2BP1 and IGF2BP3 in adult tissues is an oncogenic event, directioning tumor progression and often associated with poorer prognosis.

From a phylogenetic point of view, human IGF2BPs are paralogs and they share conserved RNA binding domains and molecular functions (Degrauwe et al, 2016). In mammals, IGF2BPs share 59% of the amino acid sequence, a percentage rising to 73% between IGF2BP1 and IGF2BP3. IGF2BPs share a molecular weight between 58 and 66 kDa, together with a common structure characterized by six RNA binding domains: two RNA-recognition motif (RRM) domains in the N-terminal portion and four hnRNP-K homology (KH) domains in the C-terminal portion (Jia et al, 2018). *In vitro* studies demonstrated that the RRM domains are involved in the stabilization of the IGF2BP-RNA complexes, whereas RNA-binding is mainly mediated by the KH domains (Farina et al, 2003; Nielsen et al, 2004). IGF2BPs mainly localize at cytoplasmic level but they can also be present in the nucleus, where they bind RNAs immediately after transcription and mediate their export (Nielsen et al, 2003.). In the cytoplasm, especially at the perinuclear level and in correspondence with specialized protrusions, IGF2BPs form ribonucleoprotein granules (RNPs) by interacting with target RNAs and with other RBPs. IGF2BPs differ from other RBP as they mainly interact with “virgin” RNAs, which have not yet bound the translational machinery (Jønson et al, 2007). This is suggested by the fact that the ribosomal subunit 60S, elongation factors such as eIF4E and eIF4G and the RNA-induced silencing complex (RISC) aren’t present in the granules formed by IGF2BPs (Jønson et al, 2007; Weidensdorfer et al, 2009).

The mechanisms through which IGF2BPs interact with RNAs still need to be further elucidated, but the most sustained hypothesis is that IGF2BPs can force the transcript into a specific conformation and promote the formation of a highly stable protein-RNA complex (Chao et al, 2010).

In general, the IGF2BP-transcript interaction can have different consequences including: promoting protection from degradation operated by endonucleases or miRNAs, allowing the transport and correct localization of the transcript, creating a temporary storage of messengers, promoting or preventing translation. It has been shown that IGF2BP1 binds to beta actin mRNA (ACTB), particularly to the cis-acting zipcode in the 3'UTR, promoting its transport and localization to protrusions of primary neurons and fibroblasts (Farina et al, 2003). Translation of the transcript is inhibited during transport and can reprise only when the transcript has reached the site where its function is required. The release signal is given by the Src kinase phosphorylation of a tyrosine residue essential for target-binding and located in a linker region between KH2 and KH3 of IGF2BP1 (Hüttelmaier et al, 2005). The simultaneous phosphorylation of two serine residues of IGF2BP2 catalyzed by mammalian target of rapamycin complex 1 (mTORC1), promotes the binding of IGF2BP2 to the 5'UTR region of the transcript of IGF2 and activates translation via an independent 5'-cap mechanism, resulting in increased synthesis of IGF2 (Dai et al, 2011). The reported mTORC2-directed phosphorylation of a serine residue located between the RRM2 domain and the KH1 domain of IGF2BP3 has been described and it has been proposed that this state of phosphorylation increases the binding of RBP to the 5'UTR of IGF2 with consequent initiation of translation and increased expression of IGF2 (Dai et al, 2013). Despite the sequence homology and the aforementioned common characteristics, there are differences between the three paralogues both in terms of the mechanism of action and in terms of specificity and affinity for the target RNAs, suggesting the absence of functional redundancy, even if the target repertoire of the IGF2BP family has not yet been fully identified (Conway et al, 2016). A partial overlap of the targets can be observed and explained as IGF2BPs can form homodimers and heterodimers on the mRNA to stabilize the complex (Nielsen et al, 2004).

1.2.2 REGULATION OF IGF2BPs EXPRESSION

The regulation of IGF2BP expression is currently one of the least studied aspects, especially at the physiological level. In fact, most of the studies carried out to evaluate this aspect refer to a pathological context, mainly tumoral. For IGF2BP3, in particular, no information concerning its physiological regulation is reported. Overall, the available evidence indicates that each paralogue possesses unique and highly cell-context dependent regulatory mechanisms including transcriptional, post-transcriptional and epigenetic control.

Several data suggest that the expression of IGF2BP1 is subject to transcriptional control by the Wnt pathway. Reportedly, β-catenin promotes IGF2BP1 expression in breast cancer cells and it has been shown that the IGF2BP1 expression correlates with the nuclear translocation of β-catenin.

Furthermore, the observation that RBP is physically associated with the β-catenin transcript and increases its stability has led to hypothesize a positive feedback regulatory mechanism (Noubissi et al, 2006; Gu et al, 2008). Similarly, the existence of a positive feedback regulation mechanism between IGF2BP1 and c-Myc has been described. Several evidence supports that c-Myc positively regulates IGF2BP1 (Noubissi et al, 2010) which, conversely, stabilizes the c-Myc transcript and protects it from endonuclease degradation (Doyle et al, 1998).

A paper by Cleynen et al, conducted on embryonic murine fibroblasts, linked IGF2BP2 transcription with the High-mobility group AT-hook factor 2 (HMGA2) which can bind an AT-rich region located in the first intron of the gene. Next to this region, IGF2BP2 gene presents a consensus sequence for Nf-kB, which, can bind to it and act synergistically with HMGA2 in the transcription activation. In the same paper, the authors showed the existence of a strong correlation between the expression of HMGA2 and IGF2BP2 also in human liposarcomas (Cleynen et al, 2007).

A role for Nf-kB has been proposed also in relation to the increase in the transcriptional activity of the IGF2BP3 promoter in a tumor context. In glioblastoma, a positive feedback mechanism has been observed between IGF2BP3 and the Nf-kB pathway: on the one hand, Nf-kB binds to the promoter of IGF2BP3 and increases its transcription, and on the other hand IGF2BP3 itself can bind the 3 'UTR region of the p65 transcript, a subunit of the heterodimer constituting Nf-kB, thus promoting its translation (Bhargava et al, 2017). Another paper showed that the transcription factor Nanog binds the promoter of IGF2BP3 and increases its expression in the tumor-initiating stem-like cell (TIC) of hepatocellular carcinoma (Chen et al, 2013). Furthermore, 5% of thyroid cancer cases present a balanced chromosomal translocation between the IGF2BP3 7p15.3 locus and the transcriptionally active thyroid adenoma-associated (THADA) 2p21 gene locus, leading to an over-expression of IGF2BP3, promoting of cell proliferation, invasion and transformation (Panebianco et al, 2017). IGF2BP3 expression appears to be regulated also at an epigenetic level. In fact, two CpG islands located in the IGF2BP3 promoter are demethylated in intrahepatic cholangiocarcinoma, in contrast to the heavy methylation present in the liver tissues of healthy controls, indicating the existence of an epigenetic deregulation mechanism associated with the expression of the protein in the tumor. (Gao et al, 2014).

Post-transcriptional control of IGF2BP, based mainly on the activity of specific miRNAs. MiRNAs identified as regulators of the expression of all three IGF2BPs include miRNAs of the lethal-7 (let-7) family, which are usually up-regulated at the end of embryonic development and down-regulated during tumor transformation. suggesting a mechanism for re-expression of oncofetal genes (Boyerinas et al, 2008).

Other miRNAs have been identified as inhibitors of IGF2BP3 expression in different tumor types, for example: miRNA-34a in gastric cancer (Zhou et al, 2017), miRNA-129-1 in glioblastoma multiforme (Kouhkan et al, 2016), miRNA -375-3p in squamous cell carcinoma of the head and neck (Cen et al, 2018), miRNA-654 in glioma (Jin et al, 2018.), miRNA-9-5p in multiple myeloma (Canella et al, 2015), and miRNA-200a in triple-negative breast cancer (Kim et al, 2018).

1.2.3 IGF2BPs' PHYSIOLOGICAL ROLE

IGF2BPs are physiologically expressed at high levels during embryonic development in most tissues. Peak expression is observed in mice at day 12.5 of embryonic development, particularly in the brain, limb sketches, muscles and epithelial tissues of various organs (Hansen et al, 2004). IGF2BP2 is the only member of the family to maintain a physiological role in adults while IGF2BP1 and IGF2BP3 are considered oncofetal proteins because their de novo expression and their up-regulation in adults are observed in tumoral context.

Several approaches were adopted to understand the physiological role of the three IGF2BPs, particularly gain- and loss-of-function analyses. IGF2BP1 knock-out mice exhibit reduced viability, dwarfism (40% smaller than wild-type), impaired intestinal development and decreased cell proliferation (Hansen et al, 2004). These data suggest a key role of IGF2BP1 in promoting growth and differentiation during development, probably through the regulation of IGF2 mRNA translation (Nielsen et al, 1999). Different studies highlighted a prominent role for IGF2BP1 in neural development. It has been observed that IGF2BP1 is expressed in fetal neural stem cells (NSCs) of the dorsal telencephalon and that its expression decreases during the late phase of development, as a result of the expression of the let-7 miRNA (Nishino et al, 2013). Deletion of IGF2BP1 in fetal NSCs has been shown to cause reduced self-renewal capacity of stem cells and early neural and glial differentiation. Furthermore, it has been found that the physiological loss of IGF2BP1 expression contributes to the decline of the functions of NSCs in adults (Nishino et al, 2013). Moreover, IGF2BP1 protein is required for the correct formation of dendrites and axons, due to the accurate spatial-temporal control of ACTB translation (Eom et al 2003.;. Zhang et al, 2001), while it is not required for the maintenance of mature dendrites, in accordance with the lack of IGF2BP1 observed in the adult brain. Overall, these data suggest that IGF2BP1 is able to control from a temporal point of view the changes, in terms of properties and functions, occurring in stem cells between embryonic development and adulthood.

One of the first single nucleotide polymorphism (SNP) found by a genome-wide association (GWA) study for type 2 diabetes mellitus is located within intron 2 of the IGF2BP2 gene (Scott et al, 2007), thus suggesting a main role for this IGF2BP in the control of the energetic metabolism. IGF2BP2 knock-out mice showed greater resistance to obesity, increased energy consumption, better response to cold exposure accompanied by increased levels of uncoupling protein-1 (UPC1) in brown adipose tissue. The molecular mechanism proposed to explain these effects is based on the observation, carried out *in vitro*, that IGF2BP2 inhibits the translation of the UPC1 protein. It has therefore been hypothesized that the absence of IGF2BP2 increases the levels of UPC1 and probably of other mitochondrial proteins, contributing to the effects observed in mice (Dai et al, 2015).

Information regarding the physiological function of IGF2BP3 is rather limited due to the lack of an *in vivo* knock-out model for the protein. The indications available to date are based on studies carried out on its orthologous, Vg-1-RBP, in Xenopus laevis, which is necessary for the migration of cells involved in the formation of the neural tube and neural crest (Yaniv et al, 2003) and for the localization of the Vg1 transcript at the vegetative pole during oogenesis (Git et al, 2009.). Its absence causes numerous aberrations especially at the level of the nervous system, but in the morphogenesis of the intestine, absence of organogenesis of the pancreas and failure to meiotic maturation (Yaniv et al, 2003; Spagnoli and Brivanlou, 2006.; Git et al, 2009). Confirming its main role during embryonic development. IGF2BP3 is expressed at high levels in fetal hematopoietic progenitor cells, including megakaryocytes, compared to its adult counterpart and its expression is responsible for the maintenance of fetal characteristics and its knock-down confers molecular and phenotypic characteristics of adult cells to neonatal megakaryocytes (Elagib et al, 2017). Interestingly, IGF2BP3 is expressed at high levels in the placental villi during the early stages of gestation. Examining its function in placental development it was found that RBP is responsible for the correct migration of trophoblast cells towards the basal decidua, a process that requires fine regulation from a spatial and temporal point of view (Li et al, 2014).

1.2.4 IGF2BPs' ROLE IN CANCER

IGF2BP1 and IGF2BP3 are considered oncofetal proteins as they are synthetized de novo and upregulated in a large number of tumors, including carcinomas, leukemias and sarcomas. The two RBPs play key roles in both tumoral onset and progression, such as staminality, inhibition of apoptosis, proliferation, migration, adhesion, chemo-resistance, by controlling the fate of specific target transcripts. At clinical level, both IGF2BP1 and IGF2BP3 currently represent promising prognostic, diagnostic and, in some cases, therapeutic biomarkers in different types of cancer.

Both these IGF2BPs can regulate transport and intracellular localization of mRNAs encoding cytoskeletal or secreted proteins, and stabilize oncogenic transcripts.
The role of each IGF2BP is highly dependent on the cellular context and on the availability of transcripts, which adds further complexity to their mechanisms of action.
The overexpression of IGF2BP1 has been observed in several tumor types, such as non-small cell lung cancer, cervical and ovarian cancer, rhabdomyosarcoma and neuroblastoma (Kato et al, 2007; Kobel et al, 2007; Bell et al, 2015; Faye et al,2015; Su et al, 2016; Zhang et al, 2018). In most cases high levels of IGF2BP1 are associated with poor survival, globally suggesting its oncogenic role in cancer (Huang et al, 2018). Several works have shown that IGF2BP1 supports the expression of classical oncogenes, such as c-Myc and KRAS, in breast cancer (Ioannidis et al, 2005), ovarian cancer (Kobel et al, 2007), and colorectal cancer (Mongroo et al, 2011). In the context of rhabdomyosarcoma, it has been observed that the role of IGF2BP1 is fulfilled by activating the translation of the apoptosis inhibitory factor-1 (cIAP-1) messenger, which promotes cancer cell survival through regulation of the Nf-kB-mediated pathway and extrinsic programmed cell death. (Stöhr et al, 2012). IGF2BP1 has been shown to regulate lamellipodia and invadopodia formation, promoting tumor cell motility. In this regard, a study conducted in osteosarcoma cell lines led to the identification of two targets of IGF2BP1, MAPK4 and PTEN. The RBP acts oppositely on the two transcripts, inhibiting the translation of MAPK4 and promoting that of PTEN (Chen et al, 2018).
Information on the oncogenic role of IGF2BP2 is limited, however a growing number of studies support the existence of an association between this protein and cancer (Cao et al, 2018.). The over-expression of IGF2BP2 has been found associated with poor prognosis in various cancers including hepatocellular carcinoma (Kessler et al, 2015), glioblastoma (Janiszewska et al, 2012.), basal-like breast cancer (Barghash et al, 2015), esophageal adenocarcinoma (Barghash, et al, 2016). Furthermore, IGF2BP2 has been proposed as a biomarker for the discrimination between endometrioid and serous endometrial adenocarcinoma (Zhang et al, 2011) and between myxoid and well differentiated liposarcoma (Cleynen et al, 2007).

1.2.5 IGF2BP3 ROLE IN CANCER

The oncogenic importance of IGF2BP3 has been observed in a large repertoire of cancers: pancreatic cancer, ovarian cancer, leukemia, glioblastoma, oral squamous cell carcinoma, mantle cell lymphoma, colorectal cancer, endometrial clear cell carcinoma, astrocytoma, hepatocellular carcinoma, glioma , multiple myeloma, lung cancer, skin squamous cell carcinoma, breast cancer, intrahepatic cholangiocarcinoma, thyroid cancer, Osteosarcoma, gastric cancer, Ewing's sarcoma, leiomyosarcoma, renal cell carcinoma (Lederer et al, 2014).

IGF2BP3 oncogenic action consists in regulating the stability, degradation and localization of RNAs and influencing the biogenesis of miRNAs. IGF2BP3 can protect its targets involved in tumor progression from miRNAs action by recruiting them into RISC / Needle-free granules (Jønson et al, 2014). IGF2BP3 can also compete with miRNAs for binding to specific sites on the 3' UTR region of specific targets (Ennajdaoui et al, 2016). Furthermore, IGF2BP3 can promote target degradation by favouring its association to Ago2 (Ennajdaoui et al, 2016) and can interfere with miRNA biogenesis by competing with Drosha in the nucleus, blocking the maturation of specific miRNAs and indirectly stabilizing target mRNAs (Wang et al, 2019). IGF2BP3 participates in the degradation of messengers and proteins through protein interaction with ribonuclease and de-ubiquitinase, respectively (Mizutani et al, 2016, Zhao et al, 2017). A further function performed by the RBP in the stabilization of transcripts consists in the formation of stress granules (SG), within which the transcripts are protected under stress conditions or during transport to specific cellular compartments (Taniuchi et al, 2014.; Kobayashi et al, 2012).

IGF2BP3 supports the growth and proliferation of cancer cells and inhibits apoptosis by positively or negatively regulating the expression of multiple targets. A well-known mechanism by which this is accomplished is the protection from degradation of target transcripts of let-7. These transcripts include known oncogenes and cell cycle factors involved in cell proliferation: HMGA2, RAS, MYC, LIN28, IGF1R, cyclins D1 and D2. Most of these have indeed been found associated with IGF2BP3 in various tumors (Jønson et al, 2014; Rivera Vargas et al, 2014; Palanichamy et al, 2016; Mancarella et al*,* 2018). LIN28, in turn, promotes the expression of proteins such as IGF2, histone H2a, cyclin A and B, CDK4, generating a positive feedback loop that supports growth (Polesskaya et al, 2007; Xu and Huang, 2009). A direct interaction has also been demonstrated between IGF2BP3 and IGF2 in leukemia (Liao et al, 2005), thyroid cancer (Panebianco et al, 2017) and glioma (Suvasini et al, 2011). Negative regulation also affects proliferation. In cervical and lung cancer cells it has been observed that the repression of EIF4E-BP2, negative regulator of the proto-oncogene eukaryotic translation initiation factor 4E (eIF4E), carried out by IGF2BP3 through ribonuclease recruitment, promotes the proliferation of tumor cells (Mizutani et al*,* 2016).

In breast cancer, IGF2BP3 represses miR145-5p by promoting the expression of its target WNT5, which in turn activates TAZ. Through the regulation of its targets, IGF2BP3 can contribute in modulating drug response. For example, IGF2BP3 overexpression, associated with LIN28, is associated with increased resistance to cisplatin treatment in ovarian cancer, probably because the two RBPs cause the down-regulation of the protein hCTR1, a transporter responsible of cisplatin entrance into the cell (Hsu et al, 2015).

By stabilizing IGF2 and / or IGF1R, IGF2BP3 influences susceptibility to anti-IGF1R therapies in Ewing's sarcoma and thyroid cancer, and to MAPK and PI3K inhibitors in glioblastoma (Suvasini et al, 2011; Panebianco et al, 2017; Mancarella et al, 2018). In triple-negative breast cancer IGF2BP3 mediates the stabilization of ABCG2 transcript, an ABC transporter (ATP-binding cassette), conferring resistance to treatment with doxorubicin and mitoxantrone (Samanta et al, 2013). Similarly, in hepatocellular carcinoma, IGF2BP3 contributes to resistance to treatment with sorafenib by modulating the expression of ABCG2 (Li et al, 2015) IGF2BP3 is significantly involved also in cell migration and metastases formation during tumor progression. The complexity of the role played by IGF2BP3 in regulating cell motility is particularly evident in the study by Ennajdaoui et al, in which a combination of genome-wide approaches to highlight in ductal pancreatic adenocarcinoma cells the association of IGF2BP3 with 164 transcripts involved in cell migration, remodeling of the cytoskeleton, cell adhesion, formation of invadopodia (Ennajdaoui et al, 2016).

In triple negative breast cancer cells, the expression of IGF2BP3 causes an increase in migration and invasion capacity, promoting the stability of MMP9 and CD164, possible mediators of cell motility (Samanta et al, 2012). MMP9 (Matrix metallopeptidase 9) is a type IV collagenase that promotes the degradation of the basement membrane, while CD164 is a membrane glycoprotein involved in cell adhesion and migration. The mechanism by which IGF2BP3 controls the fate of these two transcripts has not yet been elucidated. CD164 plays a major role in the proliferation, adhesion, and differentiation of hematopoietic stem cells. High levels of CD164 have been correlated to worse prognosis and increased migratory capabilities in different tumor types, such as bladder cancer, non-small cell lung cancer, colon cancer and triple-negative breast cancer (Samanta et al, 2012; Tang et al, 2012; Zhang et al, 2018; Wei et al, 2020). Interestingly, a functional co-expression of CD164 with the chemokine receptor CXCR4 has been observed both in ovarian cancer and in bladder cancer, sustaining that CD164 may participate in cellular response to microenvironmental stimuli such as CXCL12 (Huang et al, 2013; Zhang et al, 2018).

IGF1R and HMGA2 are both IGF2BP3 reported targets and play a role not only in cell proliferation but also in regulating migration, thus consolidating the association between IGF2BP3 expression and increased motility in melanoma (Sheen et al, 2015) and Ewing's sarcoma (Mancarella et al, 2018).

Another mechanism proposed to explain the increase in motility mediated by IGF2BP3 is the transport and localization of transcripts in specific cellular regions. In pancreatic cancer cells, IGF2BP3 and its targets ARF6 and ARGEF4 co-localize within stress granules accumulating at the level of membrane protrusions, where transcripts are translated and promote formation of protrusions and motility (Taniuchi et al, 2014).

The same research group demonstrated that the transport of stress granules containing IGF2BP3 and its transcripts along the microtubules up to the cell protrusion occurs thanks to the kinesin KIF20A (Taniuchi et al, 2014). In this example, the formation of the stress granules represents a strategy through which IGF2BP3 safely transports its transcripts to the correct localization.

Although poorly documented, the relationship between IGF2BP3 and the tumor microenvironment suggests another way in which this oncoprotein can contribute to tumor aggressiveness. The ability of cancer cells to survive and adapt to microenvironmental stressors depends on the activation of specific pathways. In this sense, IGF2BP3 represents a resistance factor since it participates in the formation of cytoplasmic stress granules, within which the mRNAs are selectively recruited and stored. In response to exposure to thermal shock and sodium arsenite, capable of inducing oxidative stress, IGF2BP3 co-localizes with typical markers of stress granules, TIA-1, G3BP1 and 2 (Taniuchi et al, 2014).

The diagnostic and prognostic significance of the expression of IGF2BP3 has been recognized in a large number of tumors, however the use of this molecule as a biomarker in clinical practice has not been implemented. Recent studies demonstrated the presence of IGF2BP3 in the serum of prostate cancer and renal carcinoma patients, thus suggesting its application as a circulating biomarker (Szarvas et al, 2014; Tschirdewahn et al, 2019).

1.2.6 IGF2BP3 ROLE IN EWING SARCOMA

Given Ewing Sarcoma high genomic stability, a prominent role in tumor progression has been proposed for post-transcriptional gene regulation mechanisms, governed by non-coding RNAs and RNA binding proteins. Studies on Ewing Sarcoma confirmed the oncogenic role of IGF2BP3, which is over-expressed both at mRNA and protein levels in Ewing Sarcoma patients. Interestingly, high expression of IGF2BP3 negatively affects both event-free survival and overall survival, indicating a role as a prognostic marker of this RBP in Ewing Sarcoma (Mancarella et al, 2018). Functional *in vitro* studies show that IGF2BP3 expression is related to anchorage independent cellular growth and with migratory abilities.

Data obtained *in vitro* were also confirmed *in vivo*, particularly in mice injected with IGF2BP3 silenced Ewing Sarcoma cell lines, which presented increased survival rates and reduced metastatic progression when compared to mice injected with IGF2BP3-expressing controls (Mancarella et al, 2018). In Ewing Sarcoma, IGF2BP3 has been described stabilizing the IGF1R transcript, thus acting on the IGF system. The silencing of IGF2BP3 reduces the cellular response to IGF, measured in terms of cell migration and growth (Mancarella et al, 2018). Moreover, a new target of IGF2BP3, ABCF1, has been described in Ewing Sarcoma.

The silencing of ABCF1 leads to increased levels of known IGF2BP3 target transcripts, associated with greater cells' aggressiveness. It has been proposed that ABCF1 associating with IGF2BP3 can limit the interaction of the RBP with other target transcripts, thus repressing its oncogenic functions. According to this hypothesis, patients with low IGF2BP3 expression and high ABCF1 expression have a better prognosis than those with high IGF2BP3 expression and low ABCF1 expression, suggesting this combined evaluation as a valid stratification method to evaluate patients' prognosis (Mancarella et al, 2018). Treatment with JQ1, a bromodomain and extra-terminal domain inhibitor (BETi) with good anti-tumor activity both in hematological and solid tumors, including Ewing Sarcoma (Jacques et al, 2016), was tested in order to exploit IGF2BP3 as a therapeutic target. JQ1 administration resulted in lower IGF2BP3 levels, associated with a reduction in the levels of some of its targets and with a dampening of anchorage-independent growth (Mancarella et al, 2018). IGF2BP3 clearly plays an important oncogenic role in Ewing Sarcoma. The high interest surrounding this RBP in the context of a tumor in which post-transcriptional regulation plays a primary role reinforces the importance of a comprehensive identification of the mechanisms of action of the protein.

1.3 TUMOR MICROENVIRONMENT

In recent years, extensive studies have focused on dissecting the interactions between the genetically altered tumor cells and the context of cellular and non-cellular components surrounding them, defined as tumor microenvironment (TME). The interactions between cancer cells and the tumor stroma, composed by the extracellular matrix (ECM) and non-neoplastic cells are responsible for the loss of tissue homeostasis and promote tumor development and progression within the TME. Indeed, these interactions are known for controlling most aspects of tumorigenesis such as tumor growth and metastasis formation, cell migration, apoptosis, neovascularization and drug resistance (Balkwill et al, 2012; Hinshaw and Shevdel, 2019). The TME features are constantly evolving, mainly depending on the dynamic release of cytokines, chemokines, matrix remodelling enzymes and other factors both from tumoral and non-tumoral cellular compoents (Balkwill et al, 2012; Hinshaw and Shevdel, 2019). The ECM, the main non-cellular component of the stroma, consists of a network of complex macromolecules assembled in 3D structures with structural and biochemical properties that can determine the interactions between tumoral and non-tumoral cells in this landscape (Henke et al, 2020).

The co-evolution towards a more activated state of both the malignant cellular subset and its surroundings is facilitated by the dynamic paracrine signalling established between the two

components and provides the essential acquisition of oncogenic features, thus corroborating the knowledge that the non-malignant components of the TME can exert a tumor-promoting function just as much as the cancer cells do (Quail et al 2013).

1.3.1 THE ROLE OF THE ECM IN THE TUMOR MICROENVIRONMENT

The Extracellular Matrix (ECM) represents the non-cellular component of the tumor microenvironment and it is mainly composed of type I collagen fybers, together with glycosaminoglycans, proteoglycans and glycoproteins (Theocharis et al 2016). In normal tissues, ECM is involved in the regulation of tissue homeostasis and development by providing a structural foundation for tissue integrity and function and regulating the availability of small molecules such as cytokines and growth factors (Karamanos et al 2021). In a tumoral context, the deregulation of its biochemical and biomechanical properties (i.e. fiber network morphology, fiber collagen content and thickness) contributes to the neoplastic progression (Najafi et al 2019). Despite the genetic alterations arising in the transformed cells are responsible for initiating and driving the malignant progression, the dynamic evolution of the ECM can actively contribute to the tumor histopathology (Henke et al, 2020).

Cell adhesion to the ECM is directly involved in the process of tumor proliferation, as growth-factor dependent intracellular signalling actively promotes the cell cycle switch and many transformed cells can synthesize their own ECM proteins (Bonnans et al, 2014). The induction of a G1/S cell cycle transition is an example of the mechanisms acquired to fulfill the escape of proliferative suppression, while, in parallel, transformed cells are able to overcome the blocking of cell cycle at the quiescent phase (G_0), a characteristic of normal cells (Hume et al, 2020). ECM ligation can temper the activity of many factors involved in tumor suppressor pathways, such as BRCA1 or TGF-β (Pickup et al, 2014). Transformed cells can also resist cell death induction via the inactivation of pro-apoptotic pathways and adhesion to the ECM can exert a bivalent function in the regulation of apoptosis evasion: while in some tumors this binding can induce expression of Bcl-2, an anti-apoptotic protein involved in cell survival, while inactivating pro-apoptotic molecules such as Bax (Sharma et al 2019; Adeshakin et al, 2021). Moreover, the biophysical properties of the ECM result in impaired drug access to tumors as the fiber densities can limit the diffusion of molecules through the interstitium (Kim et al, 2012).

Like normal tissues, tumors require an appropriate supply of oxygen and nutrients that can be provided only by an efficient vasculature. Cancer cells can deregulate the balance existing between pro-and anti-angiogenetic factors, while the tumoral ECM can enable the migration and accomodation

of newly recruited endothelial cells (Bauer et al 2009). The ECM is actively involved in the uptake of essential nutrients while promoting the activation of the PI3K pathway, thus influencing glycolisis and the cellular uptake of glucose (Hoxhaj et al 2020).

Many tumor types are characterized by a chronically inflamed TME, which can often present with fibrotic tissue and higly represented immunitary effectors. The increase in collagen and fibronectin deposition accompaining ECM fibrosis can play a role in the active recriutment of immunitary cells, promoting for instance macrophage proliferation and polarization towards a pro-tumorigenic M2 phenotype (Kim et al, 2012, Henke et al, 2020). ECM can also both support and compromise adaptive tumor immune response by, on one side, facilitating T-cells migration toward the neoplastic lesion while, on the other side, directly inhibiting T-cells proliferation and activation (Gonzalez et al, 2018). The ECM actually is the barrier that transformed cells need to overcome in order to migrate, a goal achieved via the secretion of metalloproteinases (MMP) and the formation of integrin-mediated adhesions and focal adesions, particularly on specific actin-rich protrusions, called invadopodia (Bonnans et al 2014).

1.3.2 THE NEOPLASTIC STROMA: NON-TUMORAL CELLS

The stroma surrounding the transformed neoplastic cells is highly dinamic and complex, in terms of secreted factors, extracellular components and non-tumoral cells, all contributing to tumor progression. Commonly, the non-neoplastic fraction of cells populating the tumor microenvironment consists in resident fibroblasts, contributing to the release of chemokines and growth factors, endothelial cells and perycites which can both exert a role in the aberrant angiogenesys, tumor associated immune effectors.

All these populations can impact the progression and the metastatic spread of the tumor, both directly and indirectly. For instance, the release of chemokines and the subsequent binding with their specific receptors plays a predominant role in the crosstalk regulating tumor development. Chemokines are small proteins divided into four families and characterized by a common structural composition, depending on the number of and relative spacing of the N-terminal cysteine residues (Miller et al, 2017). The CXCL12/CXCR4 axis provides a good example for the role of chemokines in the tumor-TME crosstalk.

The chemokine ligand C-X-C motif chemokine ligand 12 (CXCL12,also named SDF-1a) is known to be secreted from different non-neoplastic cells populating the TME, such as cancer associated fibroblasts and mesenchymal stem cells, and some conditions like hypoxia can ehnance its release (Manoukian et al 2021). The chemokine receptor 4 (CXCR4) is an highly conserved G protein

coupled receptor, the natural receptor of CXCL12, and its expression in cancer cells is considered a prognostic factor in different neoplasias (Chatterjee et al, 2014). The ligand/receptor interaction triggers multiple signal transduction pathways in CXCR4-positive cells, thus playing a critical role in metastasis, tumor growth and development of chemoresistance. Interestingly, a functional coexpression of CXCR4 and the sialomucin CD164 has been observed directing the response to CXCL12 in different tumor types, such as ovarian cancer and in bladder cancer (Huang et al, 2013; Zhang et al, 2018). The CXCL12/CXCR4 axis can modulate the metastatic process in several ways. For instance, CXCL12 can induce the production of matrix metalloproteases (i.e. MMP9) in cancer cells and hamper their activity in the TME, thus leading to degradation of the ECM and favouring invasion (Parmo-Cabañas et al, 2006). Moreover, this chemokine can induce the production of the vascular endothelial growth factor (VEGF) which contributes to the aberrant angiogenesis in the TME via stimulation of endothelial cells to produce MMPs and to associate in the formation of new blood vessels (Miyoshi et al, 2014). Metastatic cells of many tumor types express high levels of CXCR4 (Chatterjee et al, 2014, Krook et al, 2014). These cells can take advantage of the newly formed vessels to migrate along CXCL12 gradients, towards common metastatic sytes (i.e. bone marrow) where CXCL12 is highly expressed (López-Gil et al, 2021).

The rapid and mostly uncontrolled proliferation of transformed cells is responsible for interfering with the blood supply, thus limiting the oxygen availability. This phenomenon, termed hypoxia, is observed in the majority of solid malignancies and mostly affects those regions where the vasculature is outgrown by the tumoral mass, leading to an impaired and inadequate oxygen supply towards demanding cells, showing an increased oxygen consumption (Li et al, 2021). Hypoxic regions show a dramatic drop of oxygen levels, from the normal 2-9% to less than 2% (Jing et al, 2019). In the TME, hypoxia triggers the juxtapposition of endothelial cells to produce new but yet irregular vasculature, resulting in discontinuous and distanced capillaries whose efficiency in diffusing oxygen is compromised. At the same time, the transformed cells need to adapt to this strong microenvironmental stress via the induction of changes in gene and protein expression, often leading to the establishment of a more aggressive phenotype with an impact on the patient prognosis (Jing et al, 2019; Li et al, 2021). Hipoxya inducible factor 1α (HIF-1α) is a key player in the tumor cell adaptation to hypoxia. HIF-1α is a subunit of a heterodimeric transcription factor and its stability is directly regulated by the oxygen stastus.

Under normoxic conditions, the protein is localized in the cell cytoplasm while under hipoxyc conditions the stabilized form of HIF-1α can then translocate to the nucleus to interact with its partner HIF-1β and form the HIF-α/β heterodimeic transcriptional factor (Dengler et al, 2014).

The activation of HIF-1α can induce VEGF expression, thus stimulating the formation of new tumoral vasculature, and can at the same time mediate the induction of several metabolic changes involved in the metabolic reprogramming of the tumoral cells, via increasing of glucose uptake and decreased oxygen consumption (LaGory et al, 2016). Moreover, high levels of HIf-1α are connected, in different tumor types, to increasing expression of CXCR4 thus playing a role in the metastatic capabilities of transformed cells (Bailey et al, 2016; Jun et al 2017).

1.3.2.1 The neoplastic stroma: populations of non-immune cells.

In the context of the TME, cancer cells influence and induce the reprogramming of the surrounding normal cells. Cancer associated fibroblasts (CAFs) are stably recruited and activated fibroblasts, which secrete pro-tumorigenic chemokines and growth factors and contribute to enhancing cancer cells migratory capabilities (Liu et al 2019). Mesenchymal stem cells induced to differentiate into myofibroblasts, expressing alpha smooth muscle actin (αSMA) or into adipocytes expressing fatty acid binding protein-4 (FABP4) are also grouped under this definition (Zhang et al 2016). CAFs represent the major fraction of non-neoplastic cells pupulating the TME in carcinomas, where they are known to functionally orchestrate the epithelial-to-mesenchymal transition (EMT) via secretion of TGF-β (Ribatti et al, 2020). A study by Peña et al. showed that the expression of stanniocalcin-1 in CAFs could direct colorectal cancer metastasis, while Pelon et al. described their influence in breast cancer metastasis (Pena et al, 2013; Pelon et al, 2020). Conncected to the role of CAFs in facilitating metastatization, Gaggioli et al demonstrated their role in triggering proteolytic and structural modifications of the ECM, in order to achieve cell invasion into ECM (Gaggioli et al. 2007). The current knowledge concerning the CAFs at metastatic sites is very limited, but Kalluri et al. demonstrated the importantce of local fibroblasts in producing VEGF-A and Tenascin-C, thus preparing a suitable metastatic microenvironment (O'Connell et al. 2011). CAFs can sustain tumor growth and progression by promoting cellular proliferation in breast cancer and lung cancer (Cirri and Chiarugi, 2011). Particularly, they can sustain inflamation by the release of inflamatory cytokines in an NF-kB dependent manner, which in turn induce neoangiogenesis and macrophage recruitment, enhancing tumor growth in skin carcinoma (Erez et al, 2010). CAFs also play a role in the enhanced angiogenesis, via the secretion of factors that stimulate pericytes and endothelial cells as reported in colon cancer (Dvorak et al. 1986; Unterleuthner et al, 2020).

CAFs reportedly mediate drug-resistance of cancer cells, This function can be exerted via the regulation of vascular permeability and immune cell infiltration, as reported by Nakasone et al (Nakasone et al, 2012), or by the stimulation of cancer cells with specific factors, as reported by Wang

et al in the context of lung cancer resistance to epidermal growth factor receptor (EGFR) tyrosine kinase (Wang et al, 2009).

In the context of tumor microenvironment, endothelial cells are one of the main sources of CAFs when undergoing endothelial-to-mesenchymal transition (EndMT) in the presence of tumor growth factor (TGF)-beta (Cipriani et al, 2015). Considering the relevance of angiogenesis in tumor progression, endothelial cells play a fundamental role in this process by participating to the formation of new blood vessels (Deregibus et al, 2007). These newly formed vessels are important not only to provide nutrients and oxygen to the tumor, but also in metastasis. The role of endothelial cells in tumor microenvironment is thus involved in intravasation, which allows invasive cancer cells to translocate into the blood vessel lumen (Maishi et al, 2017; Sobierajska et al, 2020).

1.3.2.2 The neoplastic stroma: populations of immune cells.

Tumor microenvironment is also composed of a population of innate immune cells (i.e. neutrophils, or macrophages) and of adaptive immune cells (T and B lymphocytes) (de Visser et al, 2006).

Tumor-associated macrophages (TAMs) are the most frequent population of immune cells that can be found within the tumor and are considered to present an M2 phenotype (Lin and Karin 2007; Sica et al, 2008). Macrophages can be divided into two subtypes, M1 and M2 (Sica et al, 2008).

M1 macrophages are capable of killing pathogens and priming anti-tumor immune responses, express high levels of proinflammatory cytokines (TNF-a, IL-1, IL-6, IL-12 or IL-23). On the contrary, M2 or ‘‘alternatively’’ activated macrophages, present increased expression of the anti-inflammatory cytokine IL-10 (Mantovani et al, 2008). Elevated TAM content has been correlated with poorer prognosis in patients of different cancer types, such as ovarian and breast cancer, follicular B lymphoma, classic Hodgkin's Lymphoma and soft tissue sarcoma (Sica et al, 2008; Squadrito and De Palma, 2011; Ruffell et al, 2012; Chittezhath et al, 2014) and they have been associated with the promotion of different aspects of tumor progression (Shapouri-Moghaddam et al, 2018). TAMs preferentially localize in hypoxic areas of the tumor, and the consequent induction of HIF-1α induces the expression of a series of factors promoting angiogenesis, such as VEGF (Squadrito & De Palma, 2011; Jetten et al, 2014). In the context of metastatization, TAMs can reportedly produce enzymes and proteases which regulate the degradation of the ECM, i.e. MMPs and osteonectin, thus promoting cellular motility (Chittezhath et al, 2014; Belgiovine et al, 2016).

Besides TAMs, also T-cells are highly represented in the immune infiltrate of different cancer types. Interestingly, T-cells reportedly exert both tumor-suppressive or -promoting effects, depending on their effector functions (Langowski et al, 2007; DeNardo et al, 2009). Increased populations of activated cytotoxic T-cells (CTLs) or Th1 cells in colon cancer, melanoma, multiple myeloma and

pancreatic cancer has been correlated to better survival (Galon et al, 2006; Swann and Smyth, 2007). At the same time, many of the T cell subpopulations have been correlated to promoting tumor progression and metastatization (Hanada et al, 2006, Aspord et al, 2007; DeNardo et al, 2009). As an example, the presence of tumor infiltrating lymphocytes with high Th2/Th1 and CD4+/CD8+ ratios is connected to poorer prognosis in breast cancer cell (Kohrt et al, 2005), while the increased presence of Th2 CD4+ can induce tumor progression in terms of increased growth and metastatization (DeNardo et al, 2009). T-cell's functions, as well as those of TAMs, are mediated by ther release of specific cytokines and chemokines in the context of tumor microenvironment (Lin and Karin, 2007; Swann and Smyth, 2007). Interestingly, considering that these released molecules can target their downstream effectors independently on their cell of origin, the cytokine and chemokine expression profile of the tumor microenvironment may be more relevant than its specific immune cell content (Lin and Karin, 2007).

In the context of immune escape, T-cells are fundamental players in the regulation exerted by immune checkpoint molecules, such as PD1 and PDL1. PD1 is a cell surface receptor physiologically expressed on active T-cells during inflammation and immune response. The interaction of PD1 with its cognate ligand PDL1, usually expressed by tumor cells, suppresses T-cells' function causing them to change phenotype, thus, developing a T-cell tolerance, inhibiting their proliferation, lowering their cytokine production, and hindering the recognition of tumor cells (Robainas et al, 2017). From a physiological standpoint, the PD1/PDL1 interaction acts as a natural brake to temper overactivation of T-cells response while, on the other hand, overactivation of the PD1/PDL1 pathway in cancer can protect tumors from cytotoxic T-cells by disrupting the cancer immunity cycle (Chen et al, Nature 2017; Sharpe and Pauken, 2017). Highlighting new roles for the PD1/PDL1 pathway, cancer cell-intrinsic PD1 has been described in three tumor types (Yao et al, 2018): while in melanoma and liver cancer the interaction between PD1 and its ligand PDL1 had an oncogenic role, favouring tumor progression (Kleffel et al, 2015; Li et al, 2017), in non-small cell lung cancer the effect of the interaction was opposite, thus tempering tumor progression (Du et al, 2018).

other immune cells are reported to affect tumorigenesis, with an exception to be made for NK cells. These cells, in fact, are absent from most tumor infiltrates and from pre-cancerous lesions (Chang et al, 2005).

Although NK mediate potent anti-tumor cytotoxicity *in vitro*, their paucity in tumor infiltrates may be an example of the evasion mechanism preventing NK-cell recruitment to the tumor site (Bussard et al 2016). A role in cancer progression has been proposed also for neutrophils, which can alternatively promote or block tumor progression depending on the presence of TGFβ (Fridlender et

al, 2009, Wu et al, 2020), and for B-cells, which were recently shown to participate in immune escape by suppressing the activation of cancer-associated T-cells (Sarvaria et al, 2017).

1.4 EXTRACELLULAR VESICLES

Cellular behavior, both in physiological and in pathological conditions, is highly influenced not only by the genetic characteristics of the cell itself but also by signals derived from intercellular communication. Soluble factors, such as growth factors (i.e., VEGF, FGF, EGF) represent the most "classical" and simple mean to convey cell-to-cell signals, and they can exert their action both on close and distant cells (paracrine/autocrine fashion). These factors released can bind to their cognate receptors, expressed on the surfaces of target cells, thus inducing their activation and stimulating the activation of several intracellular signaling pathways.

In the last few years, a novel and very interesting method has been proposed and thoroughly studied in the context of intracellular communication. Different types of Extracellular Vesicles (EVs) are generated and released from all cell types and are responsible of the horizontal transfer of specific molecular cargos. The first description of EVs by most accounts dates back to 1967, particularly to a study by Peter Wolf focused on understanding blood coagulation. Ultracentrifuge of blood samples allowed the isolation of the so-called "platelet dust", a fraction consisting of lipid-rich particles conserving coagulant properties (Wolf et al, 1967).

Raposo et al. reported in 1996 that exosomes secreted via an MVB fusion pathway by antigen presenting cells are sufficient to present antigen *in vitro* and *in vivo*, thus proving that exosomes are signaling entities (Raposo et al, 1996). Trying to extend this knowledge to EVs in general and proposing them as signaling entities, Ratajczak et al. and Valadi et al. showed that EVs contain RNAs that could be transferred between cells in a functional way (Ratajczak, et al, 2006, Valadi et al, 2007).

1.4.1 MICROVESCICLES OR EXOSOMES?

EVs can be divided into two major subgroups, microvesicles (MVs) and exosomes, which can be distiguisheb based on their size and on their cellular origin.

Cargo characterization of both classes of EVs showed that they can contain various types of proteins, such as RNA binding proteins, transcriptions factors, cytosolic signaling proteins, cell surface receptors and extracellular matrix proteins. Moreover, EVs also contain different kinds of nucleic acids, as small RNAs, RNA transcripts and fragments of genomic DNA (Jeppesen et al, 2019).

MVs (sometimes also referred to as large EVs, shedding vesicles or oncosomes) are generated from cells by the outward budding of the plasma membrane (Maas et al. 2017; Latifkar et al. 2019). Particularly, discrete microdomains along the plasma membrane, enriched in lipid rafts, cholesterol, and phosphatidylserine, begin to protrude outward, until the neck of the vesicle is sufficiently small and undergoes a fission event, which results in the release of the vesicle from the cell surface (Maas et al, 2017; van Niel et al, 2018). Almost all types of cells can release MVs, but it has been demonstrated that highly aggressive forms of cancer cells tend to produce more MVs when compared to lower grade cancer cells, or normal cells (Menk et al, 2020). A mutant form of the EGF receptor, the EGF receptor variant type III (EGFRvIII) and ADP-ribosylation factor 6 (ARF6) were identified as critical regulators of MV biogenesis. Via the activation of different signaling pathways, both these molecules induce an actin-cytoskeletal rearrangement which in the end is necessary for the budding of MVs from cellular surface (Heijnen et al, 1999; Muralidharan-Chari V et al, 2009; Palmisano et al, 2012). The lipid composition of the plasma membrane also plays an important role in MVs generation and release (van Niel et al, 2018). Particularly, when the typical asymmetric distribution of different lipids between the inner and the outer layers of the plasma membrane is loss (i.e., under conditions where cytosolic calcium levels are increased), the curvature of the plasma membrane is favored and MVs budding is promoted (Latifkar et al, 2019; Clancy et al, 2021)

The second major class of EVs is represented by exosomes (also called small EVs or microparticles), They differ from MVs as they are smaller and actively released through endosomes. Specifically, during the endolysosomal degradation pathway, multivesicular bodies (MVBs) are subject to a maturation process inducing invagination and budding events of their limiting membranes, resulting in the formation of smaller intraluminal vesicles (ILVs) in the lumen of the MVB. Most MVBs are trafficked to the lysosome and degraded, some of them are redirected to the cell surface. At this point, the MVBs fused with the plasma membrane and release exosomes in the extracellular space (Hessvik et al, 2018; Latifkar et al, 2019). Harding et al. visually observed MVB fusion with the plasma membrane for the first time, in 1983. Exosomes were characterized for the first time in this study, together with the one by Pan and Johnstone.

Both researches showed that the transferrin receptor was associated with vesicles of about 50–120 nm in diameter, which were actively secreted by reticulocytes during their maturation into red blood cells (Harding et al, 1983; Pan and Johnstone, 1983).

MVB fromation is well characterized and is mainly directed by the family of endosomal sorting complex required for transport (ESCRT) proteins which can direct both membrane deformation and fusion (Hanson and Cashikar, 2012). These proteins are divided into four classes, ESCRT-0, -I, -II, and -III, differing as each plays a distinct role in promoting MVB generation. Specifically, the binding

between ESCRT-III and ESCRT-II directly promotes membrane invagination and fission, inducing ILVs formation. ESCRT-0, -I, and -II are responsible of the recruitment of ubiquitinated proteins to the surfaces of MVBs (Vietri et al, 2018). Tipically, these organelles are transported and fused to the lysosomes, where their content is degraded. That's not the case of those MVBs which are responsible for exosomal release, as they are instead redirected to the cellular surface and fuse with the plasma membrane, thus releasing their ILVs (exosomes) into the extracellular compartment (Vietri et al, 2018). ESCRT proteins are not the only ones influencing exosomal biogenesis. Tetraspanins are membrane spanning proteins, with a reported role in the regulation of endocytic trafficking. Several members of this family, such as CD9, CD63 and CD81, are known to localize to MVBs and are reportedly enriched in exosomes (Johnstone et al, 1991; Kowal et al, 2016). Tetraspanins play a relevant role in exosome biogenesis, as shown by CD63 knock-out which reduced exosomal production in HEK293 cells, compared to wild-type control cells (Hurwitz et al, 2016). Moreover, a role for CD63 has been reported in protein sorting into exosomes. Under conditions where CD63 expression was knocked-down by shRNA in HEK293 cells ectopically expressing the Epstein-Barr virus latent membrane protein 1 (LMP1), the amount of LMP1 detected in exosomes appeared to be reduced, thus suggesting it was dependent on CD63 (Verweij et al, 2011; Hurwitz et al, 2017). CD9 and CD82 have halso been shown to help recruit proteins into exosomes and, particularly, exosomes derived from HEK293 cells ectopically expressing these tetraspanins were highly enriched in β-catenin (Chairoungdua et al, 2010). Another protein family, the RAB family of small GTP binding proteins, has been shown to play a role in MVBs formation and trafficking, as well as in exosomal release. The RAB family comprises around 70 members, key regulators of intracellular vesicle trafficking processes (Langemeyer et al, 2018; Blanc et al, 2018). Particularly, RAB5 promotes the formation of early endosomes by activating phosphatidylinositol 3-kinase VPS34 to generate phosphatidylinositol-3-phosphate (PI3P), which is then enriched on endosomal membranes and induces the recruitment of early endosome antigen 1 (EEA1) to promote the fusion of endocytic vesicles in the early stages of MVBs generation.

As the maturation of endocytic vesicles into late endosomes and MVBs, RAB5 is replaced by RAB7, which suggests a role also for this protein in exosomal production (Langemeyer et al, 2018). A role for RAB11, RAB27, and RAB35 was suggested in mediating the docking of MVBs to the cell surface. Knock-down experiments were carried out for all of these three proteins: fluorescence microscopy analysis showed that cells lacking RAB11, RAB27, or RAB35 accumulated MVBs along the inner surface of their plasma membrane and their ability to release exosomes was reduced. These findings suggest that RAB11, RAB27, and RAB35 are all important for MVBs docking to the plasma membrane. Protein cargo of exosomes produced by cells depleted of RAB27 was not impoverished,

suggesting that RAB27 is not involved in protein sorting into exosomes (Savina et al, 2005; Ostrowski et al, 2010).

Notably, exosomal biogenesis can also be ESCRT-independent as demonstrated by Stuffers et al in HEp-2 epithelial cells depleted of several components of critical relevance for the ESCRT complex formation (Stuffers S et al, 2009). The sphingomyelin ceramide can promote ESCRT-independent biogenesis of exosomes thanks to its ability to spontaneously assemble in microdomains on the membranes of the MVBs. Due to its small polar head group, high local concentrations of ceramide can induce the inward budding of the MVB's membrane (Trajkovic et al. 2008).

1.4.2 THE ROLE OF EXOSOMES IN TUMOR PROGRESSION

The relevance of exosomal-mediated intercellular communication has been of major interest since the discovery of this type of extracellular vesicles. Microvesicles were initially thought to be the mechanism through which cells could dispose of waste materials, partially due to their intimate connnection with lysosomes in terms of biogenesis (Buratta et al 2020). Studies through the years not only helped characterizing in a more proper way the cargo of exosomes, highliting that it's loading is an active process which is not so in line with the idea of a "trash bin" vesicles, but also identified a plethora of mechanisms which are finely tuned by the messages carried by exsosomes between cells. The physiological role of exosomes has been mostly studied in the context of reproduction and embryonic development, as they have been identified in semen, amniotic fluid, breast milk (Yáñez-Mó et al, 2015). Seminal plasma-derived exosomes are involved in sperm maturation (Sullivan et al, 2005) and can influence immune surveillance at the level of genitalia (Vojtech et al, 2014; Madison et al, 2015). A role in immune defense, and particularly in the induction of anti-viral response, has been proposed also for placental exosomes (Delorme-Axford et al 2013; Menon et al, 2019). Exosomes present in breast milk are linked to promoting postnatal health both by transfer of miRNAs with immune-related functions and can enhance the number of peripheral blood-derived T-regulatory cells, thus modulating immune tolerance (Admyre et al, 2007).

As intercellular communication is crucial for cells when adapting to intra- and extra-cellular alterations, it comes with no surprise that the role of exosomes has been mostly investigated in the context of pathology and prevalently of cancer.

The contribution of exosomes in the context of tumor progression can be retrieved at two levels, both as mediators of the interaction between tumoral cells and as involved in the interplay with the surrounding tumor microenvironment (TME).

1.4.2.1 Tumor-derived exosomes and tumor growth

Tumor-derived exosomes can induce the initiation of cell transformation, as reported in breast cancer and prostate cancer, where exosomes transfer specific miRNA signature that induces neoplasia (Das et al 2018), or glioma, where exosomes from cells with high aggressiveness induce transformation of fibroblasts or normal mammary epithelial cells (Figueroa et al, 2017; Ghaemmaghami et al 2020). The transfer of exosomal EGFRvIII receptor induces the activation of the MAPK and AKT signaling pathways to sustain glioma progression (Read et al, 2017). These same pathways, as well as CD97 expression, mediate the response to tumor-derived exosomes uptake in gastric cancer (Li et al, 2015). The role of tumor-derived exosomes in evasion of cell death has been reported in other cancer types. In bladder cancer, as well as in hepatocellular carcinoma, exosomal transfer facilitates cell-death evasion by the inducing of the up-regulation of Bcl-2 and cyclin-D1 expression and down-regulation of Bax and caspase-3 in exosome-receiving cells. (Yang et al, 2013; Alzahrani et al, 2018). The importance of exosomes in sustaining tumor expansion can also be ascribed to the evidence that they may serve as a survival mechanism in response to an environment that is highly stressful with limiting amounts of nutrients and oxygen. It has been shown that the EVs from cancer cells can protect recipient cells from nutrient deprivation-induced cell death (Hanahan and Weinberg 2011; Meehan et al 2016). Moreover, tumor-derived exosomes can exert complex effects on neighboring stromal cells such as endothelial cells and fibroblasts. Glioblastoma-derived exosomes containing RNAs, and angiogenic proteins are uptaken by recipient cells, thus promoting primary tumor growth and endothelial cell proliferation (Skog et al, 2008). As well, pancreatic cancer-derived exosomes can activate angiogenesis-related gene expression in endothelial cells (Nazarenko et al, 2010). Tumor-derived exosomes containing TGF-β can convert fibroblasts into myofibroblasts and thus contribute to tumor growth and local invasion (De Wever et al, 2008; Webber et al, 2010). Exosomes derived from breast cancer cells can promote a myofibroblastic phenotype in adipose tissue-derived mesenchymal stem cells, resulting in increased expression of the tumor-promoting factors TGF-β, VEGF, SDF-1 and CCL5 (Cho et al, 2012).

1.4.2.2 Tumor-derived exosomes and angiogenesis

Tumor-derived exosomes manipulate the microenvironment also by promoting angiogenesis, a critical process to maintain tumor growth. To overcome the limitation in oxygen and nutrients, cancer cells actively recruit endothelial cells to induce the formation of new blood vessels. This can be achieved via the transfer of specific factors via exosomes. The VEGF (vascular endothelial growth factor) signaling pathway is the most promising angiogenic target due to its key role in angiogenesis.

Glioblastoma-derived exosomes carrying VEGF induce angiogenesis and the promotion of vascular permeability (Treps et al, 2017), another essential step for tumor dissemination. Breast-cancer cells produce EVs presenting VEGF on their surface, capable of activating VEGF receptors on target cells and stimulating blood vessel formation (Feng et al, 2017). In epidermoid cancer cells, exosomes were reported to carry the EGF receptor, which could be transferred to human umbilical vein endothelial cells (HUVECs) and induce the production of VEGF (Al-Nedawi et al, 2008). Glioblastoma-derived exosomes also contain high levels of miR-221, associated with proteoglycans glypican-1 and syndecan-4, involved in the increased revascularization that characterizes this acutely sngiogenic tumor (Choi D et al 2018). The transfer of miRNA by exosomes also increased angiogenesis in multiple myeloma, via the targeting of HIF-1 (Umezu et al, 2014), and in gastric cancer, via the transfer of the proto-oncogene c-MYB (Yang et al, 2018). The exosomal transfer of miR-23a was linked to increased angiogenesis in nasopharyngeal carcinoma, where it induced the repression of Tsga10 (Bao et al, 2018), and in lung cancer, by the targeting of the tight junction protein ZO-1 (Hsu et al, 2018).

1.4.2.3 Tumor-derived exosomes and immune infiltrate

In the high complexity of tumor microenvironment, immune escape is considered an important hallmark of cancer, largely contributing to tumor progression (Thorsson et al, 2018). Interestingly, tumor-derived exosomes hae been reported to contribute to immune escape in different types of cancers and with various mechanisms.

One of the best understood and most studied mechanism in cancer-mediated immusosuppression is represented by the interaction of the cell surface receptor Programmed Death 1 (PD-1), expressed by various types of immune cells, particularly by CD8+ T cells, with its cognate ligand Programmed Death-Ligand 1 (PD-L1), usually expressed by tumor cells. This interaction can suppress T-cells' function, causing them to change phenotype, developing a T-cell tolerance and hindering the recognition of tumor cells (Robainas et al, 2017). Chen et al. demonstrated that in metastatic melanoma cells release high quantities of exosomes presenting PDL1 on their surface, which can bind PD-1 and prevent T cell activation (Chen et al, 2018).

A similar observation was reported also in prostate cancer, colorectal cancer, head and neck cancer, and glioblastoma (Chen et al, 2018; Theodoraki et al 2018; Ricklefs et al, 2018; Poggio et al, 2019,). Moreover, PD-L1 levels in circulating melanoma-derived exosomes positively correlated with response to immunoterapy, whereas it correlated with disease progression in head and neck squamous cell carcinoma patients (Theodoraki et al 2018). Taken togethere these studies show the potential of PD-L1 expressing exosomes as metrics of disease and immune activity, hence of response to

immunoterapy. Another layer to the explanation of exosomal PD-L1 role in cancer immune escape is provided by the observation of Chen et al, that cancer cell-derived EVs containing PD-L1, when administered to mice via tail vein injections, could induce a significant decrease in the total levels CD8+ T cells, suggesting that exosomes can suppress immunity both within the local tumor microenvironment, as well as systemically (Chen et al, 2018; Poggio et al, 2019).

The increase of extracellular adenosine is another strategy through which tumor cells can mediate immunosuppression. Extracellular adenosine binding to the A2A or A2B adenosine receptor, expressed in immune cells, can stimulate the biosynthesis of cyclic AMP (cAMP), which inhibits the immune activation (van Calker et al, 1979; Huang et al ,1997). A role for tumor-derived exosomes in modulating this pathway has been reported in head and neck cancer, where they regulate the synthesis of adenosine by transporting high levels of this process such as CD39 and CD73 (Clayton et al, 2011; Bastid et al, 2015).

Several studies reported a role for tumor-derived exosomes in mediating macrophages' polarization toward the tumor-promoting M2 phenotype, mostly via the transfer of specific miRNA cargos. This was observed in epithelial ovarian cancer (Ying et al, 2016), where exosomes enriched with miR-222-3p can enhance STAT3 activation in receiving macrophages, or in colorectal cancer, exosome-mediated transfer of miR-25-3p, miR-130b-3p, and miR-425-5p induces PTEN suppression and the subsequent M2 polarization of macrophages (Wang et al, 2020). Moreover, exosomes produced by hypoxic pancreatic cancer cells reportedly shuttle miR-301a-3p to macrophages, promoting M2 polarization via PTEN/PI3K signaling (Wang et al, 2018).

The activation of the NF-κB signaling pathways in macrophages is associated with the expression of pro-inflammatory factors such as IL-6, TNF-α, and CCL2. Tumor-derived exosomes from breast cancer and gastric cancer reportedly activate NF-κB in receiving macrophages (Chow et al, 2014; Wu et al, 2016).

1.4.2.4 Tumor-derived exosomes e cellular migration

Most studies on the role of exosomes in influencing tumor progression have focused on the ability of these vesicles to direct and facilitate the metastatic process, either in terms of induction of epithelial-mesenchymal transition, preparation of the prometastatic niche or through the transfer of metastatic capability (acquired by de novo mutations, epigenetic alterations or through the activation of cell signalling in the absence of genetic mutations) from cells with high metastatic capability to cells with low metastatic capability. (Steinbichler et al, 2017; Rajagopal et al, 2018).

The elucidation of the mechanisms through which exosomes induce the initiation of EMT are of recent interest. During EMT, ECM is degraded and tumor epithelial cells change morphologically and functionally to become more invasive. Tumor cells lose their epithelial features and gain mesenchymal properties, becoming aggressive and attaining stem cell-like properties (Whiteside et al, 2017). Many inducers of EMT have been identified in exosomal cargos, including transforming growth factor β TNFα, IL6, tumor susceptibility gene 101, AKT, integrin-linked kinase 1, β-catenin, hepatoma-derived growth factor, casein kinase II, annexin A2, integrin 3, Caveolin 1, MMPs and miRNA (Felicetti et al, 2009; Chairoungdua et al, 2010; Garnier et al, 2013; Jeppesen et al, 2014; Tauro et al, 2015; Webber et al, 2015). Moreover, Garnier et al. performed proteomic analysis on exosomes derived from epithelial and mesenchymal cells of squamous cell carcinoma and detected different proteomic signatures of EVs linked to EMT pathways which influences cell transition (Garnier et al, 2013). Exosomal LMP1, an Epstein Barr (EBV)-encoded primary oncogene, contributes to severe metastatic features of NPC by upregulating EMT which is accompanied by the expression of cancer stem cell markers (Yoshizaki et al, 2013). Tumor-derived exosomes enriched with miR-301a-3p in pancreatic cancer cells enhance transition of macrophages into the M2 phenotype in hypoxic conditions. This transition promotes migration and EMT of pancreatic cancer cells which is due to activation of PTEN/PI3K pathway (Wang et al, 2018). Matrix metalloproteinase (MMP) 13-containing exosomes facilitate the metastasis of nasopharyngeal cancer (NPC) cells (an endemic type of head and neck cancer) and it is through induction of EMT (You et al, 2015). Similarly, exosomes purified from highly metastatic breast cancer cells can induce an EMT-like process in epithelial cells (Galindo-Hernandez et al, 2014).

A major role reported for melanoma-derived exosomes is consistent with the “seed and soil” theory by Paget (1889), proposing that the interaction between cancer cells (seeds) and the microenvironment of the metastatic organ (soil) can direct the metastatic organ tropism by inducng the development of a pro-tumorigenic nyche, an environment distant from the primary tumor that is suitable for the survival and outgrowth of incoming circulating tumor cells (Peinado et al, 2012).

The preference of melanoma cells for spreading to lymph nodes has been ascribed to an exosomal-mediated establishment of a tumor-promoting environment in this metastatic site (Hood et al, 2011). Similarly, exosomes derived from melanoma with high metastatic capacity can help creating a favorable environment for tumor proliferation by stimulating bone marrow-derived cells (Peinado et al, 2012). Evidences obtained in melanoma have been also confirmed in other tumor types, such as pancreatic cancer metastatizing within lungs or lymph nodes (Jung et al, 2009) or renal cancer metastatizing within lungs (Grange et al, 2011). Tumor-derived exosomes can induce a molecular alteration in resident cells within the metastatization syte, like the up-regulation of matrix

metalloproteinases (MMP2, MMP3, and MMP14) and the down-modulation of cadherin-17 in lung fibroblasts or lymph node stromal cells (Rana et al, 2013) or TLR3 activation in lung epithelial cells (Liu et al, 2016). Interestingly, they can also exert their action by actively recruiting non-tumoral cell populations, such as fibroblasts, endothelial cells and macrophages, in the metastatization syte, further supporting the formation of the pro-tumorigenic nyche (Peinado et al, 2012; Costa-Silva et al, 2015). As an example, tumor-derived exosomes isolated from highly metastatic colorectal cancer can establish a favorable metastatic microenvironment by recruiting CXCR4-expressing stromal cells (Wang et al, 2015) and the aforementioned upregulation of TLR3 in lung epithelial cells is reported to promote chemockine secretion inducing the recruitment of immune cell populations, such as neutrophils, macrophages and monocytes at the metastatic site (Liu et al,2016).

The role of tumor-derived exosomes in promoting migration, invasion and metastasis is also exerted via the transfer of a metastatic phenotype from cells with high metastatic capability to cells with low metastatic capability, as a consequence of the horizontal transfer of key factors, both mRNAs or proteins, involved in tumor progression. Proteins such as caveolins, MET proto-oncogene and S100 family members are shuttled in exosomes produced by metastatic hepatocellular carcinoma cells and can induce, upon transfer to non-motile cells, the activation of MAPK and PI3K signalling pathways and the upregulation of matrix metalloproteinases (Mashouri et al, 2019). Exosomes derived from epithelial ovarian cancer cells containing CD44 can increase matrix metalloproteinase 9 (MMP9) production in human peritoneal mesothelial cells, thus increasing their invasion (Nakamura et al, 2017). Exosomal miR-222-3p has been associated to increased invasion of NSCLC cells by the targeting of SOCS3 (Suppressor of cytokine signaling 3), a negative regulator of the JAK/STAT signaling pathway (Wei et al, 2017). It also plays a role in enhancing migration and invasion abilities of breast cancer cells via the activation of the NF-κB signaling pathway (Ding et al, 2108).

1.4.2.5 Stromal cells of the tumor microenvironment and exosomes

The investigated role in the croostalk between cancer cells and the surrounding microenvironment is a two-directions complex interplay. The majority of studies in the last years focused on the biology and the function of tumor-derived exosomes, yet exosomes produced by the stromal components of tumor micreonvironment can modulate the phenotype of cancer cells as well (Balaji et al, 2021; Malla et al, 2021). The most represented stromal compoents of tumor microenvironment are cancer associated fibroblasts (CAFS). They derive from the differentiation of fibroblasts, bone marrow-, adipose-derived MSCs and endothelial cells (Kendall et al, 2014; Shiga et al, 2015; Alkasalias et al,

2018). Tumor-derived exosomes can induce the conversion of fibroblast cells into CAFs via the abundant cargo-presence of TGFβ, which can activate the SMAD pathway (Chowdhury et al, 2015). Once activated, CAFs can secrete exosomes that promote tumor growth: Hu et al reported that CAF-derived exosomes can drive proliferation in colorectal cancer (Hu et al, 2015), while the work by Rodrigues et al demonstrated that the shuttling of IL6, activin-A and G-colony stimulating factor mediated by CAF-derived exosomes could promote dedifferentiation in lung cancer cells (Rodrigues et al, 2018). Further evidence of the role for CAF-derived exosomes relies in the trafficking of miRNAs, such as miR21-5p, miR378e, miR143-3p and miR92a-3p, enhancing stemness, EMT, chemoresistance and metastasis in breast cancer, colorectal cancer and ovarian carcinoma (Yeung at al, 2016; Donnarumma et al, 2017; Hu et al, 2019).

Mesenchymal Stem Cells (MSCs) present in the tumor microenvironment, due to their multipotency, can differentiate into multiple cell lineages (i.e. CAFs, macrophages or endothelial cells) to modulate pro-tumorigenic environment (Direkze et al, 2004; Janeczek Portalska et al, 2012; Atiya et al, 2020). MSCs-derived exosomes can modulate cancer homeostasis, chemoresistance, angiogenesis and metastasis. Bone Marrow-derived MSCs drive pro-tumorigenic effects by transferring cargo proteins, such as UBR2, which can induce the upregularion of stemness-mediated genes in gastric cancer cells (Mao et al, 2017), or miRNAs, such as the NOTCH-activating miR142-3p, which can trigger- EMT and chemoresistance to doxorubicin in colon cancer cells (Li et al, 2018). Moreover, BM-MSCs- derived exosomes carry miR-23b and miR-21, which can promoted cell proliferation in breast cancer (Ono et al, 2014).

Besides cancer cells, tumor microenvironment is characterized not only by stromal cell populations, but also by stressing and adverse conditions, such as oxygen and nutrients deprivation, constantly challenging the survival of cancer cells. To tolerate such adverse circumstances, tumor-derived exosomes can be loaded with specific regulatory factors such as miRNAs.

Hypoxia-induced exosomes of cancer cells were shown to transfer long non-coding RNAs (lncRNA) to adjacent bladder cancer cells, which can reportedly enhance EMT and metastatization via the inhibition of E-cadherin associated with the elevated expression of vimentin and MMP9 (Xue et al, 2017).

1.4.3 EXOSOMES AND BONE SARCOMAS

Bone sarcoma cells, as many other cancer cells, produce exosomes which are released in the surrounding TME. Their interest relies both in the specifc biomolecules packed in exosomal cargos,

which could be used as biomarkers, and the molecular changes they induce in surrounding recipient cells, both malignant or not-malignant, as further clarification of tumor progression.

As the most common malignant bone tumor in children and adolescents, Osteosarcoma is characterized by rapid proliferation and erarly metastasis, resulting in elevated malignancy and unfavourable prognosis. Emerging evidence show that Osteosarcoma development can be mediated by exosomes, which can transfer key molecules such as DNA and different types of RNAs which can have an impact on many aspects of tumor biology.

To date, miRNAs are the most investigated molecules whithin Osteosarcoma exosomes' cargo as increasing evidence has been collected regarding their functions in influencing tumor progression. MiRNA sequencing experiments on a series of human Osteosarcoma cell lines with differential metastatic potential identified a signature of four miRNAs, namely miR-21-5p, miR-143-3p, miR-148a-3p and 181a-5p, which are higly enriched in exosomes derived from highly metastatic cell lines when compared to non-metastatic Osteosarcoma cells. Gene ontology analysis performed on predicted target genes for these miRNAs suggested a role in regulating cell migration, adhesion, apoptosis and angiogenesis (Jerez et al, 2019). Interestingly, the role of exosomal miR-143 in dampening the migratory phenotype of Osteosarcoma cells had already been proposed (Shimbo et al, 2014). High expression of exosomal but not cellular miR-675 level was observed in metastatic OS cell lines in contrast to nonmetastatic counterparts, further evidencing the role of this exosomal miRNA in influencing cellular migration and invasion via inducing a decrease of Calneuron1 expression levels in recipient cells (Gong et al, 2018). Osteosarcoma cells with high levels of miR-195-3p can produce exosomes enriched in this microRNA, thus promoting proliferation and migration of recieving cells (Ye et al, 2020). Recently, also exosomal miR-1307 has been correlated to the modultion of Osteosarcoma progression, particularly via the inhibition of its direct target AGAP1, an Arf GTPase-activating protein (Han et al, 2021).

Drug resistance is a significant problem with chemotherapy in Osteosarcoma patients, as it may induce a rapid increase in metastasis (He et al, 2014). Exosomes released by drug-resistant Osteosarcoma cells can mediate acquired multidrug resistance (MDR) in recieving cells. Particularly, exosomes generated from doxorubicin-resistant cells contain high levels of MDR1 and P-glycoprotein mRNA, which can enhance the ability of the surrounding Osteosarcoma cells to resist doxorubicin action (Levchenko et al, 2005; Torreggiani et al, 2016). The identification of the most effective chemotherapeutic agent for each individual patient represents another major challenge in Osteosarcoma, as ineffective chemotherapy leads to increased mortality and decreased quality of life in patients. Xu et al. investigated the RNA cargo of exosomes isolated form the sera of patients with

differental chemotherapeutice response. They identified a signature of miRNAs, namely miR-124, miR-133a, miR-135b, miR-148a, miR-199a-3p, miR-27a, miR-385, and miR-9, which are deregulated in poor responders. Moreover, the same group observed that exosomal mRNAs including Annexin2, Smad2, MTAP, CIP4, PEDF, WWOX, Cdc5L, P27, could help discriminate good and poor responders to treatment (Xu et al, 2017).

The identification of exosomal microRNAs in Osteosarcoma patients' sera holds an important diagnostic and prognostic promise. Fujiwara et al. identified 236 serum miRNAs highly expressed in Osteosarcoma patients when compared to controls. Among them, miR-17-5p and miR-25-3p resulted higly expressed in Osteosarcoma cells and were were abundantly released in tumor-derived exosomes. Interestingly, serum miR-25-3p levels at diagnosis were correlated with patient prognosis and reflected tumor burden in both *in vivo* models and patients, suggesting a potential role for this micro RNA as a noninvasive biomarker for prognostic prediction and tumor monitoring in Osteosarcoma patients (Fujiwara et al, 2017).

In the context of tumoral microenvironment, exosomes play their role as intercellular communication tools not only between Osteorsarcoma cells, but also between tumoral and surrounding normal cells. Osteosarcoma-derived exosomes can induce malignant transformation in normal receiving cells by sustaining proliferation, metastasis and antiapoptotic properties (Urciuoli et al, 2018). Osteosarcoma-derived exosomes can induce lung fibroblast reprogramming by activating TGFb1 and SMAD2 pathway, thus directing their activation toward the CAF phenotype and promoting Osteosarcoma metastatization to the lungs (Mazumdar et al, 2020). Further sustianing the role for Osteosarcoma derived exosomes in promoting metastasis to local or distant tissues, Cheng et al. observed that these exosomes can induced macrophage M2 polarization by regulating the expression of Tim-3, T cell immunoglobulin and mucin domain 3 (Cheng et al, 2021).

The M2 polarization promoted by exosomes released by metastatic Osteosarcoma cells can induce, via TGFb2 production, the development of an immunosuppressive and tumor-promoting microenvironment, consistent with the poor prognosis for this tumor type (Wolf-Dennen et al, 2020). Moreover, Osteosarcoma derived exosomes induce the activation of IL-6/STAT3 signaling pathway in mesenchymal stem cells (MSCs), thus promoting tumoral proliferation and metastasis (Lagerweij et al, 2018).

Notably, not only Osteosarcoma-derived exosomes influence the surrounding normal cells to sustain tumor progression. CAFs have a reported role in affecting tumor cell malignancy and they were demonstrated increasing Osteosarcoma migratory abilities by the transfer of exosomal miR-1228 and the subsequent downregulation of endogenous SCAI mRNA, similarly to what is reported in breast

cancer cells (Lin et al, 2015; Wang et al, 2019). Interestingly, exosomal miR-29a released by macrophages in the context of Osteosarcoma promotes cancer cell invasion and proliferation (Zhang et al, 2021). The role of exosomes secreted by MSCs in influencing Osteosarcoma cells'phenotype has been evaluated in different sudies. Particularly, MSC-exosomes promote Osteosarcoma growth and metastasis via the paracrine activation of the Hedgehog pathway (Qi et al, 2017), by inducing HIF-1α expression via the activation of the PI3K/AKT pathway (Lin et al, 2019), and by promoting oncogenic autophagy both *in vitro* and *in vivo* (Huang et al, 2020). MSC-exosomes also carry specific microRNAs which lay a role in modulating receiving Osteosarcoma cells phenotype, such as miR-208a which negatively targets PDCD4 and induces the activation of the ERK1/2 signaling pathway (Qiu et al. 2020) or miR-206 which, on the contrary can inhibit tumor progression by targeting TRA2B (Zhang et al, 2020).

Research in the field of exosomes in Ewing Sarcoma, the second most common bone tumor in children and young adolescents, is rather recent, as in 2013 Miller et al. described for the first time exosomal release by Ewing Sarcoma cell lines (Miller et al, 2013). Moreover, the authors hilightesd that Ewing Sarcoma-derived exosomes carry the EWS-FLI1 transcript in their cargo, an observation which was further confirmed in exosomes isolated from the blood of mice harboring Ewing Sarcoma xenografts by Tsugita et al. Interestingly, EWS-FLI1 transcript was observed to be transferred between different Ewing Sarcoma cell lines but not into Osteosarcoma cells, thus suggesting its selective transfer (Tsugita et al, 2013).

Ewing Sarcoma derived exosomes carry a broad spectrum of RNAs, particularly the small ones, but the EWS-FLI1 transcript is not the only mRNA which is specifically loaded into these vescicles.

Microarray analysis performed on isolated exosomal RNA hilighted an enrichment of transcripts involved in signal transduction, particularly G-protein coupled signalling and neurotransmitter signalling, together with stemness (Miller et al, 2013).

The expression of a group of transcripts highly characteristic of Ewing Sarcoma, such as the histone methyltransferase Enhancer of Zeste Homolog 2 (EZH2) which is a transcriptional target of EWS-FLI1, was assessed and exosomal levles appeared to be accordingto the cellular ones (Miller et al, 2013).

MicroRNA cargo of Ewing Sarcoma derived exosomes has also started to be investigated. Particularly, Ewing Sarcoma cells with silenced expression of CD99, a characteristic surface marker of this tumor type, produced exosomes containing not only lower levels of the protein itself (Llombart bosch et al, 2009; Ventura et al, 2016), but also increased levels of miR-34a, whose transfer represses the Notch pathway and inhibits NF-kB transcriptional activity. Neural differentiation of the recieving cell is observed, similarly to what happens with direct CD99 silencing (Ventura et al, 2016).

Moreover, CD99-depleted exosomes contain high levels of miR-199a-3p, responsible of growth inibithion and impaired migration of recipient cells as seen in other cancers (De Feo et al, 2019). On the contrary, the same study demonstrated that the uptake of CD99-positive exosomes derived from cells expressing the protein led both to an increase in cell proliferation and migration in recipient cells, whereas poor neural differentiation was observed (De Feo et al, 2019).

Interestingly, exosomal miRNA content doesn't appear to rely only on the cell of origin but also on the influence exerted by the surrounding microenvironment. In fact, miR-210 was observed to be the most upregulated miRNA under hypoxic conditions both in Ewing Sarcoma cells and exosomes (Kling et al, 2020). Hypoxia is a major feature of Ewing Sarcoma microenvironment and has been demonstrated to affect cellular proliferation and migration (Knowles et al, 2010). The work by Kling et al also identified a role for hypoxia in determining exosomal secretion and specific miRNA loading, particularly via the regulation exerted by Hypoxia Inducible Factor 1-a (HIF 1α) on miR-210 exosomal packaging. Another evidence of the impact that the TME can exert on exosomal biogenesis in Ewing Sarcoma was obtained via the development of a bioengineered tumor model: 3D culture and extracellular matrix (ECM) composition had an influence on exosomal size distribution, which was more similar to the one detected in patients'plasma rather than in cell culture supernatants (Villasante et al, 2016).

The examples presented so far higlight the role of Ewing Sarcoma derived exosomes in regulating the fate of surrounding tumoral cells and the impact that the TME can have on exosomal biogenesis, yet the influence exerted by these vesicles on the cellular components still needs to be clarified.

The cargo of exosomes derived from bioengineered tumors was successfully tranferrerd into normal recipient cells, such as human MSCs, osteoblast and osteoclasts, and a modulation of EZH2 mRNA levels was observed in all three cellular types, suggesting a transfer of exosomal mRNA cargo (Villasante et al, 2016). Yet, the functional consequences of this uptake in normal recipient cells still need further elucidation both *in vitro* and *in vivo*.

To date, no information is available on the influence of Ewing Sarcoma derived exosomes on many of the non-tumoral cell lineages populating the TME, yet during the last year Gassmann et al. collected evidence of their interaction with the immune cells. Despite being a yet poorly investigated field, Ewing sarcoma is known for showing a limited immune infiltrate. Overall, it iss predominantly composed by tumor associated macrophages (TAM) (Fujiwara et al, 2011) while CD8(+) T lymphocytes infiltrate is even less represented (Machado et al, 2018). In their study, they showed that

Ewing Sarcoma exosomes sustain pro-inflammatory signaling while impairing the maturation of myeloid cells, namely CD14+ monocytes and CD33+ myeloid cells, thus influencing both innate and adaptive immunity. The vesicles are shown to induce prolonged cytokine and chemokine release, particularly of IL-6, IL-8 and TNF by myeloid cells, CD14+ cells differentiated in the presence of Ewing Sarcoma derived exosomes exhibited a semi-mature immunosuppressive phenotype, consisting in reduced expression of co-stimulatory molecules associated with DC maturation and with MDSC phenotypes (Gassmann et al, 2021).Similar effects were reported in hematological and other solid malignancies, which hints of common mechanisms operating in different types of cancer (Maus et al, 2017; Ning et al, 2018). Moreover, to sustain the indication that exosomes released by Ewing Sarcoma cells may affect both innate and adaptive immunity, the CD14+ cells differentiated in the presence of Ewing Sarcoma derived exosomes induce diminished activation of CD4+ and CD8+ T cells, by reducing their proliferation and IFN release. Ewing Sarcoma EVs may thus contribute to the observed scarce infiltration of Ewing Sarcoma tumors with T cells, M1 macrophages, and mature DCs, as well as the prevalence of pro-tumorigenic immunosuppressive M2 macrophages and resting DCs in the Ewing Sarcoma TME (Fujiwara et al, 2011; Sthal et al, 2019).

2 AIM OF THE STUDY

The interactions between cancer cells and the context of cellular and non-cellular components surrounding them, defined as Tumor Microenvironment (TME), are responsible for the loss of tissue homeostasis and promote tumor development and progression. Indeed, these interactions are known for controlling most aspects of tumor progression, such as tumor growth, neovascularization, drug resistance, apoptosis, cell migration and metastasis formation.

Ewing Sarcoma, the second most common malignant mesenchymal tumor in young patients, is characterized by a particularly adverse prognosis associated with metastatic disease at diagnosis.

The overall stability of Ewing Sarcoma genome reinforces the need to study epigenetic or mRNA post-translational modification mechanisms, such as the oncofetal RNA binding protein (RBP) Insulin-like Growth Factor 2 mRNA Binding Protein 3 (IGF2BP3/IMP3), to understand more in-

depth tumor progression. In Ewing Sarcoma, IGF2BP3 plays a well-known oncogenic role in sustaining cell migration both *in vitro* and *in vivo*, correlating with the poorest outcomes of the patients. Yet a comprehensive identification of the malignant processes mediated by this RBP in the interaction with the tumor microenvironment still needs further investigation.

The aim of the present study was indeed to evaluate the relevance of IGF2BP3 in the communication between Ewing Sarcoma cells and tumor microenvironment, in order to gain deeper insight on this tumor progression mechanisms and to further explore the role of IGF2BP3 as a prognostic or diagnostic marker. To do so, we evaluated the role of IGF2BP3 in

- response to the stress-adaptive conditions characterizing Ewing Sarcoma TME, such as hypoxia, with a particular focus on metastatic progression;
- communication between Ewing Sarcoma cells, which can influence their phenotypes via exosome-mediated horizontal transfer of the RBP and its client mRNAs;
- interaction between Ewing Sarcoma cells and the immune effectors populating the TME.

Therefore, the PhD project was built on the intention of providing a deeper insight on Ewing Sarcoma progression and metastasis formation, by elucidating the IGF2BP3-dependent mechanisms through which the tumoral cell interacts with the surrounding microenvironment.

3 RESULTS

3.1 GENERATION OF A NOVEL CRISPR/CAS9 IGF2BP3 KNOCKOUT MODEL IN EWING SARCOMA CELLS

Recent research from our laboratory broadly investigated the functional role of IGF2BP3 in Ewing Sarcoma. For *in vitro* studies, canonical cell lines were employed and two IGF2BP3 knockdown experimental models were previously obtained. Specifically, IGF2BP3 was silenced via transfection with the pLKO.1 vector containing the IGF2BP3-specific short hairpin RNA on A673 and TC-71 cells (Figure 1), as they present the highest IGF2BP3 levels correlated with strongest malignant features in a panel of classical Ewing Sarcoma cell lines (Mancarella 2018). In this section, we will refer to IGF2BP3 knockdown cells as “shIMP3” and to the mock-transfected cells as “shGFP”.

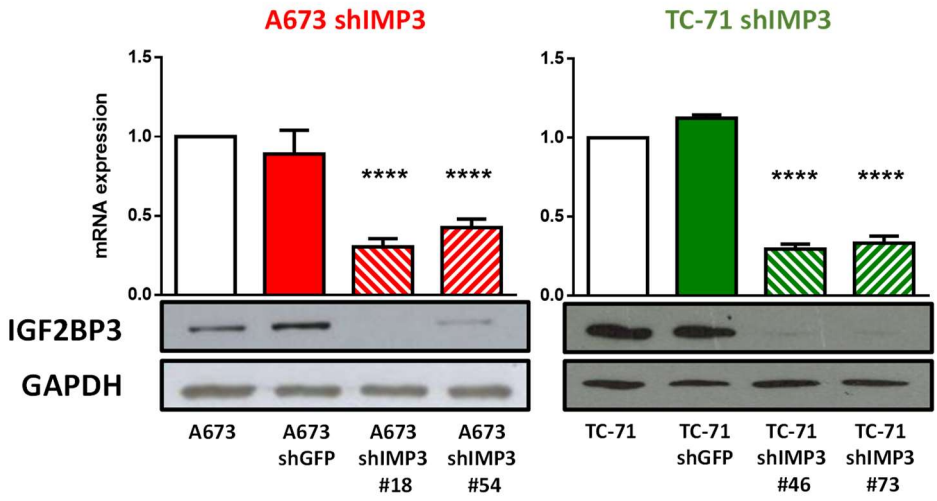

Figure 1. IGF2BP3 levels in A673 and TC-71 shIMP3 models.
*IGF2BP3 mRNA and protein levels evaluation in IGF2BP3 knockdown (shIMP3) A673 and TC-71 cells compared to parental control and to mock-transfected cells (shGFP). GAPDH was used as housekeeping gene or loading control. mRNA expression is reported as RQ and bars represent the mean ± SD of at least three independent replicates, ****p < 0.0001, one-way ANOVA. A representative Western Blot is shown.*

3.1.1 IGF2BP3 IN PATIENT-DERIVED XENOGRAFTS CELL LINES

The faithfulness of classical preclinical models has been recently debated, particularly as one of the reasons behind the difficult translation of preclinical discoveries into effective therapies. In the last decades research has concentrated on the development of Patient Derived Xenografts (PDXs) and companion cell lines as one of the strategies to overcome the limited predictive value of classical cell lines. To obtain PDXs, primary patient specimens are implanted into immunodeficient mice shortly after explant.

Tumors grown in mice are then harvested and minced to obtain PDX-derived cell lines, which are stabilized under 2D *in vitro* colture conditions. PDX and matching cell lines share elevated genotypic and phenotypic similarity between themselves and with the tumor of origin, a characteristic that makes this model extremely intriguing (Shi et al, 2020). A collection of Patient Derived Xenografts from Ewing Sarcoma tumors had previously been obtained in our laboratory in collaboration with the laboratory of Professor P.L. Lollini (Dipartimento di Medicina Specialistica, Diagnostica e Sperimentale, Laboratorio di immunologia e biologia delle metastasi, Bologna). The genetic representativeness of PDX and PDX-derived cell lines has recently been confirmed in our laboratory in CIC-DUX4 (Capicua–double homeobox 4) sarcomas, a subcategory of small round blue cell tumors resembling the morphological phenotypes of Ewing sarcoma (Carrabotta et al, 2021). Based on this knowledge, *IGF2BP3* expression levels were tested via Real Time-qPCR in a group of tumor

samples with corresponding PDXs and, when available, their corresponding PDX-derived cell lines (Figure 2A). No significant statistical difference was observed between the mean of the three groups of samples. Expression levels resulted evened out in PDXs when compared to tumors and cell lines and this could be ascribed to the presence of necrotic or murine cells in sample preparation. Interestingly, PDX-EWS#5-C and PDX-EWS#2-C cell lines, which presented very high and very low levels of both IGF2BP3 mRNA and protein (Figure 2B), were derived from tumor samples which respectively presented one of the highest and one of the lowest *IGF2BP3* expression levels. This observation confirms the high representativeness of PDX-derived cell lines when compared to the tumor of origin.

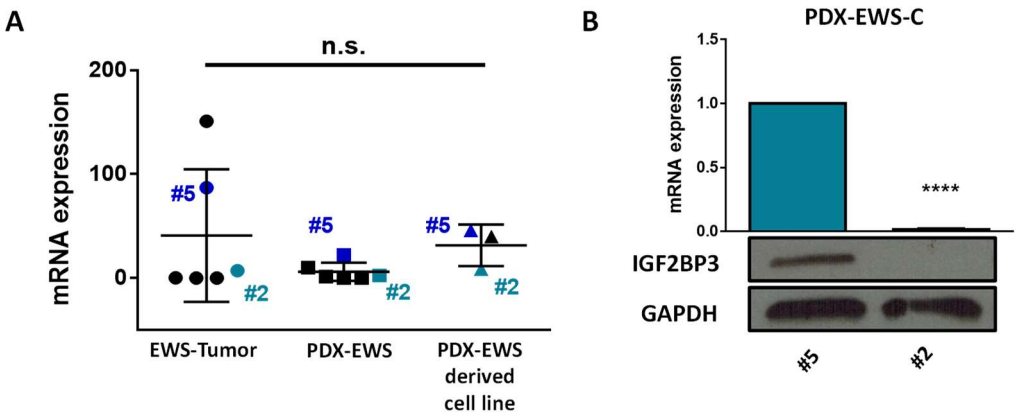

Figure 2. PDX and PDX-derived cell lines are representative of IGF2BP3 levels of the tumor of origin
(A) *IGF2BP3 mRNA levels evaluated via Real Time-qPCR in 6 Ewing Sarcoma tumor samples, 6 corresponding Patient-Derived Xenografs (PDX-EWS) and 3 stabilized PDX-EWS derived cell lines. Relative mRNA expression reported as RQ is shown. Each symbol represents a single sample and the line marks the mean ± SD of each group. GAPDH was used as housekeeping gene. Human mesenchymal stem cells were used as calibrator. n.s, not significant, one-way ANOVA.* ***(B)*** *IGF2BP3 mRNA and protein levels evaluation in PDX-EWS #2-C compared to PDX-EWS #5-C PDX-derived cell line. GAPDH was used as housekeeping gene or loading control. mRNA expression is reported as RQ and bars represent the mean ± SD of at least three independent replicates. ****$p < 0.0001$, one-way ANOVA. A representative Western Blot is shown*

3.1.2 GENERATING A CRISPR/CAS9 IGF2BP3-KNOCKOUT MODEL

The described presence of high or low levels of IGF2BP3 in PDX-derived cell lines does not necessarily make the comparison between their phenotype representative of IGF2BP3-induced malignancy. In fact, since IGF2BP3 is constitutively down-modulated in PDX-EWS#2-C cell line, the tumor cell has likely activated collateral compensatory pathways in order to maintain the malignant phenotype. Based on these considerations, we decided to use PDX-EWS#5-C cell line to perform IGF2BP3 knockout (KO) via the Crispr/Cas9 system. In this section, we will refer to IGF2BP3 knockout cells as “gIMP3” and to the mock-transfected cells as “gSCR”.

CRISPR (Clustered Regularly Interspaced Short Palindromic Repeats) is a microbial nuclease system involved in defense against invading plasmids and phages. Microbial CRISPR locus is a combination

of CRISPR-associated (Cas) genes and non-coding RNA elements which can program the specificity of the CRISPR-mediated nucleic acid cleavage. Lentiviral CRISPR/Cas can infect a broad variety of mammalian cells by co-expressing a mammalian codon-optimized Cas9 nuclease along with a single guide RNA (sgRNA) to facilitate genome editing (Doudna and Charpentier, 2014, Shalem et al, 2014).

For our purposes PDX-EWS#5-C cells were infected with the lentiviruses carrying the lentiviral CRISPR plasmid expressing the corresponding gRNA. Plasmids containing the sgRNA sequences were kindly designed and provided by professor A.M. Mercurio (University of Massachusetts Medical School). Infected cells were selected in puromycin 2μg/ml and subsequently amplified in puromycin 0.5 μg/ml to constitute liquid nitrogen stocks. IGF2BP3 KO was evaluated at protein level via Western Blotting and the clones showed no detectable expression of the protein, confirming a successful silencing (Figure 3A). The total absence of IGF2BP3 protein in gIMP3 cells is a remarkable difference with what is observed in shIMP3 models, as the two mechanisms differ in their targets: while short hairpin directly bind mRNAs, leading them to disruption, the Crispr/Cas9 system is designed to specifically cleave the gene of interest at DNA level, *de facto* disrupting the cellular ability to produce the corresponding mRNA. Our PDX-EWS #5 gIMP3 cells were then characterized in terms of cellular proliferation, migration and anchorage-independent growth with respect to their corresponding mock-silenced control (gSCR). gIMP3 cells doubling time was comparable to the gSCR one, hinting that IGF2BP3-KO didn't affect significantly cell proliferation (Figure 3B). On the contrary, IGF2BP3-KO was associated with a significant reduction in migration ability in a transwell assay (Figure 3C), and correlated with a reduced ability to form colonies under anchorage-independent conditions (Figure 3D).

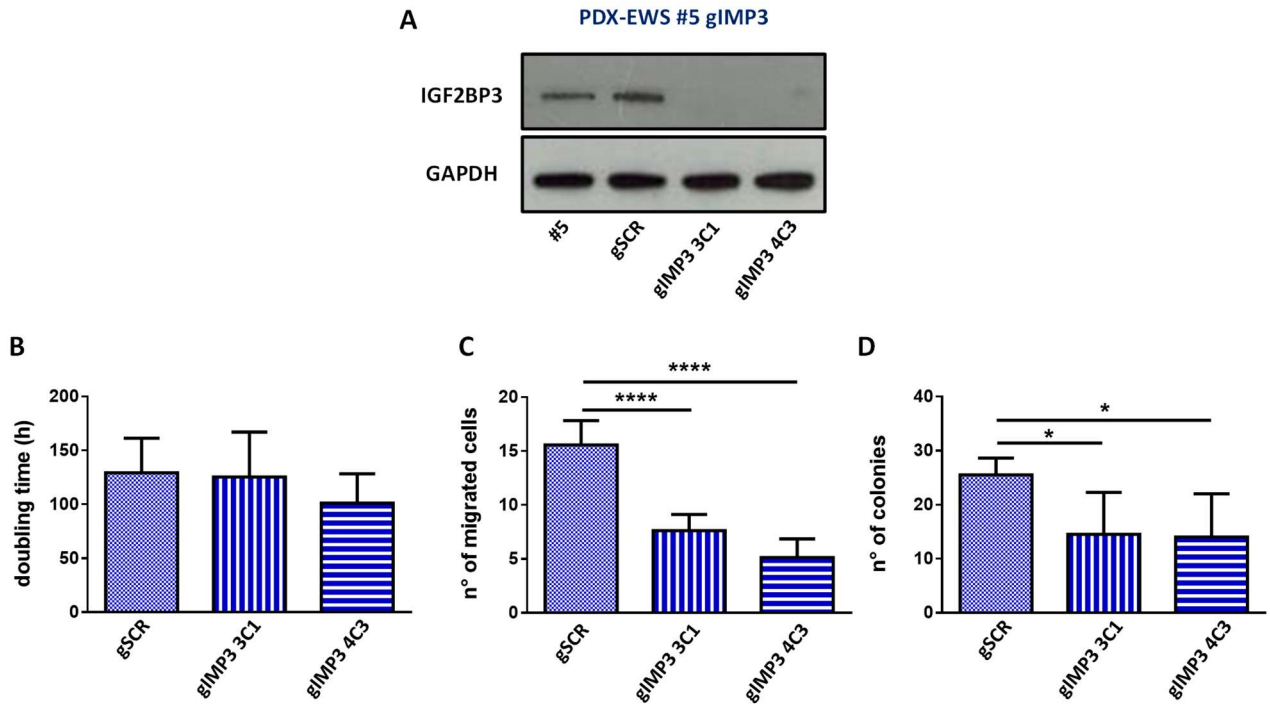

Figure 3. Characterization of a Crispr/Cas9 IGF2BP3-knockout model in PDX-EWS #5-C cell line
(A) *IGF2BP3 protein levels evaluated in IGF2BP3-KO (gIMP3) PDX-EWS #5-C g cells compared to parental control and to gSCR mock-transfected cells. GAPDH was used as loading control. A representative Western Blot is shown.* ***(B)*** *Proliferation of gIMP3 cells compared with that of gSCR control. Bars are representative of mean ± SD of at least two independent experiments are shown.* ***(C)*** *Basal migration of gIMP3 cells compared with that of gSCR control. Bars represent number of migrated cells. Mean ± SD of at least two independent experiments performed in duplicate is shown. ****$p < 0.0001$, Student's t-test vs gSCR.* ***(D)*** *3D growth in soft agar of gIMP3 cells compared with gSCR control. Bars represent number of colonies. Mean ± SD of at least two independent experiments performed in duplicate is shown. *$p < 0.05$, Student's t-test vs gSCR.*

3.2 IGF2BP3-MEDIATED CELLULAR RESPONSE TO TUMORMICROENVIRONMENT

3.2.1 IGF2BP3 IS ASSOCIATED WITH METASTASIS IN EWING SARCOMA

Data previously published by our laboratory showed a lower incidence of metastasis in Crl:CD-1-nu/nu BR mice after intravenous injection of IGF2BP3-depleted cells when compared to controls (Mancarella et al, 2018).

The correlation between IGF2BP3 expression levels and Ewing Sarcoma metastasis was further explored performing Real-Time qPCR on a set of 48 RNA samples derived from primary Ewing Sarcoma lesions and on 44 RNA samples extracted from metastatic tissues. Clinical-pathological features of primary Ewing Sarcoma patients included in the study are presented in Table 5.

Interestingly, *IGF2BP3* expression was higher in metastatic specimens when compared to primary untreated tumors, used as controls (Figure 4).

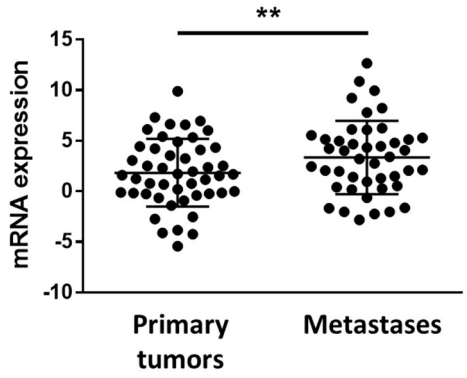

Figure 4. Correlation between IGF2BP3 and metastatic disease in Ewing Sarcoma patients
*Scatter plot representing IGF2BP3 mRNA levels determined via Real Time-qPCR in primary (48) or metastatic (44) Ewing Sarcoma specimen. GAPDH was used as housekeeping gene. Mean ± SD of relative mRNA expression, reported as log2, is shown. Human mesenchymal stem cells were used as calibrator. **p < 0.01. Student's t-test.*

3.2.2 IGF2BP3 IS ASSOCIATED WITH IMMUNOLOGICAL AND CHEMOKINE-MEDIATED SIGNALING PATHWAYS

During cancer progression, the repertoire of chemokines, cytokines, and growth factors that orchestrates normal immune and inflammatory responses can be redirected to create an immunosuppressive state that facilitates invasion and metastasis.

A set of 6 primary localized EWS specimens, with very low or very high expression of IGF2BP3, had previously been analyzed in our laboratory via RNAseq, identifying a signature of 814 differentially expressed genes involved in immunological and chemokine-mediated signaling pathways (Mancarella et al, 2020). Thus, to further define which IGF2BP3-related mechanisms might have a relevance in the context of tumor microenvironment, we took advantage of the stably IGF2BP3-silenced A673 model to perform a comprehensive analysis of the expression levels of a panel of 84 mRNA involved in mediating communication between tumor cells and the cellular mediators of inflammation and immunity via the Human Cancer Inflammation & Immunity Crosstalk RT² Profiler PCR Array. 13 out of 84 analyzed mRNAs resulted differentially expressed between IGF2BP3-silenced Ewing sarcoma cells and controls (Table 1). 10 out of 13 deregulated mRNAs were upregulated and the majority of them (i.e., *CD274*, *IL15*, *PDCD1*, *PTGS2*) is known to participate in immune responses, hinting that IGF2BP3 could play a role in the interaction of Ewing Sarcoma cells with the immune system. Only three mRNAs, *TLR3*, *CXCR4* and *CCL2* resulted downregulated and, interestingly, both *CXCR4* and *CCL2* participate in chemokine-mediated signaling pathways, sustaining a functional association between IGF2BP3 and chemokine signaling pathways.

Pathway	Gene Symbol	Gene Name	Fold Regulation (IGF2BP3- *vs* IGF2BP3+)
Immune Responses	**CD274**	*Programmed Cell Death 1 Ligand 1*	**2.85**
	IL15	*Interleukin 15*	**2.38**
	PDCD1	*Programmed Cell Death Protein 1*	**2.32**
	PTGS2	*Prostaglandin-Endoperoxide Synthase 2*	**2.18**
Interferon Signaling	**GBP1**	*Guanylate-Binding Protein 1*	**4.14**
	IRF1	*Interferon Regulatory Factor 1*	**3.79**
Toll-Like Receptor Signaling	**MYD88**	*Myeloid differentiation primary response 88*	**2.28**
	TLR3	*Toll-like receptor 3*	**-2.50**
Chemokines and Chemokine Receptors	**CCR7**	*C-C chemokine receptor type 7*	**3.83**
	CXCR4	*C-X-C Motif Chemokine Receptor 4*	**-2.49**
	CCL2	*C-C Motif Chemokine Ligand 2*	**-53.30**
Growth Factors and Receptors	**EGFR**	*Epidermal Growth Factor Receptor*	**2.79**
Other Cytokines	**KITLG**	*KIT Ligand*	**3.67**

Table 1. Human Cancer Inflammation & Immunity Crosstalk RT² Profiler PCR Array: mRNAs differentially expressed in A673 shIMP3 model

3.2.3 IGF2BP3 ACTS AS AN UPSTREAM REGULATOR OF CXCR4

CXCR4 is the most common chemokine receptor expressed in human cancer and mediates migration towards its ligand, CXCL12 (Teicher and Fricker, 2010). Its upregulation has been already associated with the metastatic process in many tumors, including Ewing Sarcoma (Krook et al, 2014).

We performed qRT-PCR and Western Blotting analyses to confirm the association between IGF2BP3 and CXCR4 levels in Ewing Sarcoma cells, observing a downmodulation of CXCR4 in IGF2BP3-silenced cells when compared to controls (Figure 5).

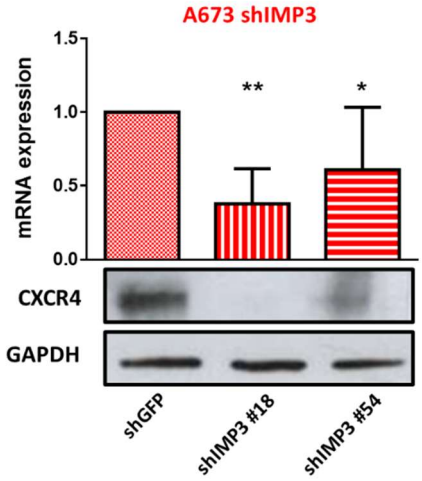

Figure 5. CXCR4 levels are related to IGF2BP3 expression in Ewing Sarcoma

*CXCR4 expression analyzed via Real Time-qPCR and Western Blot in shIMP3 or mock-transfected (shGFP) A673 cells. GAPDH was used as housekeeping gene or loading control. mRNA expression is reported as RQ and bars represent the mean ± SD of at least three independent replicates. * p<0,05, **p < 0.01, one-way ANOVA. GAPDH was used as housekeeping gene or loading control. A representative Western Blot is shown.*

3.2.4 IGF2BP3 INFLUENCES CELLULAR MIGRATION IN HYPOXIC CONDITIONS

We decided to investigated the contribution of the IGF2BP3/CXCR4 axis in the stress-adaptive response of Ewing Sarcoma cells under hypoxic conditions (1% O_2), since this is a major feature of this tumor type microenvironment (Knowles et al, 2010). Moreover, the upregulation of CXCR4 in Ewing Sarcoma exposed to hypoxia is reported (Krook et al, 2014). Cells cultured in hypoxic conditions showed a trend of reduced proliferation in an IGF2BP3-independent manner (Figure 6A). On the other hand, a reduction in migration was observed in A673 shIMP3 cells cultured under hypoxia (Figure 6B). Interestingly, IGF2BP3 silencing was associated with a significant reduction in migration in response to CXCL12, both in normoxic and hypoxic conditions (Figure 6C).

CXCR4 levels were assessed and, according to previously reported evidences, Ewing sarcoma high-IGF2BP3 expressing cells exposed to hypoxia displayed the induction of both CXCR4 and Hypoxia Inducible Factor alpha (HIF1-α).

Interestingly, shIMP3 cells did not display any increase of CXCR4 even under hypoxic conditions, an observation that can explain the reduced migration in response to CXCL12 in the context of oxygen deprivation (Figure 6D). Overall, these data suggest that the IGF2BP3/CXCR4 axis guides the migration toward the ligand CXCL12 and that IGF2BP3 represents a putative novel mediator of stress response.

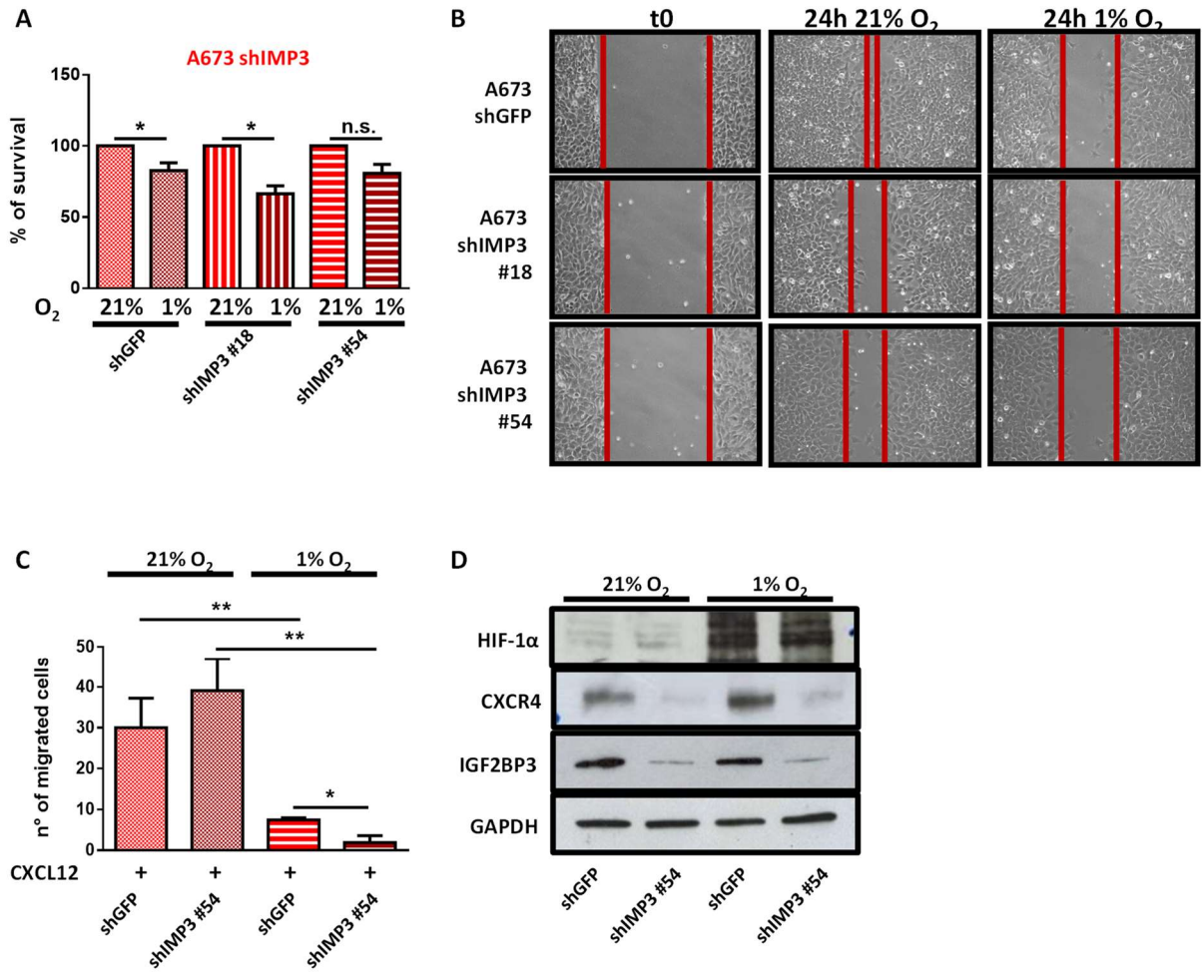

Figure 6. CXCR4 and hypoxia in Ewing Sarcoma

Effects of normoxic (21% O_2) o hypoxic (1% O_2) conditions on shIMP3 or mock-transfected (shGFP) A673 cells. ***(A)*** *Proliferation evaluated via trypan blue count. Bars representative of mean ± SD of at least two independent experiments are shown. * $p<0.05$, n.s. not significant, Student's t-test.* ***(B)*** *Migration evaluated via scratch test. A representative photograph for each condition is shown.* ***(C)*** *Migratory response to a CXCL12 (100 ng/ml) gradient evaluated via transwell analysis. Bars representative of mean ± SD of three independent experiments are shown. * $p < 0.05$, ** $p < 0.01$, Student's t test.* ***(D)*** *Protein evaluation via western blot displaying HIF-1α, CXCR4 and IGF2BP3 expression. GAPDH was used as housekeeping gene or loading control. A representative Western Blot is shown.*

3.2.5 IGF2BP3 REGULATES CD14 LEVELS IN EWING SARCOMA

A direct relationship between IGF2BP3 and CXCR4 has never been reported. Yet IGF2BP3 is known to sustain the expression of CD164, a type 1 integral transmembrane sialomucin involved in regulating adhesion and migration of cancer cells (Samanta et al, 2012; Lederer et al, 2014), which can also act as a functional regulator of CXCR4 in different tumor types (Forde et al, 2007). The role of CD164 in Ewing Sarcoma has never been studied.

The interaction between IGF2BP3 and CD164 had previously been investigated in our laboratory via Ribo-Immunoprecipitation (RIP) assay: *CD164* mRNA appeared to be highly enriched after immunoprecipitation with anti-IGF2BP3 antibody (Mancarella et al, 2020), suggesting that IGF2BP3 might regulate mRNA stability and expression levels of *CD164*. We further pursued this evidence by investigating CD164 protein levels in A673 and TC-71 shIMP3 models. The results showed significantly lower levels of the sialomucin when comparing low-IGF2BP3 expressing cells to the mock-silenced controls and confirmed the concurrent reduced expression of the RBP and CD164 (Figure 7).

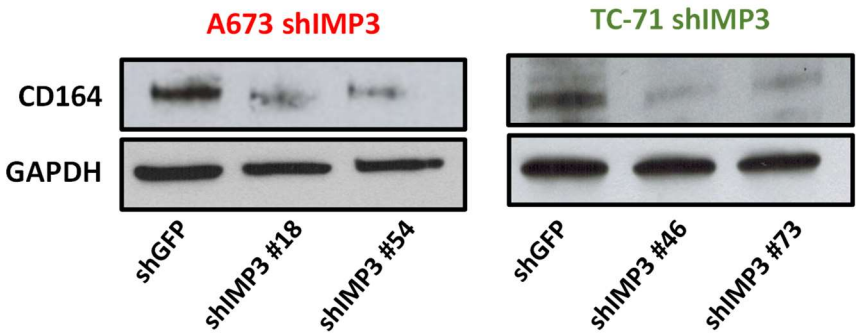

Figure 7. CD164 levels depend on IGF2BP3 expression in Ewing Sarcoma
CD164 expression analyzed via Western Blot in IGF2BP3-depleted or empty vector-transfected (shCTR) A673 and TC-71 cells. GAPDH was used as loading control. Representative Western Blots are shown.

3.2.6 JQ1 TREATMENT REGULATES CD164 LEVELS ACCORDING TO IGF2BP3 DOWNMODULATION IN EWING SARCOMA

JQ1 is a powerful bromodomain and extra-terminal domain inhibitor (BETi) (Filippakopoulos et al, 2010.). Experimental evidence indicates that JQ1 is able to inhibit the expression of IGF2BP3 and its target transcripts in leukemia cells and ES cells (Dawson et al, 2011; Mancarella et al, 2018). Knowing this, the association between the expression of the RBP and CD164 was further assessed after a 48-hour treatment with increasing doses of the drug on TC-71 parental cells.

Interestingly, alongside the significant reduction in *IGF2BP3* mRNA, the treatment results in a significant reduction in the level of *CD164* mRNA in a dose-independent manner (Figure 8).

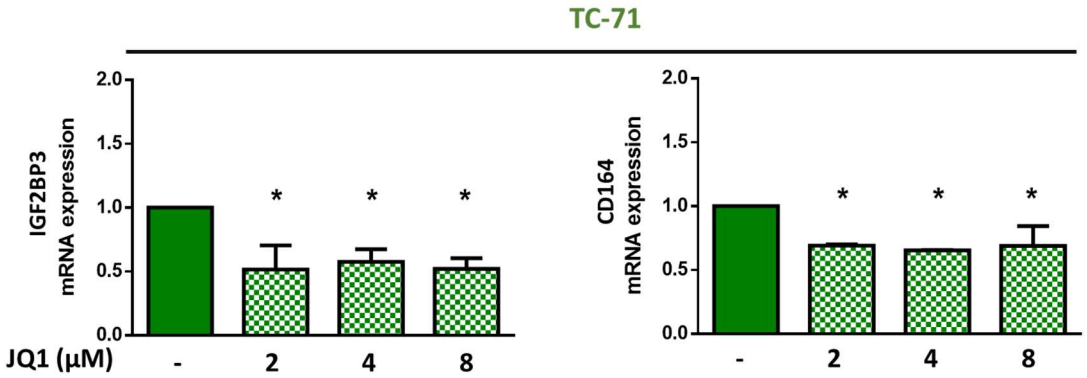

Figure 8. Effect of JQ1 treatment on the IGF2BP3 / CD164 axis
*IGF2BP3 (left) and CD164 (right) levels were evaluated via Real Time-qPCR on TC-71 cells after 48h treatment with increasing doses of JQ1. Data normalization was performed on untreated control. mRNA expression is reported as RQ and bars represent the mean ± SD of at least three independent replicates. * p-value <0.05, one-way ANOVA.*

3.2.7 CD164 AND CXCR4 INTERACTION MEDIATES MIGRATORY RESPONSE TO CXCL12

CD164 and CXCR4 are reported to colocalize at the plasma membrane and to interact in mediating the cellular response to CXCL12. To evaluate whether the functional interaction between CXCR4 and CD164 exists in Ewing Sarcoma cells, we performed confocal microscopy. In absence of CXCL12, both CXCR4 and CD164 resulted equally distributed between cell membrane and cytoplasm while CXCL12 presentation induced a redistribution of both receptors, which then colocalized at plasma membrane level (Figure 9A).

To further confirm the role of the CD164/CXCR4 axis in Ewing Sarcoma cells, CD164 was silenced using siRNAs in A673 and TC-71 cell lines (Figure 9B). The migratory ability towards a CXCL12-gradient of silenced cells compared to controls was then evaluated and CD164 reduction resulted in impaired migratory skills, accordingly to the model proposed (Figure 9C).

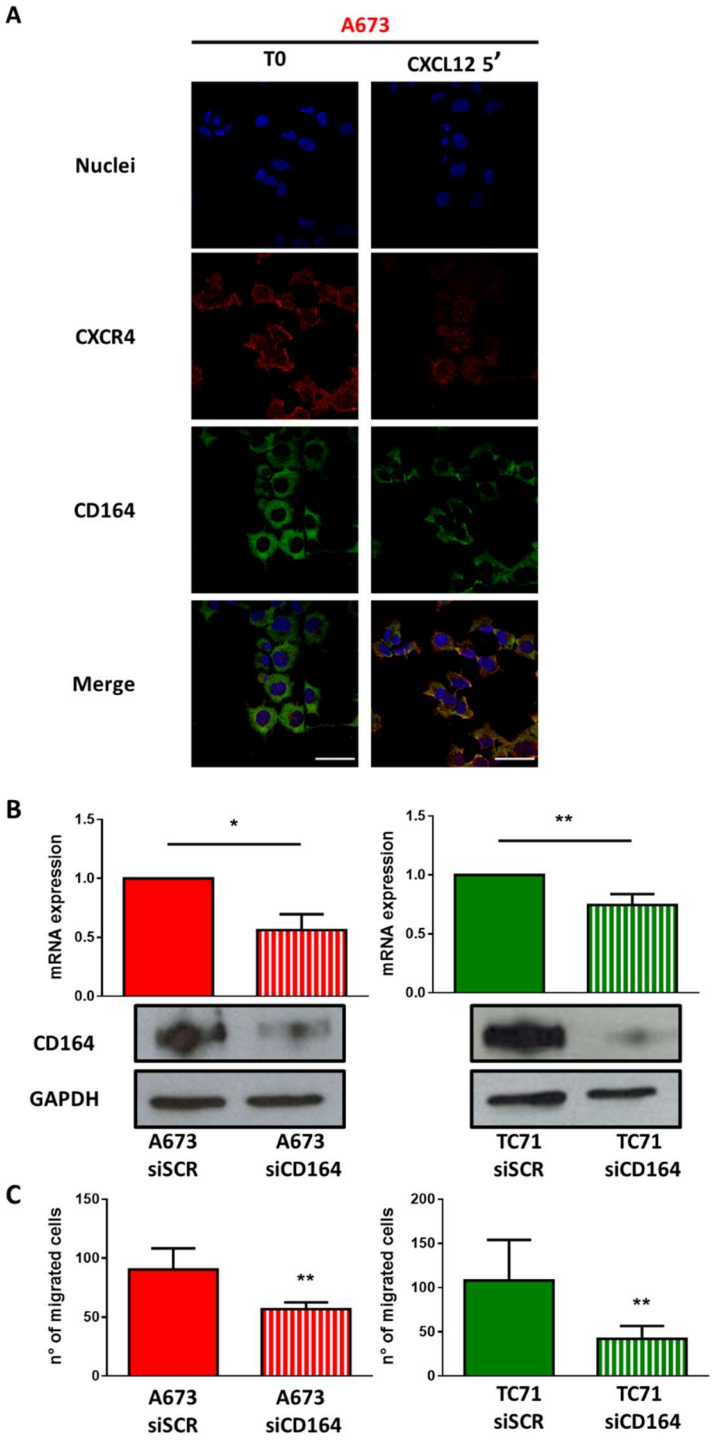

Figure 9. CD164 and CXCR4 interact on plasma membrane and direct cellular response to CXCL12 stimulus
(A) *Colocalization of CD164 and CXCR4 was assessed in A673 cells by immunostaining and confocal microscopy. Cells were stimulated (right column) with CXCL12 100 ng/ml for 5 min or left unstimulated (left column). Images were taken using confocal microscopy (scale bar 25 µm).* ***(B)*** *Real Time-qPCR and Western blotting for CD164 evaluation on A673 and TC-71 cells transfected with siCD164 and in corresponding siSCR mock-silenced controls. was evaluated via Real Time-qPCR and Western Blotting. GAPDH was used as housekeeping gene or loading control. Real Time-qPCR is the mean of at least three independent replicates, relative mRNA expression reported as RQ is shown. A representative Western Blot is shown. * p<005, **p < 0.001, Student's t-test.* ***(C)*** *Migration of A673 and TC-71 cells treated with CD164 siRNA or control scramble siRNA using a CXCL12 (100 ng/ml) gradient. Mean ± SE of at least two independent experiments is shown. **p < 0.001, Student's t-test.*

3.2.8 CLINICAL RELEVANCE OF CD164/CXCR4 IN EWING SARCOMA

The relevance of CD164 and CXCR4 was further evaluated at clinical level. We took advantage of the clinical samples previously used to study IGF2BP3 levels and performed Real Time-qPCR both on primary tumors and metastatic specimens. A significant statistical correlation is present between *IGF2BP3* and *CD164* as well as *CXCR4* both in primary and in metastatic lesions (Figure 10A). Spearman coefficients showed a strong correlation between *CD164* and *CXCR4* in the two groups of samples. No significant difference in both *CD164* and *CXCR4* mRNA levels was highlighted between the two group of samples (Figure 10B).

Nevertheless, the correlation between *CD164/IGF2BP3* and *CXCR4/IGF2BP3* was represented by a higher Spearman coefficient in metastases rather than in primary tumors, thus sustaining the relevance of the proposed IGF2BP3/CD164/CXCR4 axis in metastatic progression in Ewing Sarcoma.

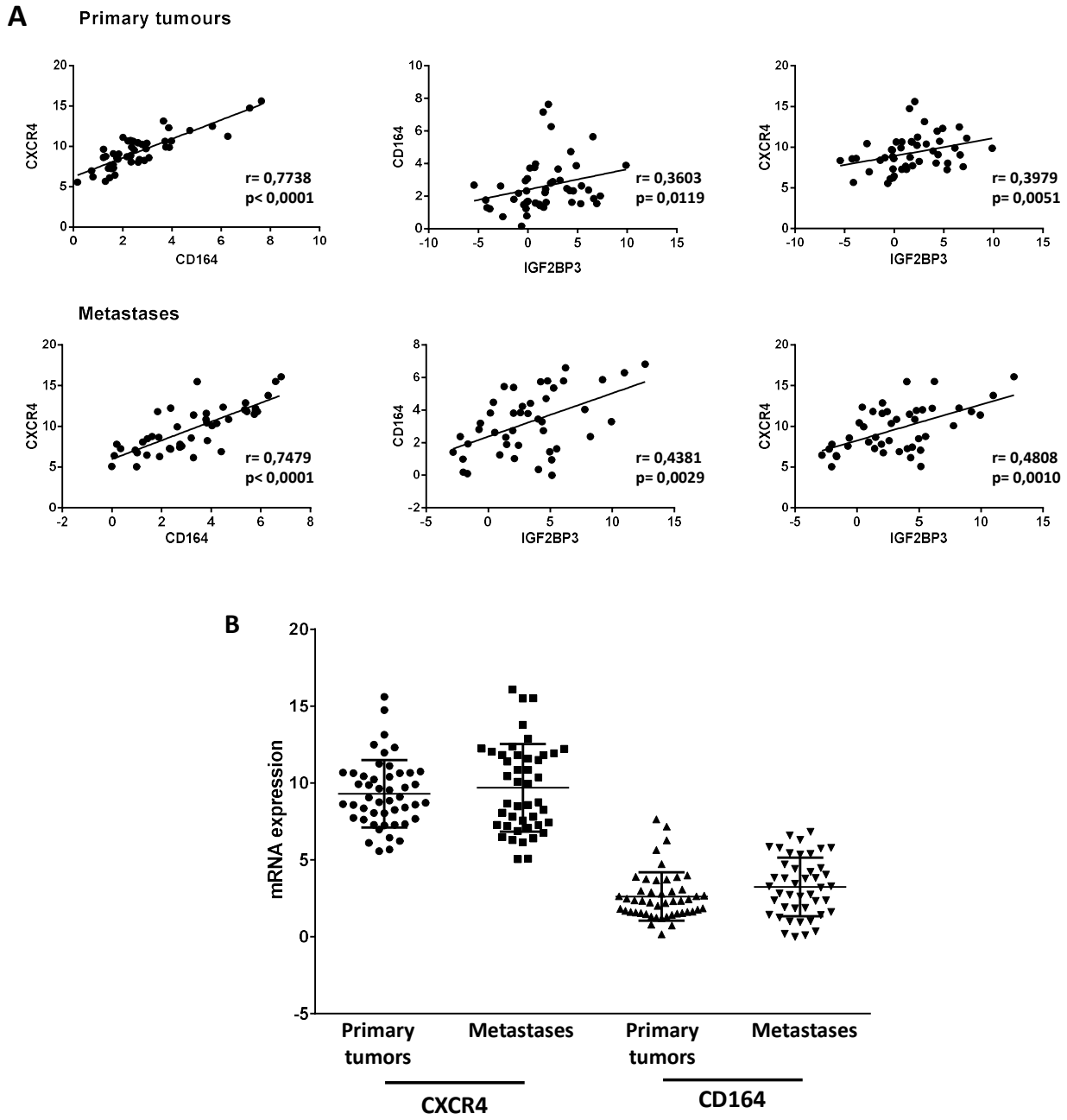

Figure 10. IGF2BP3/CD164/CXCR4 correlation in Ewing Sarcoma patients

Evaluation, in 48 primary Ewing Sarcoma primary tumors and 44 metastatic lesions, of CD164 and CXCR4 mRNA levels via Real Time-qPCR. ***(A)*** *Scatter plots displaying correlations between IGF2BP3, CD164, and CXCR4. Relative mRNA expression reported as -ΔΔCt is shown. Human mesenchymal stem cells were used as calibrator. Correlation coefficient (r) and p-value were calculated using Spearman's rank test.* ***(B)*** *Scatter plot representative of CXCR4 and CD164 mRNA levels. GAPDH was used as housekeeping gene. Mean ± SD of relative mRNA expression reported as -ΔΔCt is shown. Human mesenchymal stem cells were used as calibrator. n.s, not significant. Student's t-test.*

3.3 THE ROLE OF EXTRACELLULAR IGF2BP3 IN EWING SARCOMA

3.3.1 CHARACTERIZATION OF EWING SARCOMA DERIVED EXOSOMES

Exosomes are small extracellular vesicles physiologically produced by many cell types. Horizontal transfer of key molecules entrapped in exosomal cargo mediates intercellular communication, both between cancer cells themselves and between the tumor and the surrounding microenvironment, and leads to regulation of physiological and pathological processes in receiving cells (Wortzel et al, 2019). To date, no information is available about a role for IGF2BP3 in exosome-mediated communication, yet the ability of RNA Binding Proteins to form RBP-RNA complexes has been described as one of the mechanisms facilitating RNA loading into exosomes. (Statello et al, 2018).

We decided to evaluate whether IGF2BP3 could be loaded into Ewing Sarcoma derived exosomes and, preliminary to every further experiment, we proceeded to properly characterize the extracellular vesicles. To do so, we followed the indications reported on the "Minimal Information for Studies of Extracellular Vesicles ("MISEV") guidelines" (Théry et al, 2018).

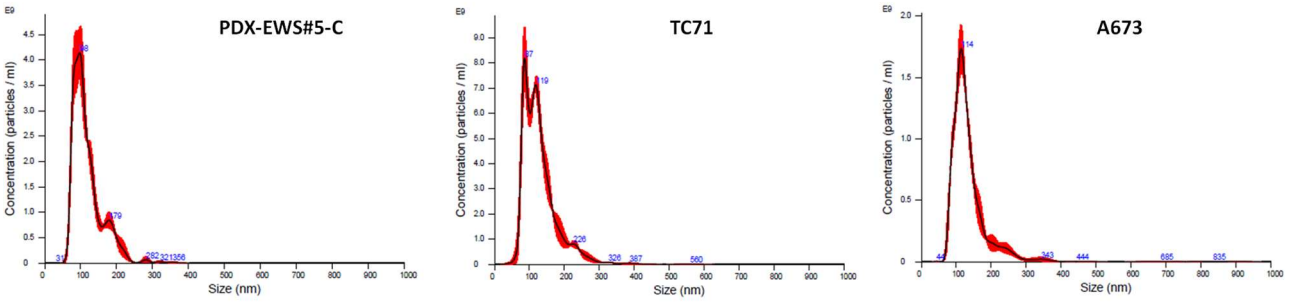

Figure 11. Characterization of Ewing Sarcoma derived exosomes

Representative graphs from NanoSight™ analysis displaying the distribution in terms of size (nm, x-axis) and concentration (particles/ml, y-axis) of exosomes isolated from PDX-EWS #5-C, TC-71 and A673 cell lines.

We started by taking advantage of different cellular models with differential levels of IGF2BP3 and assessed extracellular vesicles' size and concentration via NanoSight analysis (Figure 11), together with total protein yield (Table 2). We observed that all cell lines produced exosomes of around 130-150 nm of diameter, which is consistent with exosomal size. Modest size differences could be observed, as they range from the approximately 118 nm of PDX-EWS#2-C derived exosomes to the 187 nm of PDX-EWS#5-C gIMP3 4C3 derived ones.

Overall, shIMP3 or gIMP3 derived exosomes present higher diameters when compared to corresponding control cells, but this observation wasn't recapitulated in PDX-EWS#2-C derived exosomes. TC-71 cells, independently on their IGF2BP3 content, produced more exosomes (approximately 6 x 10^{11}) in comparison to other cell lines (ranging from 0.765 x 10^{11} to 2,750 x 10^{11}), but no significant differences associated to IGF2BP3 expression were observed. The evaluation of total exosomal protein content, used as an indirect quantification of exosomes, didn't highlight any significant difference between exosomes derived from different cell lines.

We performed Western Blotting to evaluate the presence of exosomal protein markers in our vesicles' preparations. The Endoplasmic Reticulum marker Calnexin was detectable only in cell lysates, confirming the endosomal origin of the extracellular vesicles. Moreover, classical exosomal markers such as HSP90, ALIX and TSG101 were enriched only in vesicles' preparations (Figure 12).

Cell line	Mean Exosomes' size (nm)	Exosomes' concentration (10^{11} particles/ml)	Total protein amount (µg)
A673	134.5 ± 4.2	1.150 ± 0.0333	2201.6 ± 296.4
A673 shGFP	116.8 ± 3.1	1.520 ± 0.0922	2267.2 ± 270.7
A673 shIMP3 #18	155.0 ± 2.6	1.500 ± 0.0410	2098.7 ± 275.4
A673 shIMP3 #54	148.5 ± 3.2	0.765 ± 0.0476	1957.9 ± 364.5
TC-71	128.8 ± 3.6	6.330 ± 0.0 168	2318.7 ± 264.6
TC-71 shGFP	126.2 ± 0.8	6.950 ± 0.0309	2079.2 ± 242.3
TC-71 shIMP3 #46	137.0 ± 3.2	5.720 ± 0.0362	2284.1 ± 304.8
TC-71 shIMP3 #73	135.6 ± 3.7	5.890 ± 0.5960	2376.9 ± 298.1
PDX-EWS#2-C	117.9 ± 1.8	2.750 ± 0.0843	1894.8 ± 291.2
PDX-EWS #5-C	146.5 ± 5.5	0.8650 ± 0.02619	2507.2 ± 185.9
PDX-EWS #5-C gSCR	149.1 ± 2.9	1.160 ± 0.0436	2650.1 ± 747.5
PDX-EWS #5-C gIMP3 3C1	177.6 ± 2.3	1.040 ± 0.0811	2909.7 ± 843.2
PDX-EWS #5-C gIMP3 4C3	186.8 ± 3.8	1.160 ± 0.0301	1687.1 ± 363.4

Table 2. Evaluation of exosomal characteristics.

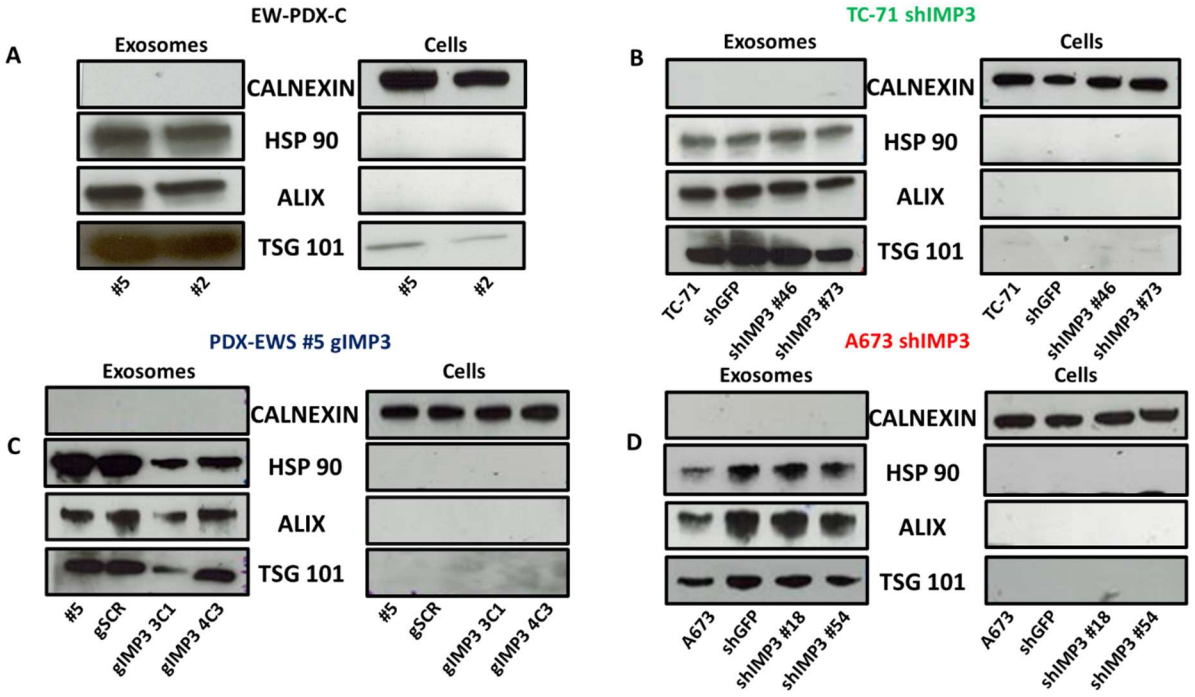

Figure 12. Exosomal markers in Ewing Sarcoma derived exosomes

Evaluation of Calnexin, HSP90 α/β, ALIX and TSG101 in exosomal preparations and corresponding cell lines. A representative Western Blot is shown for each model (PDX-EWS #2-C, PDX-EWS #-C gIMP3, TC-71 shIMP3 and A673 shIMP3).

3.3.2 IGF2BP3 IS RELEASED BY EWING SARCOMA CELLS

IGF2BP3 has been found to be released both in renal carcinoma and pancreatic cancer (Szarvas et al, 2014; Tschirdewahn et al, 2019) but no evidence is yet available about a possible secretion of IGF2BP3 in Ewing Sarcoma. Based on this information, PDX-EWS cell lines with differential expression of IGF2BP3, together with TC-71 shIMP3 and A673 shIMP3 models, and performed an ELISA test. We observed that IGF2BP3 is indeed heterogeneously released by Ewing Sarcoma cells in culture medium but the levels of secreted IGF2BP3 are not consistent with the cellular ones. Interestingly, the same test was conducted also on culture supernatants from the PDX-EWS#5-C gIMP3 model and we observed no IGF2BP3 release from gIMP3 cells, which is consistent with their knockout origin (data not shown).

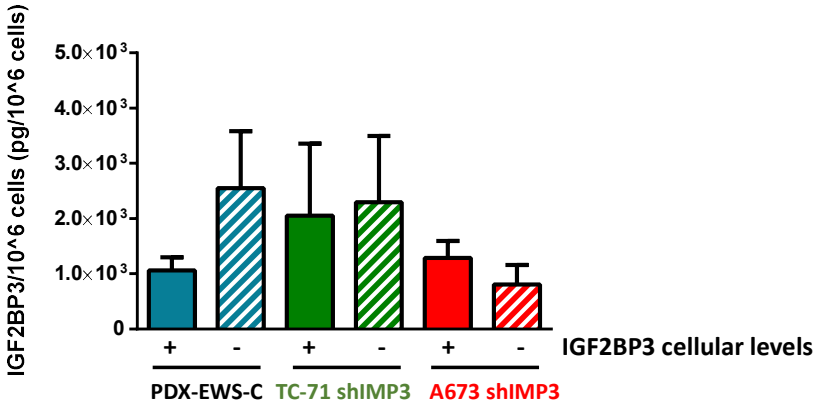

Figure 13. IGF2BP3 is secreted by Ewing Sarcoma cells
ELISA test performed on cell supernatants from a panel of Ewing Sarcoma cells. Bars representative of IGF2BP3 concentration/10^6 cells. The mean ± SD of two independent experiments is shown.

3.3.3 SECRETED IGF2BP3 IS ENCAPSULATED IN EXOSOMES

Exosomes play a major role in mediating the transfer of key molecules between cells, thus we hypothesized that secreted IGF2BP3 could be encapsulated in exosomes. IGF2BP3 protein levels were assessed in PDX-EWS cell lines and TC-71 shIMP3 model, together with PDX-EWS #5 gIMP3 and A673 shIMP3 models. In contrast with the results obtained when evaluating the total release of the RBP, we observed that IGF2BP3 was present in exosomes derived from IGF2BP3+ cell lines but was absent or heavily down-modulated in exosomes derived from cells lacking for the RBP (Figure 14A). We also evaluated *IGF2BP3* mRNA levels in PDX-EWS cell lines, TC-71 shIMP3 and A673 shIMP3 models, observing that also *IGF2BP3* mRNA is differentially loaded between exosomes derived from PDX-EWS#2-C and shIMP3 cells, with relative controls (Figure14B). Since PDX-EWS #5 gIMP3 cells present IGF2BP3- knockout, we investigated only the presence of IGF2BP3 protein in this model. We therefore determined that IGF2BP3 is loaded into exosomes both at protein and mRNA level, accordingly to the cellular levels of the RBP. We further hypothesized a prominent role for exosomal IGF2BP3, rather than total released IGF2BP3, in the intercellular communication between Ewing Sarcoma cells.

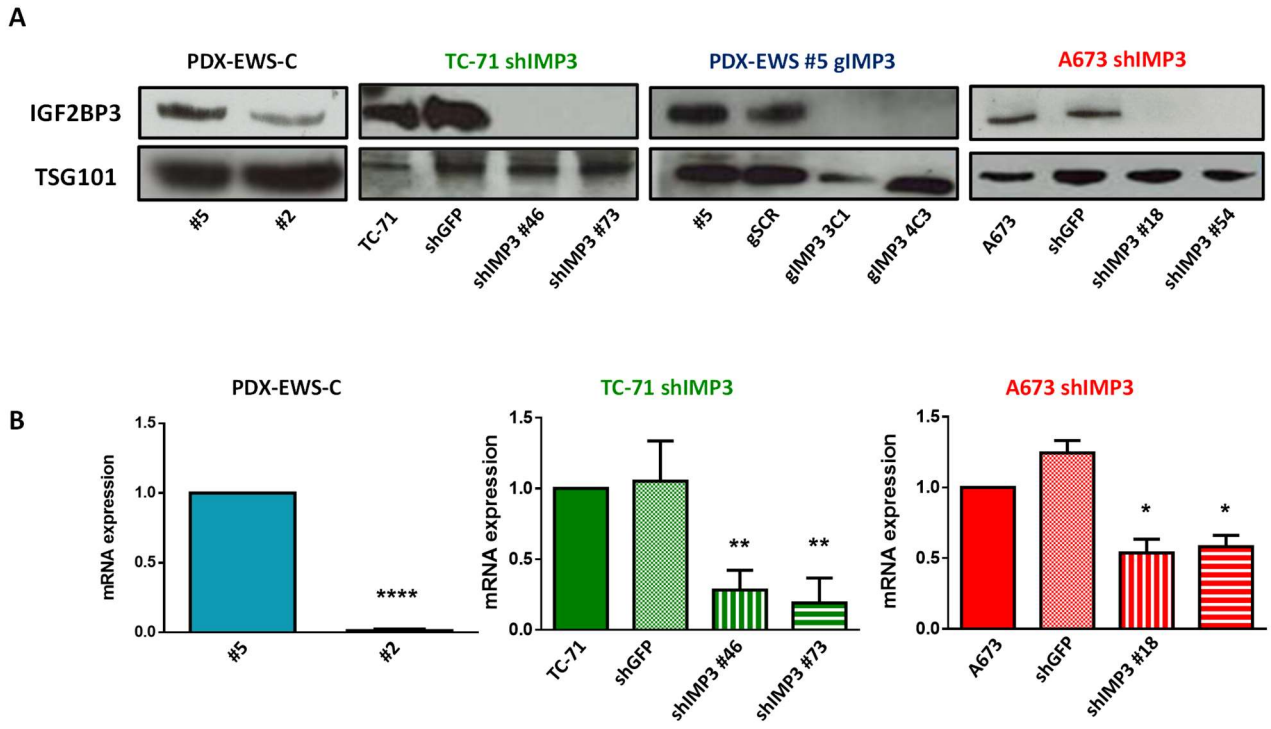

Figure 14. IGF2BP3 is loaded into exosomes released by Ewing Sarcoma cells
IGF2BP3 levels were evaluated via Western Blot ***(A)*** *and Real Time-qPCR* ***(B)*** *in exosomes (precipitated via (U) for Western Blotting and via (EQ) for Real Time-qPCR) released by Ewing Sarcoma cell lines and corresponding IGF2BP3-deprived cells (PDX-EWS cell lines, PDX-EWS #-C gIMP3, TC-71 shIMP3 and A673 shIMP3). Data normalization was performed on exosomes from the parental cell lines. Relative mRNA expression reported as RQ is shown. The mean ± SD of two independent experiments is shown. GAPDH was used as housekeeping gene. * p-value <0.05, ** p-value <0.01, one-way ANOVA. TSG 101 was used as loading control. A representative Western Blot is shown for each model.*

3.3.4 UPTAKE OF IGF2BP3 EXOSOMES DOESN'T AFFECT CELLULAR PROLIFERATION

In order to proceed with the characterization of the phenotypical effects of IGF2BP3+/- exosomes on receiving Ewing Sarcoma cells, we verified their cellular uptake by labeling exosomes with the fluorescent dye PKH67 (Figure 15A). Interestingly, PDX-EWS#5-C TC-71 cells exposed to and incorporating IGF2BP3+ exosomes displayed no difference in cell proliferation when compared to cells receiving IGF2BP3- exosomes derived from PDX-EWS#2-C cells. This observation was further sustained in TC-71 cells receiving exosomes from TC-71 shIMP3 model: no differences were observed in cell growth (Figure 15B).

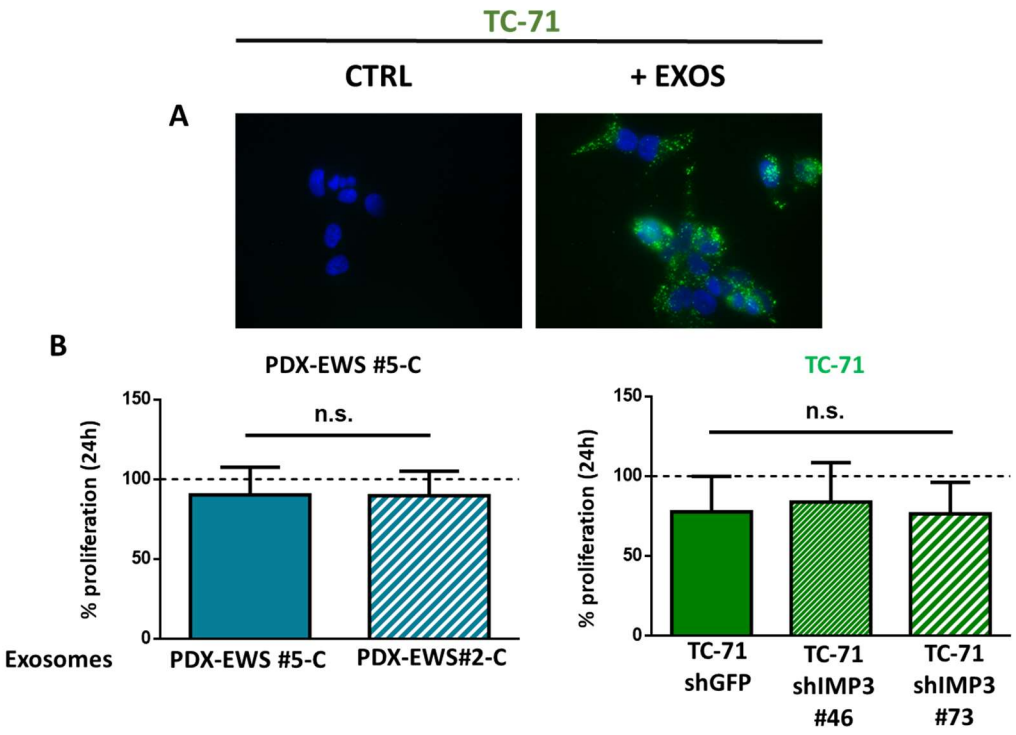

Figure 15. Exosomal uptake and cell proliferation
(A) *Fluorescent microscopy image of exosome uptake by TC-71 cells treated with IGF2BP3+ exosomes (EQ). Internalized vesicles, labeled with PKH67, were evidenced as a green fluorescent signal inside recipient cells. Scale bar: 50 µm.* ***(B)*** *Evaluation by MTT assay of cell proliferation after administration of IGF2BP3+ or IGF2BP3- exosomes (EQ) in PDX-EWS #5-C or TC-71 cell line. The mean ± SE of two independent experiments is shown. n.s., not significant.*

3.3.5 EXOSOMAL IGF2BP3 SHUTTLES CLIENT mRNAs INVOLVED WITH CELLULAR MIGRATION INTO RECEIVING CELLS

IGF2BP3 is an RNA binding protein exerting its oncogenic role by directly binding client mRNAs, which can be protected from degradation and overexpressed in tumoral cells. *CD164* and *IGF1R* are two IGF2BP3-client mRNAs whose expression plays a prominent effect on migratory properties of Ewing Sarcoma cells expressing IGF2BP3 (Mancarella et al, 2018; Mancarella et al, 2020). Via Real Time qPCR, we evaluated the cargo of PDX-EWS#5-C and PDX-EWS#2-C exosomes to assess the levels of these mRNAs. Both *CD164* and *IGF1R* appeared to be loaded and upregulated in exosomes derived from IMP3pos PDX-EWS#5-C cell line. This observation was further sustained when *CD164* and *IGF1R* levels were evaluated in exosomes derived from TC-71 shIMP3 cells (Figure 16A, B). Interestingly, we also observed a decrease in *CXCR4* mRNA levels, which was more prominent in PDX-EWS#2-C *vs* PDX-EWS#5-C derived exosomes rather than in the TC-71 shIMP3 model (Figure 16C). The levels of these mRNAs were assessed also in exosomes derived by PDX-EWS #5 gIMP3 cells (Figure 16A, B, C).

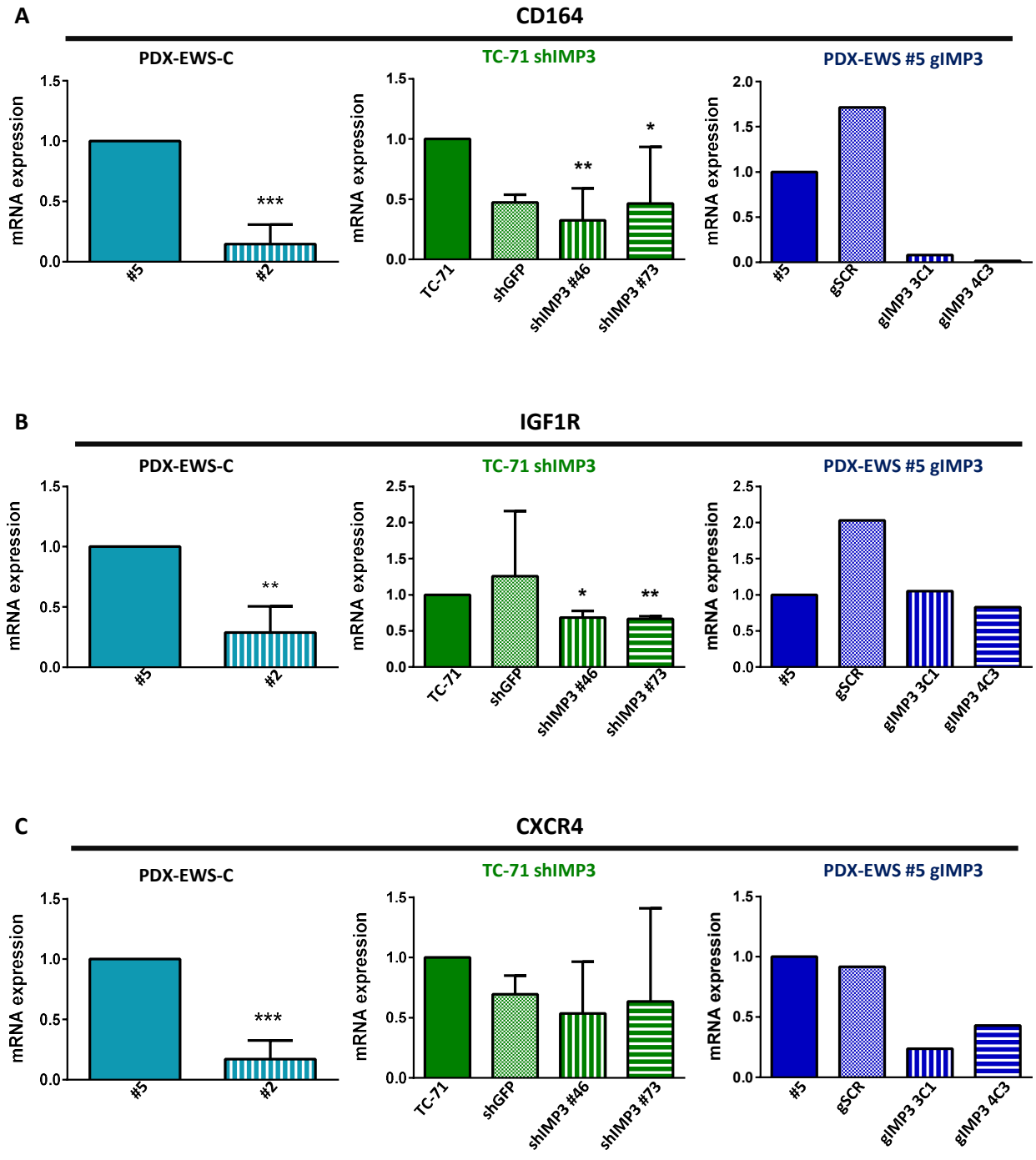

Figure 16. IGF2BP3 shuttles client mRNAs into exosomal cargo

Real Time-qPCR evaluation of CD164 ***(A)****, IGF1R* ***(B)*** *and CXCR4* ***(C)*** *levels in the cargo of exosomes (EQ) released by PDX-EWS cell lines, TC-71 shIMP3 and PDX-EWS #-C gIMP3. Data normalization was performed on exosomes from the parental cell lines. Relative mRNA expression reported as RQ is shown. The mean ± SD of two independent experiments is shown. GAPDH was used as housekeeping gene. For PDX-EWS cell lines and TC-71 shIMP3 derived exosomes, the mean ± SE of two independent experiments is shown. * p-value <0.05, ** p<0.01, *** p<0.001, Student's t-test vs parental control. For PDX-EWS #5 gIMP3 exosomes, a single representative experiment is shown.*

Unfortunately, only a trend consistent with what we observed in the other models is present and this can be ascribed to the small amount of RNA contained into exosomes, which represents a major challenge in terms of RNA extraction and purity. For the same reason, mRNA content of A673 shIMP3 derived exosomes couldn't be effectively explored.

To evaluate whether IGF2BP3-client mRNAs are transferred into receiving cells upon exosomal administration, we treated the parental TC-71 cell line with Actinomycin D, which blocked endogenous transcription, significantly reducing *CD164* and *IGF1R* cellular mRNA levels. Treated cells were then fused with the corresponding IGF2BP3+ exosomes for another hour: we observed that *CD164* and *IGF1R* mRNA levels were partially restored, confirming the transfer of both exosomal mRNAs into receiving cells (Figure 17).

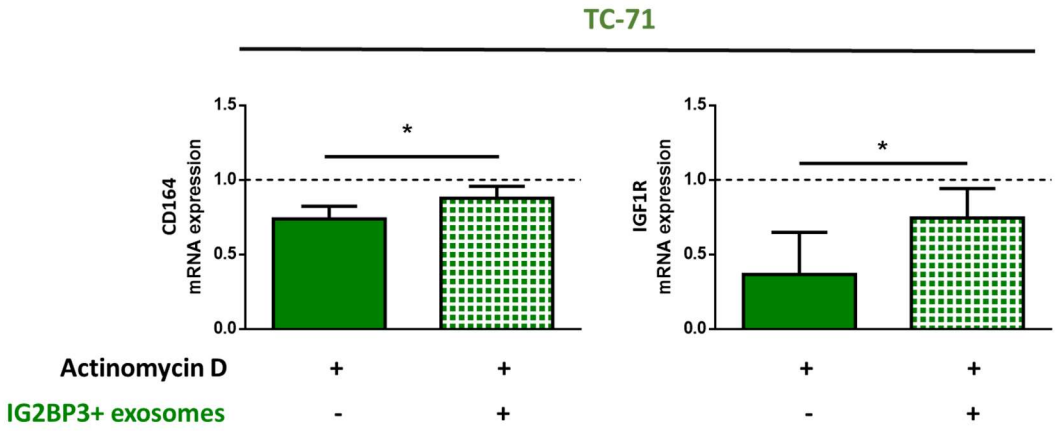

Figure 17. IGF2BP3-client mRNAs are transferred into receiving cells
*Real Time-qPCR evaluation of CD164 (left) and IGF1R (right) in TC-71 cells receiving IGF2BP3+ exosomes ((EQ), from TC-71 cell line) after 1 hour treatment with 5 μg/ml Actinomycin D. Data normalization was performed on exosomes from the parental cell lines. Relative mRNA expression reported as RQ is shown. The mean ± SD of two independent experiments is shown. GAPDH was used as housekeeping gene. * p-value <0.05, Student's t test.*

3.3.6 EXOSOMAL IGF2BP3 INFLUENCES THE MIGRATION OF RECEIVING EWING SARCOMA CELLS

IGF2BP3 reportedly exerts its pro-tumorigenic role in Ewing Sarcoma by favoring cell migration and metastatization, thus we wanted to assess whether exosomal transfer of IGF2BP3 could be one of the mechanisms through which this phenotype is achieved. We performed a wound healing assay on TC-71 cells after the administration of exosomes derived from IGF2BP3+ or IGF2BP3- cell lines from TC-71 shIMP3 model. We observed that IGF2BP3+ exosomes sustained the migratory phenotype of the cells while it appeared to be impaired in cells receiving the IGF2BP3- ones.

Further sustaining that this effect was ascribable to exosomes, we also performed this test after the administration of complete or exosome-deprived culture medium derived from IGF2BP3+ or IGF2BP3- cell lines from TC-71 shIMP3 model. The administration of complete supernatants reflected what was observed after exosomal administration, whereas the migration of cells receiving exosome-deprived supernatants was totally impaired (Figure 18).

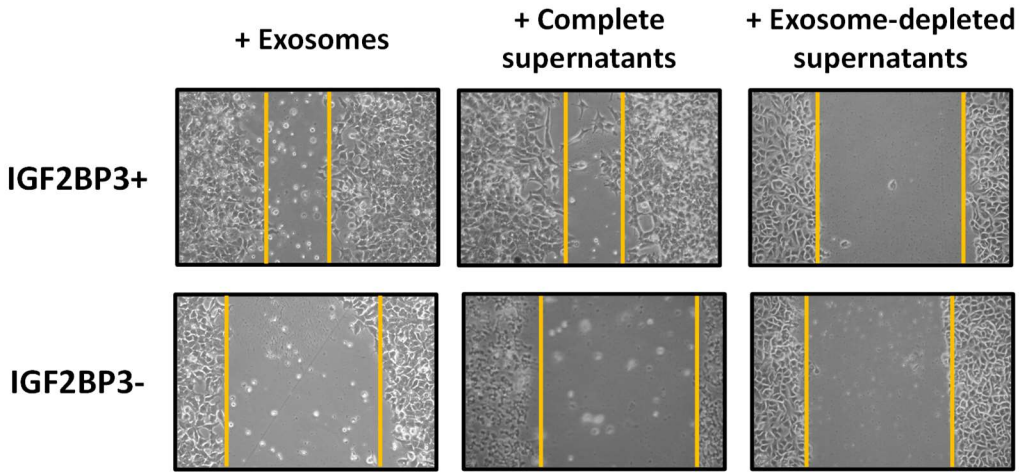

Figure 18. Exosomal IGF2BP3 mediates migratory response in Ewing Sarcoma
Scratch test on TC-71 cells receiving exosomes, complete supernatants or exosome-depleted supernatants from TC-71 shIMP3 model. A representative image is shown for every condition.

3.3.7 EXOSOMAL IGF2BP3 SUSTAINS MIGRATORY RESPONSE TO CXCL12 VIA CD164/CXCR4 AXIS IN EWING SARCOMA CELLS

We already described (Paragraphs 2.4, 2.7) the role played by IGF2BP3 in regulating Ewing Sarcoma aggressiveness in terms of cellular migration and metastatic potential in response to CXCL12. Thus, we wanted to assess whether exosomal IGF2BP3 could contribute to this phenotype.

Hence, we performed transwell migration assay on PDX-EWS#5-C cell line in presence of CXCL12 upon fusion with PDX-EWS#5-C and PDX-EWS#2-C derived exosomes and observed that cells receiving IGF2BP3+ exosomes migrated at higher rates when compared to those receiving IGF2BP3- exosomes. This observation was further sustained in TC-71 cells fused with exosomes derived from parental or shIMP3 models: exosomes from IGF2BP3+ cells fostered migration of TC-71 cells whereas IGF2BP3- did not (Figure 19A).

Migratory response to CXCL12 is mediated by the receptor CXCR4, thanks to its interaction with CD164, a direct IGF2BP3 client, at plasma membrane level. We previously demonstrated that *CD164* mRNA is present in exosomal cargo, depending on IGF2BP3 levels, and is transferred into receiving cells upon exosomal fusion.

We performed Western Blot analysis on exosomes-receiving cells and observed that the expression of CD164 was higher in cells fused with IGF2BP3+ exosomes, derived from both PDX-EWS and TC-71 shIMP3 models, when compared to cells receiving IGF2BP3- exosomes. Interestingly, CXCR4 levels also appeared to be equally modulated upon exosomal exposure (Figure 19B).

To further sustain that the transferring of exosomal *CD164* is responsible for the differential migratory phenotype observed, we treated TC-71 shIMP3 cells with exosomes from parental TC-71 cells and observed that receiving cells displayed increased levels of CD164. A moderate increase was observed also when evaluating CXCR4 levels (Figure 19C).

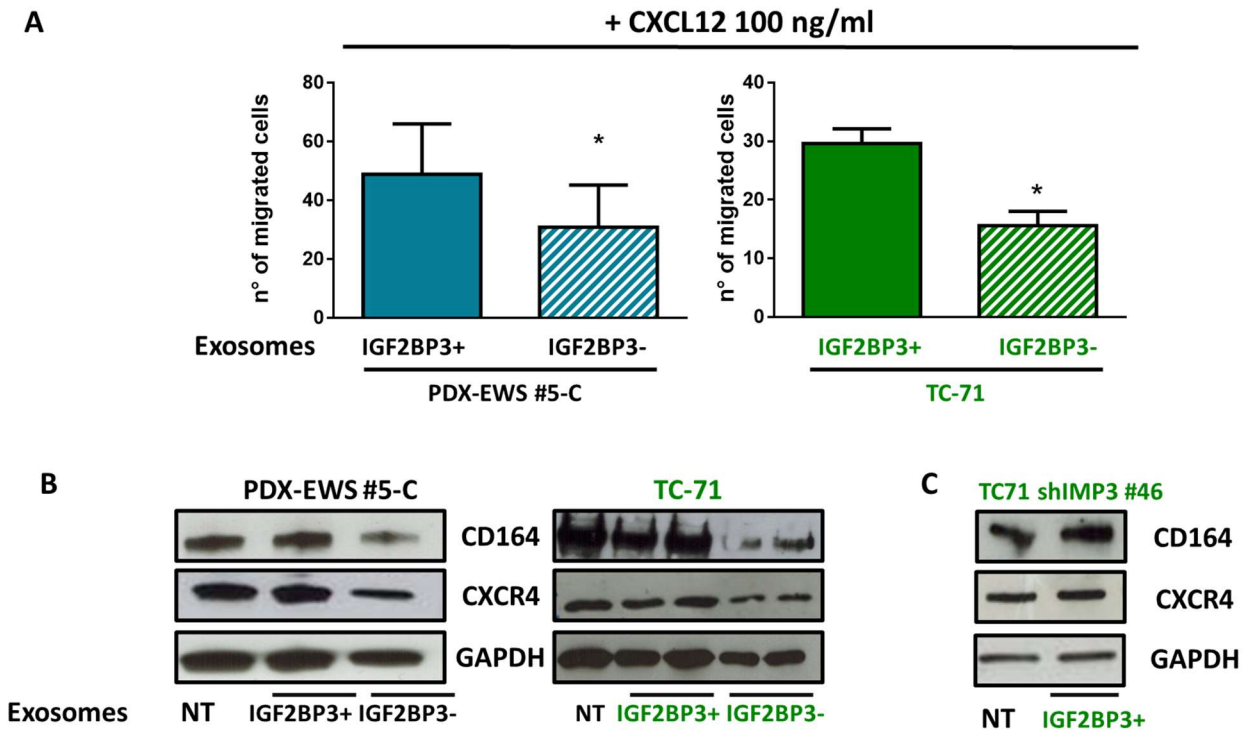

Figure 19. Exosomal IGF2BP3 mediates migratory response to CXCL12

(A) *Migration of Ewing Sarcoma cells fused with IGF2BP3+ or IGF2BP3- exosomes (EQ) using a CXCL12 (100 ng/ml) gradient. Bars representative of mean ± SD of at least two independent experiments are shown. *p < 0.05, Student's t-test.* ***(B)*** *CD164 and CXCR4 expression evaluated via Western Blotting in PDX-EWS #5-C and TC-71 cells receiving IGF2BP3+ or IGF2BP3- exosomes (EQ) or* ***(C)*** *in TC-71 shIMP3 #46 receiving IGF2BP3+ exosomes (EQ) from TC-71 parental cells. GAPDH was used as loading control. A representative Western Blot is shown.*

3.3.8 IG2BP3+ EXOSOMES INDUCE SIGNALING PATHWAY ACTIVATION IN RECEIVING EWING SARCOMA CELLS

The signaling pathways triggered by binding of CXCL12 to CXCR4 are multiple and include both the mitogen-activated protein kinases (MAPK) pathway and the phosphatidylinositol 3-kinase (PI3K) pathway (Ganju et al, 1998; Gassmann et al, 2009).

We investigated these pathways via Western blotting analysis performed on PDX-EWS#5-C and TC-71 cells receiving exosomes. We observed that cells fused with IGF2BP3+ exosomes presented higher levels of both total and phosphorylated forms of ERK when compared to cells receiving IGF2BP3- exosomes (Figure 20A). Moreover, TC-71 shIMP3 cells receiving parental TC-71 IGF2BP3+ exosomes displayed an increase in ERK levels, accompanied by an increase in its phosphorylation (Figure 20B). Interestingly, we also observed an increased activation of both AKT and mTOR in PDX-EWS#5-C and TC-71 cells fused with IGF2BP3+ exosomes (Figure 20C). TC-71 shIMP3 cells receiving TC-71 IGF2BP3+ exosomes present a modest increase in AKT phosphorylation (Figure 20D). These data suggest that exosomes, depending on their IGF2BP3 levels, can prominently mediate the activation of the MAPK signaling pathway, thus sustaining cellular response to CXCL12 signaling.

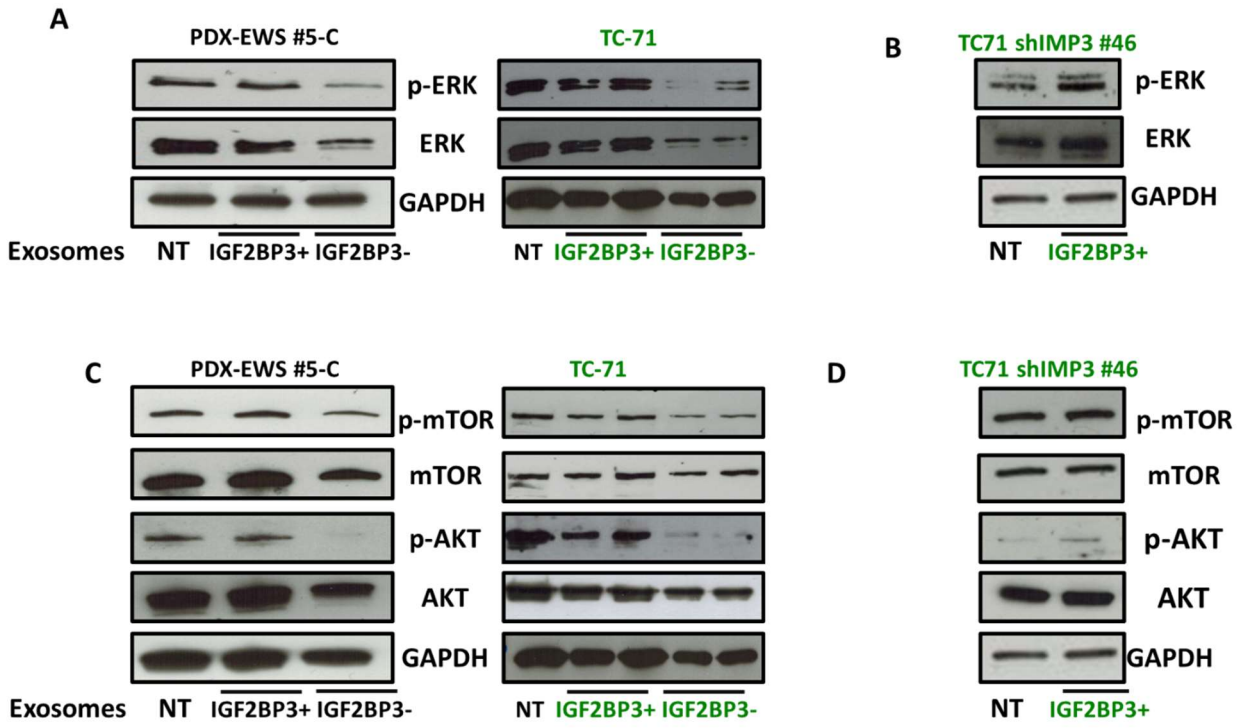

Figure 20. Cellular response to exosomal administration
Western blotting showing ERK and AKT/mTOR activation in PDX-EWS#5-C and TC-71 cells receiving IGF2BP3+ or IGF2BP3- exosomes (EQ) ***(A, C)*** *or in IGF2BP3-depleted cells (TC-71 shIMP3 #46) receiving only IGF2BP3+ exosomes (EQ)* ***(B, D)****. GAPDH was used as loading control. A representative Western Blot is shown.*

3.3.9 EXOSOMAL IGF2BP3 INFLUENCES EWING SARCOMA MIGRATORY RESPONSE TO IGF1

In Ewing Sarcoma IGF2BP3 acts on the IGF system by stabilizing the IGF1R transcript, modulating the response of cells to the IGF1 ligand, measured in terms of cell migration and growth (Mancarella et al, 2018). Thus, we performed transwell migration assay on PDX-EWS#5-C and TC-71 cell lines in presence of IGF1 gradient after fusion with IGF2BP3+ or IGF2BP3- exosomes. We observed that cells receiving IGF2BP3+ exosomes migrated at higher rates when compared to those receiving IGF2BP3- exosomes (Figure 21A) and expressed IGF1R at higher levels (Figure 21B). Transferring of exosomal *IGF1R* can be held accountable for the differential phenotype observed, as TC-71 IGF2BP3-deprived cells fused with parental TC-71 IGF2BP3+ exosomes displayed and increase in cellular IGF1R levels (Figure 21C).

Activation of IGF1R receptor upon ligand binding reportedly activates downstream signaling pathways including the MAPK and the PI3K pathways (Fruman et al, 2017; Liu et al, 2018). Interestingly, we have already demonstrated that exposure to IGF2BP3+ exosomes induce the activation of both these signaling pathways (Figure 20).

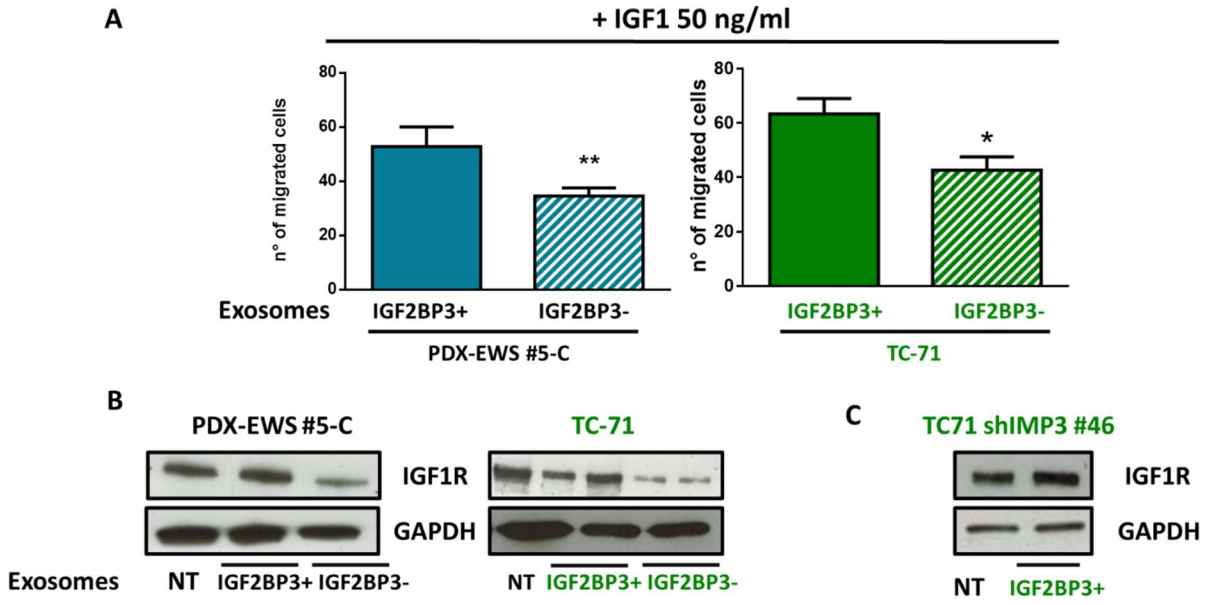

Figure 21. Exosomal influence on IGF1/IGF1R axis in Ewing Sarcoma

*(A) Migration of Ewing Sarcoma cells treated with IGF2BP3+ or IGF2BP3- exosomes (EQ) using a IGF1 (50 ng/ml) gradient. Bars representative of mean ± SE of at least two independent experiments are shown. * $p < 0.05$, ** $p<0.01$, Student's t-test.* ***(B)*** *IGF1R expression evaluated via Western Blotting in PDX-EWS #5-C and TC-71 cells receiving IGF2BP3+ or IGF2BP3- exosomes (EQ) or in* ***(C)*** *IGF2BP3-depleted cells (TC-71 shIMP3 #46) receiving only IGF2BP3+ exosomes (EQ). GAPDH was used as loading control. A representative Western Blot is shown.*

3.3.10 EXOSOMAL IGF2BP3 SUSTAINS EWING SARCOMA CELL MIGRATION INDEPENDENTLY ON THE MODEL OF ORIGIN

We wanted to confirm that the observed phenotype was not dependent on the model of origin of the exosomes used for the experiment. To do so, we took advantage of exosomes derived from PDX-EWS #5 gIMP3 cells. We performed a scratch test on TC-71 cell line and administered IGF2BP3+ or IGF2BP3- exosomes derived from PDX-EWS#5 gIMP3 model. We observed that wound closure was quicker in cells receiving IGF2BP+ exosomes (Figure 22A). Since migration of Ewing Sarcoma cells didn't appear to be influenced by the origin of the administered exosomes but only by their IGF2BP3 cargo, we repeated transwell migration assay in presence of CXCL12 or IGF1 gradients after fusing TC-71 cells with PDX-EWS #5 gIMP3 derived exosomes and confirmed that cells receiving IGF2BP3+ heterologous exosomes migrated at higher rates when compared to those receiving IGF2BP3- exosomes (Figure 22 B).

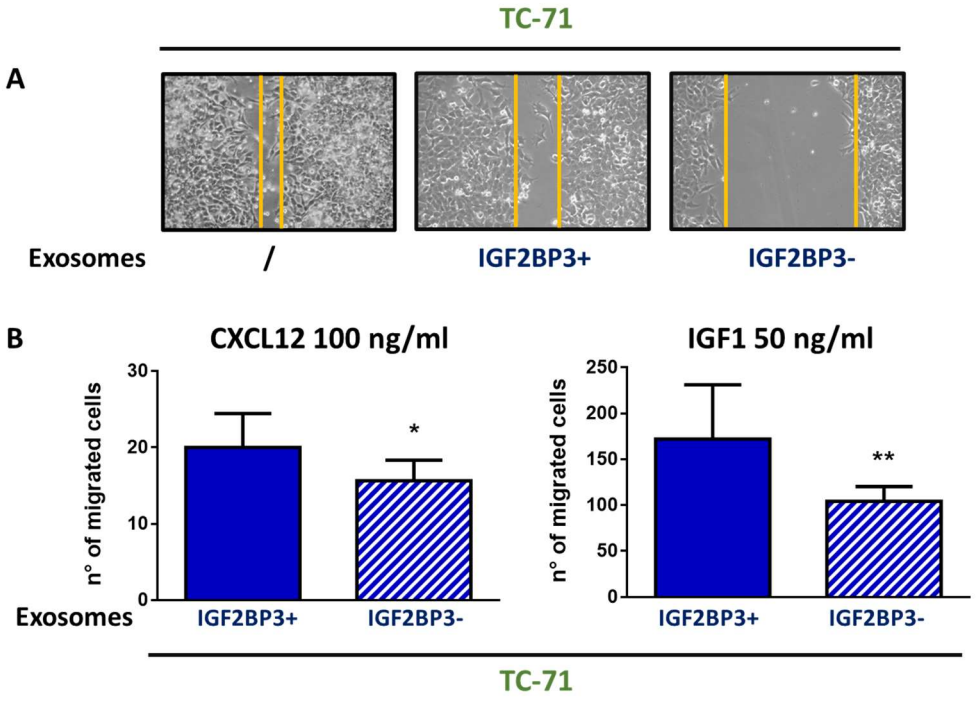

Figure 22. Effect of heterologous exosomes administration on Ewing Sarcoma cells

(A) *Scratch test on TC-71 cells receiving exosomes (EQ) from PDX-EWS #5 gIMP3 model. A representative image is shown for every condition (scale bar).* ***(B)*** *Migration of Ewing Sarcoma TC-71 cells treated with IGF2BP3+ or IGF2BP3- exosomes (EQ) from PDX-EWS #5-C gSCR model using a CXCL12 (100 ng/ml, left) or an IGF1 (50 ng/ml, right) gradient. Mean ± SE of at least two independent experiments is shown. *p < 0.05, ** p<0.01, Student's t-test.*

3.3.11 CHARACTERIZING miRNA CONTENT OF IGF2BP3+/- EXOSOMES

MicroRNAs (miRNAs) are small non-coding RNAs involved in regulating gene expression and highly enriched in exosomal cargo (Yu et al, 2016).

In an attempt to better characterize the cargo of our IGF2BP3+ and IGF2BP3- exosomes, to further clarify their role in sustaining Ewing Sarcoma aggressiveness, we decided to perform miRNA sequencing on exosomes derived from TC-71 and A673 shIMP3 models.

We identified 105 Differentially Expressed (DE) miRNAs between IGF2BP3- and IGF2BP3+ exosomes in TC-71 shIMP3 model; out of them, 61 resulted upregulated while 44 were downregulated (logFC > |0.5|, *p*-value < 0.05). In the A673 shIMP3 model, 150 miRNAs were DE between IGF2BP3- vs IGF2BP3+ exosomes, 92 of which were upregulated and 58 downregulated (logFC > |0.5| and *p*-value <0.05). When comparing the DE miRNAs in the two aforementioned models, we identified a group of 13 common miRNAs (10 upregulated and 3 downregulated (Table 3 and 4). Taking advantage of the miRNA-target prediction tool miRabel, we observed that among them, hsa-miR-218-5p is predicted *in silico* to target IGF1R. Further studies are ongoing in order to properly evaluate the putative targets of these miRNAs, both experimentally validated or predicted *in silico*, to elucidate the mechanisms underlying the effect of exosomal uptake in receiving cells.

Preliminarly, we also queried the online miRNA-target prediction tool MiRWalk to identify which pathways could result affected by the exosomal miRNA cargo. We performed Gene Set Enrichment Analysis on the 132 genes found to be targeted by DE miRNAs identified in the TC71 shIMP3 model and on the 249 genes identified as targets of the DE miRNAs in A673 shIMP3 model. This analysis identified MAPK cascade and positive regulation of cell migration as the most affected pathways by DE miRNAs in TC-71 model (Figure 23A). Similarly, the same pathways were identified by performing the same analysis on the targets of A673 shIMP3 DE miRNAs (Figure 23B). These observations further sustain the role of exosomes with differential levels of IGF2BP3 in modulating the migratory capabilities of the receiving cells. It also offers an interesting hypothesis on the mechanisms leading to the modulation of ERK levels upon exosomal administration (Figure19A, B).

Common Upregulated miRNAs							
A673 shIMP3				TC-71 shIMP3			
miR_ID	**logFC**	**FC**	**PValue**	**miR_ID**	**logFC**	**FC**	**PValue**
hsa-miR-12136	1,493422	2,815559	0,019198	**hsa-miR-12136**	0,926806	1,901063	1,37356E-05
hsa-miR-146b-5p	0,832863	1,781217	0,026404	**hsa-miR-146b-5p**	0,842031	1,792571	3,39901E-05
hsa-miR-218-5p	1,05833	2,082519	0,022928	**hsa-miR-218-5p**	0,664592	1,58512	0,001975191
hsa-miR-222-3p	1,120757	2,17461	0,022732	**hsa-miR-222-3p**	0,539278	1,453245	0,014594074
hsa-miR-3127-5p	1,326267	2,507531	0,020257	**hsa-miR-3127-5p**	1,714803	3,282519	5,80411E-05
hsa-miR-4485-3p	0,92758	1,902083	0,025282	**hsa-miR-4485-3p**	0,798055	1,738755	0,009791387
hsa-miR-654-3p	1,077437	2,110283	0,022773	**hsa-miR-654-3p**	0,621046	1,537989	0,029518645
hsa-miR-664a-5p	1,633841	3,103381	0,0174	**hsa-miR-664a-5p**	1,252117	2,381906	0,006507622
hsa-miR-6767-5p	4,084732	16,96785	0,00019	**hsa-miR-6767-5p**	3,249473	9,510179	0,040156542
hsa-miR-944	**1,391265**	**2,623086**	**0,019812**	**hsa-miR-944**	**0,875614**	**1,834789**	**0,022086131**

Table 3. Common Upregulated miRNAs from TC71 shIMP3 and A673 shIMP3 exosomes

Common Downregulated miRNAs							
A673 shIMP3				TC-71 shIMP3			
miR_ID	**logFC**	**FC**	**PValue**	**miR_ID**	**logFC**	**FC**	**PValue**
hsa-miR-144-3p	-0,86266	0,549939	0,030091	**hsa-miR-144-3p**	-0,58723	0,665619	0,013778103
hsa-miR-4470	-3,17159	0,110983	0,041473	**hsa-miR-4470**	-3,72947	0,075391	0,015536532
hsa-miR-6865-5p	-3,17834	0,110465	0,041721	**hsa-miR-6865-5p**	-3,18254	0,110143	0,035713968

Table 4. Commond Downregulated miRNAs from TC71 shIMP3 and A673 shIMP3 exosomes

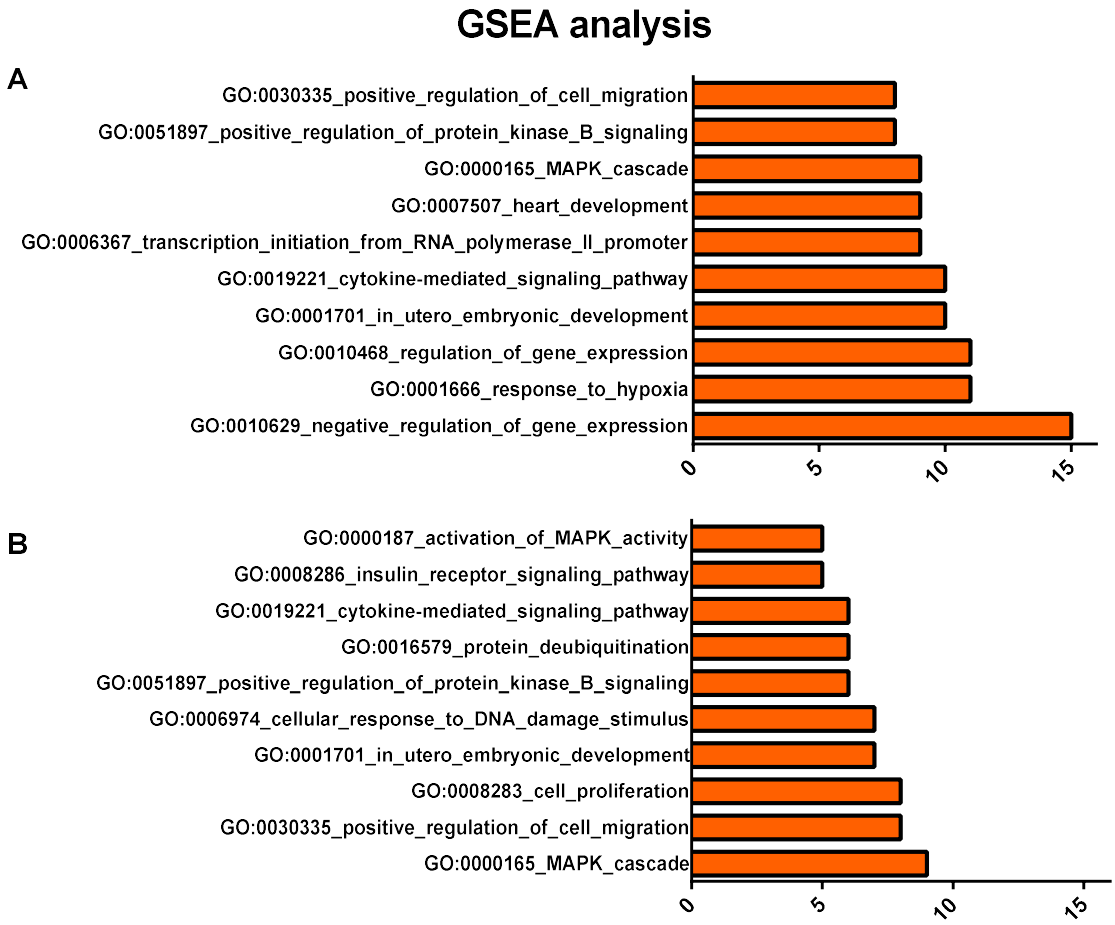

Figure 23. Influence of exosomal miRNA cargo on receiving cells

Results of Gene Set Enrichment analysis performed on genes identified as targets of those miRNAs that resulted deregulated in exosomes derived from TC-71 shIMP3 ***(A)*** *and A673 shIMP3* ***(B)*** *models. Top 10 entries are shown.*

3.4 IGF2BP3 IN THE CONTEXT OF THE IMMUNE MICROENVIRONMENT

Previously reported results obtained in this research group suggested that IGF2BP3 might play a relevant role in the context of immune tumor microenvironment. In fact, from the analysis conducted via the Human Cancer Inflammation & Immunity Crosstalk RT² Profiler PCR Array (Qiagen) identified a set of mRNAs known to participate in immune responses (i.e., *CD274*, *IL15*, *PDCD1*, *PTGS2*) which were upregulated in A673 cells deprived of IGF2BP3 (Table 3, paragraph 2.2).

3.4.1 IGF2BP3 DOESN'T REGULATE THE EXPRESSION OF IMMUNE CHECKPOINTS IN EWING SARCOMA CELLS

Among the genes that appeared to be overexpressed in IGF2BP3-depleted cells when compared to controls, we identified *PDCD1* and *CD274*, respectively encoding for PD1 and PDL1.

PD1, a cell surface receptor physiologically expressed on active T-cells, can act as a natural brake to T-cells response by binding its ligands PDL1 or PDL2 (Sharp and Pauken, Nat Rev Immunol 2017). Cancer cell-intrinsic PD1 was described to favor tumor progression in melanoma and liver cancer (Kleffel et al, Cell 2015; Li et al, Hepatology 2017), whereas it plays an oncosoppressive role in non-small cell lung cancer (Du et al, Oncoimmunology 2018).

To validate the suggested upregulation of PD1 and PDL1, we performed Real Time-qPCR in both A673 and TC-71 shIMP3 models. A general trend of upregulation was observed for *PDCD1* and *CD274* mRNA levels when comparing low-vs high-IGF2BP3 expressing cells but no statistical significance was found (Figure 24A).

We performed Western Blotting analysis and observed that both PD1 and PDL1 weren't modulated in accordance with IGF2BP3 levels in either A673 or TC-71 shIMP3 model (Figure 24B).

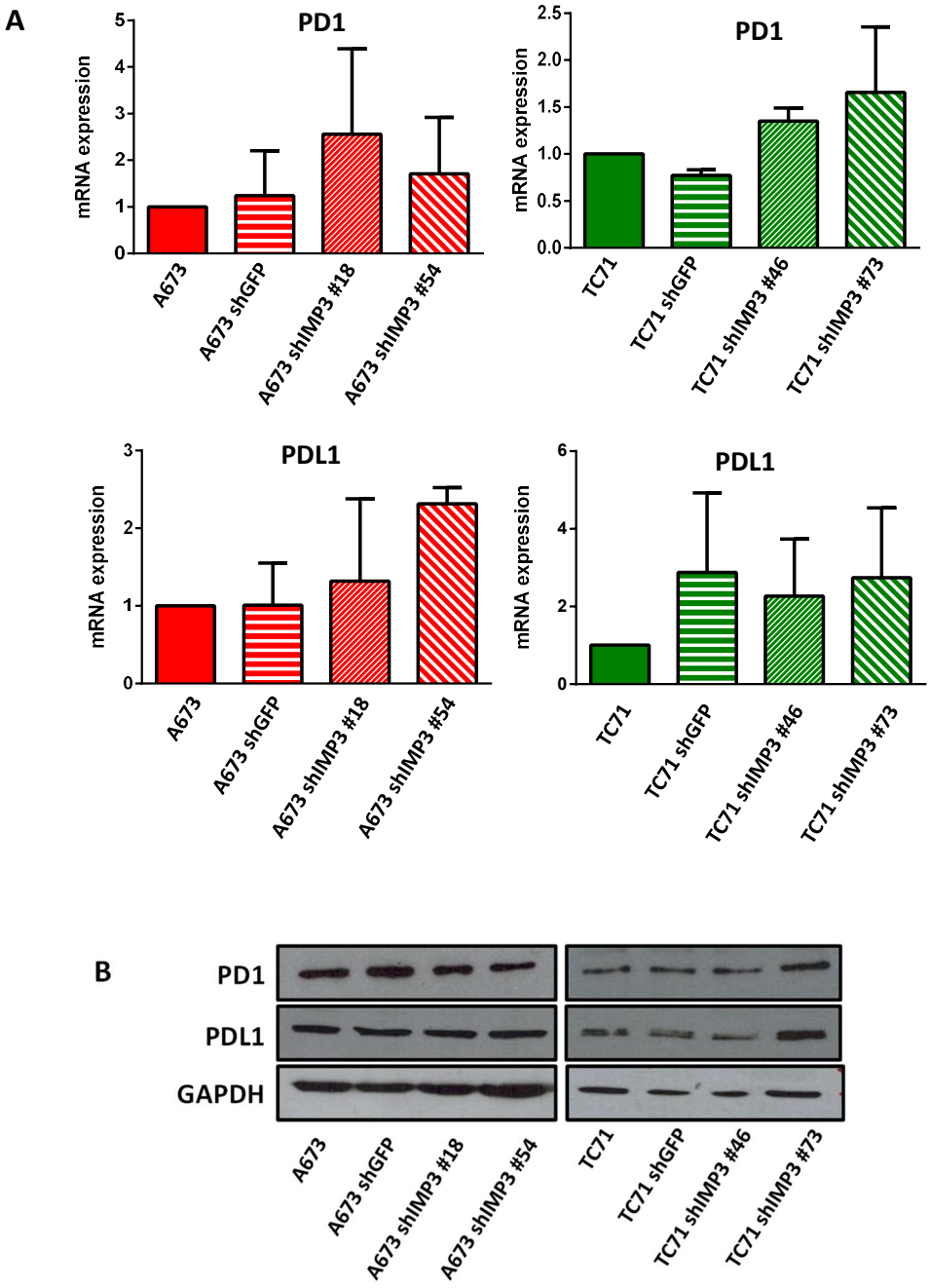

Figure 24. PD1 and PDL1 levels in IGF2BP3-depleted cells.
(A) *PD1 and PDL1 mRNA levels were analyzed via Real Time-qPCR in IGF2BP3-depleted or empty vector-transfected (shCTR) A673 and TC-71 cells. Relative mRNA expression reported as RQ is shown. GAPDH was used as housekeeping gene. The mean ± SE of two independent experiments is shown. n.s, not significant, one-way ANOVA.*
(B) *Western Blot analysis on PD1 and PDL1 in IGF2BP3-depleted or empty vector-transfected (shCTR) A673 and TC-71 cells. GAPDH was used as loading control. Representative Western Blots are shown.*

3.4.2 JQ1 TREATMENT DOESN'T MODULATE THE PD1/PDL1 AXIS IN EWING SARCOMA CELLS

According to recent data available in literature, the BET inhibitors have the interesting ability of affecting the expression of both IGF2BP3 and PD1/PDL1 axis (Boi et al, Oncotarget 2016; Mancarella et al, Clin Cancer Res 2018; Hogg et al, Cell reports, 2017).

Moreover, in paragraph 2.6, we observed that JQ1 treatment on TC-71 cell line reduced not only *IGF2BP3* but also *CD164* levels, *de facto* confirming the association between the two molecules.

Based on this knowledge, we evaluated *PD1* and *PDL1* levels on TC-71 cell line after 48h of treatment with increasing doses of JQ1. We observed a significant inhibition of *PD1* expression, already at low doses of treatment, whereas *PDL1* levels didn't vary significantly (Figure 25). These data sustain the lack of association between PD1/PDL1 and IGF2BP3 in Ewing Sarcoma cells.

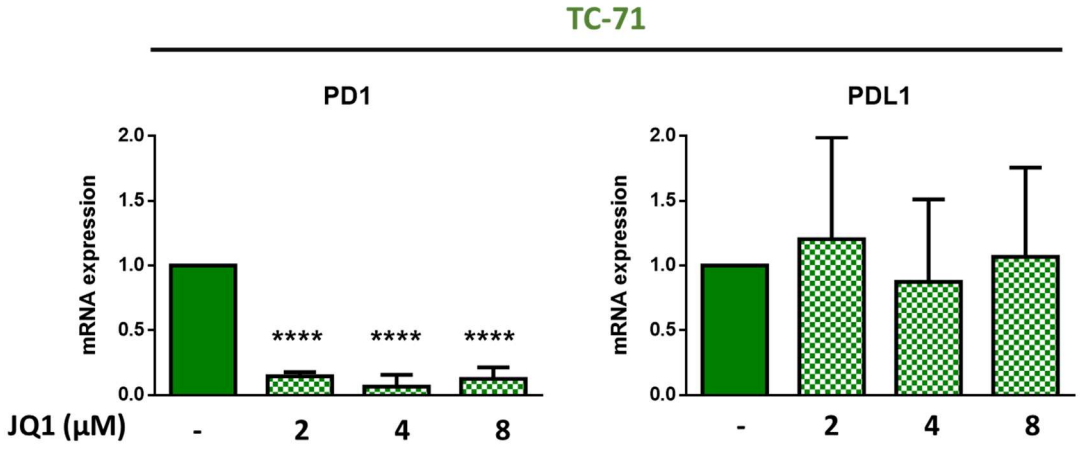

Figure 25. Effect of JQ1 treatment on PD1/PDL1

(A) *PD1 (left) and PDL1 (right) mRNA levels were evaluated via Real Time-qPCR on TC-71 cells after 48h treatment with increasing doses of JQ1. Data normalization was performed on untreated control. Real Time-qPCR is the mean of at least three independent replicates, relative mRNA expression reported as RQ is shown. The mean ± SE of two independent experiments is shown. **** p-value <0.05, one-way ANOVA.*

4 DISCUSSION

The present work confirmed both at clinical and preclinical levels the the fundamental role of IGF2BP3 in directioning Ewing Sarcoma metastatization, identifying a novel IGF2BP3/CD164/CXCR4 functional axis, and explored for the first time the contribution of exosome-secreted IGF2BP3 in the context of this tumor microenvironment.

Ewing Sarcoma is the second most common malignant mesenchymal tumor in young patients. (Grünewald et al, 2018). The presence of metastases in Ewing Sarcoma is the major adverse prognostic factor and, reportedly, the complex and multifaceted progression to metastatization is profoundly linked with stress adaptation, induced by adverse conditions typical of the tumor microenvironment such as exposure to hypoxia and nutrient deprivation (Bailey et al, 2016; Krook et al, 2014). From a genetic point of view, the EWSR1/FLI1 chromosomal translocation is the main oncogenic feature of Ewing Sarcoma, driving pathogenesis and tumor progression (Arvand and Denny, 2001) in the proper context of adjuvant factors, such as an active Insulin-like Growth Factor (IGF) system (Scotlandi et al, 2002) and the presence of the membrane glycoprotein CD99 (Manara et al, 2016). Beside this driver mutation, Ewing Sarcoma presents a very low rate of somatic mutations (Crompton et al, 2014) and this stability is conserved in metastases, whose genetic profile is almost indistinguishable from that of the primitive tumor (Scotlandi et al, 2009.). Therefore, epigenetic or post-transcriptional mechanisms may play a prominent role in directing Ewing Sarcoma progression and metastatization.

RNA-binding proteins (RBPs) are major regulators of gene expression at a posttranscriptional level. both in physiological and pathological conditions (Coppin et al, 2018). Of particular interest, RBPs appear to play a prominent role in regulating many aspects of cancer progression, (i.e. stemness, cell proliferation, tumor dissemination) and may act as promising biomarkers of tumor progression (Pereira et al, 2017, Mancarella 2020).

The role of RBPs in the context of Ewing Sarcoma has been marginally investigated. Data published from our laboratory demonstrated that the RBP Insulin-Like Growth Factor 2 mRNA Binding Protein 3 (IGF2BP3) is a relevant modulator of Ewing Sarcoma aggressiveness, as it is expressed at high levels in clinical specimens and its higher expression correlates with a poor prognosis. In addition, experimental evidence shows that the elevated expression of IGF2BP3 promotes growth in the absence of anchorage and motility *in vitro* as well as the ability to metastatize *in vivo* (Mancarella 2018).

Real time-qPCR analysis on clinical specimens showed how IGF2BP3 is expressed and significantly up-regulated in Ewing Sarcoma metastatic lesions when compared to primary localized tumors, further confirming the prominent role of this RBP in the metastatic progression of this tumor type.
Metastatic progression of solid tumors depends not only on the intrinsic changes in cells acquiring a more motile phenotype, but also on the interplay with the demanding microenvironment surrounding them (Bailey et al, 2016). Previously published evidence shows that IGF2BP3 can promote Ewing Sarcoma cells migration *in vitro* by supporting *IGF1R* translation, through an IGF-dependent mechanism (Mancarella et al, 2018).
To further highlight the IGF2BP3-related mechanisms involved in the interplay of Ewing Sarcoma cells with the microenvironment, a comprehensive analysis of a panel of mRNA involved in Cancer Inflammation and Immunity Crosstalk pathways, was performed. The analysis identified 13 putative novel downstream effectors of IGF2BP3 that were modulated in IGF2BP3-silenced Ewing sarcoma cells compared to controls. The identified genes suggested a role for the RBP both in the interaction between tumor and immune microenvironment and in the chemokine-mediated signaling pathways, confirming previous RNA-sequencing analysis (Mancarella et al, 2020).
CXCR4 was identified among the genes modulated upon IGF2BP3 differential expression. CXCR4 modulation has already been identified as one of the effectors of increased migration in response to hypoxic stress and lack of growth factors in Ewing Sarcoma (Bailey et al, 2016, Bennani-Baiti at al, 2010). Our results demonstrated for the first time a correlation between CXCR4 and IGF2BP3, as both CXCR4 mRNA and protein levels were down-modulated in IGF2BP3-deprived cells. Data from literature report that in normal conditions CXCR4 is expressed at low levels and only by a minority of Ewing Sarcoma cells, while hypoxic stress conditions can induce an increase both in the levels of CXCR4 transcript and protein (Krook et al, 2014). Hence, we decided to take a further step in analysing the role of IGF2BP3 in the context of CXCR4-mediated response to hypoxia Our results demonstrated that the response of Ewing Sarcoma cells to hypoxic stress appears to be directly modulated by the levels of IGF2BP3 in terms of migration towards CXCR4 natural ligand, CXCL12 (Stromal Cell Derived Factor, SDF1). In the absence of CXCL12 stimulation, the different levels of IGF2BP3 do not correlate with a differential response to oxygen deprivation, neither in terms of proliferation nor migration. On the other hand, in hypoxic conditions CXCL12 induces an increased chemotactic migration of cells expressing IGF2BP3, associated with the up-regulation of the CXCR4 receptor in response to the increase of HIF1α. This same modulation, both in terms of receptor availability and of migration capability, is not induced in IGF2BP3- cells, lacking of CXCR4 in basal conditions.

This observation is consistent with data reporting that microenvironmental stress can promote cellular migration towards sites of metastasis rich in CXCL12, such as lungs and bone marrow (Krook et al, 2014). Our data confirm the reported fundamental role of CXCL12 as a stimulus for Ewing Sarcoma migration and, for the first time, report a role for IGF2BP3 in regulating the CXCR4/CXCL12 mediated response to hypoxia, thus indicating that this RBP can mediate cell motility also through IGF-independent mechanisms (Mancarella et al, 2018).

A direct relationship between IGF2BP3 and CXCR4 mRNA has never been reported.

CD164 (endolyn) belongs to the sialomucin family and regulates the adhesion of CD34+ cells to bone marrow stroma, and their recruitment into cycle (Forde et al, 2007). An oncogenic role for this molecule is reported (Tang et al, 2011, Havens et al, 2006, Huang et al, 2013, Chen et al, 2016) but, with the exception of sporadic evidence (Grunewald et al 2013), CD164 role in Ewing Sarcoma progression has never been deeply investigated. Preliminary RIP assay data produced from our laboratory suggested the existance of a direct association between IGF2BP3 and CD164 in Ewing Sarcoma cells (Mancarella et al, 2020). Our research work confirmed these evidences, demonstrating that IGF2BP3 regulates *CD164* expression levels in Ewing Sarcoma. These data are in accordance with what was observed by the works from Hafner et al and Samanta et al, respectively *in silico* and in triple-negative breast cancer (Hafner et al, 2010; Samanta et al, 2012). The association between IGF2BP3 levels and CD164 expression in Ewing Sarcoma is further sustained by the observation that cells treated with the BETi JQ1 presented decreased levels of both the RBP and its target, as observed in leukemia cells and Ewing Sarcoma cells (Filippakopoulos et al, 2010, Dawson et al, 2011; Mancarella et al, 2018). Interestingly, in Jurkat cells CD164 physically associates with CXCR4 following stimulation with CXCL12 and promotes cell motility (Forde et al, 2007) and a similar mechanism has been reported in ovarian and colon cancer cell lines (Huang et al, 2013, Tang et al, 2012). According to reported literature, we observed the existence of a direct functional interaction between CD164 and CXCR4 also in Ewing Sarcoma, as the two proteins colocalize at plasma membrane level after stimulation with CXCL12. This observation sustains the existence of a functional relationship between CD164 and CXCR4 in Ewing Sarcoma cells, which appears to be fundamental to mediate the migratory response to CXCL12 stimulus. In fact, CD164 loss-of-function models display a strong impairment in terms of chemo-directed migration. These data, taken all together, demonstrate the existence of a functional axis that indirectly connects IGF2BP3 and CXCR4, through the mediation of CD164, and that this axis modulates the migratory response to the chemo-mediated stimulation carried out by CXCL12.

The relevance of the proposed IGF2BP3/CD164/CXCR4 axis in Ewing Sarcoma is further supported by its evaluation in clinical samples. Real time-qPCR analysis showed that neither CD164 nor CXCR4 levels were up-regulated in metastatic lesions compared to primary Ewing Sarcoma tumors. Yet, we demonstrated that a statistically significant correlation exists between CD164/CXCR4, CD164/IGF2BP3 and CXCR4/IGF2BP3, as in primary tumors as in metastasis. This observation suggests a major relevance for the concomitant up-regulation of CD164 and CXCR4 at clinical level. In summary, data presented so far identified the existence of a novel functional oncogenic axis composed by IGF2BP3/CD164/CXCR4, acting as an IGF-independent mechanism modulating Ewing Sarcoma aggressiveness in terms of metastatization. This discovery could open new interesting perspectives from a diagnostic/prognostic and therapeutic point of view.

In terms of immune infiltrate composition, Ewing Sarcoma is classified as a "desert tumor" (Grünewald et al, 2018; Chen and Mellman, 2017), as its major feature is a substantial paucity of immune cells. The predominant presence of CD8+ T cells correlates with reduced tumor progression (Berghuis et al, 2011) while a modest presence of Tumor Associated Macrophages (TAMs) is associated with poorer prognosis (Inagaki et al, 2016; Lau et al, 2007). The influence of these two populations of immune cells on Ewing Sarcoma prognosis hints the existance of a cross-talk with the tumor itself. Yet, the presence of the immune infiltrate doesn't seem to be sufficient to control Ewing Sarcoma progression. The previously reported results evaluating the influence of IGF2BP3 levels on a panel of mRNAs involved in Cancer Inflammation and Immunity Crosstalk Pathways hinted a role for the RBP in the interaction with the immune microenvironment of Ewing Sarcoma and particularly highlighted the upregulation of both PD1 and PDL1 in cells deprived of IGF2BP3 when compared to controls. From a physiological standpoint, PD1 is a cell surface receptor physiologically expressed on active T-cells during inflammation and immune response and the canonical PD1/PDL1 interaction acts as a natural brake to overactivation of T-cells response. On the other hand, it can protect tumors from cytotoxic T-cells by disrupting the cancer immunity cycle (Robainas et al, 2017, Sharp and Pauken, 2018; Chen et al, Nature 2018). Many research groups recently investigated PD1/PDL1 expression in Ewing Sarcoma cells, obtaining ambiguous results (Spurny et al, 2018; Pinto et al, 2017; Kim et al, 2013; per Van Erp et al, 2017; Machado et al, 2018). The hypothesis of a concomitant upregulation of PD1/PDL1 in association with lower IGF2BP3 was of major interest as it hinted the existance of an autocrine loop between these two molecules both expressed by Ewing Sarcoma cells. The role of cancer cell intrinsic PD1 has been studied only in melanoma, liver cancer and non-small cell lung cancer (Kleffel et al, 2015; Li et al, 2017, Du et al, 2018).

The proposed correlation between IGF2BP3 and PD1 or PDL1 couldn't be validated either at mRNA or protein level. Treatment with the IGF2BP3-targeting BETi JQ1 (Dawson et al, 2011; Mancarella et al, 2018) induced a dose independent abrogation of PD1, while it didn't modulate PDL1 levels, further sustaining the absence of correlation between IGF2BP3 and PD1/PDL1 levels. The data collected and presented so far, didn't highlight a correlation between IGF2BP3 and PD1/PDL1 levels, thus leave the questions about the role of these molecules in Ewing Sarcoma still unanswered.

Intercellular communication within the scenario of the tumor microenvironment is emerging as a crucial mechanism to explain the progression of many cancer types. Exosomes are specialized Extracellular Vesicles (EVs) and represent a broadly recognized candidate to explain the intercellular horizontal transfer of oncogenic signals and molecules, as they are actively released by tumor cells and enriched with proteins and RNAs (Théry et al, 2002, Kalluri et al, 2020).
Extracellular Vesicles can be divided into two major subgroups, microvesicles (MVs) and exosomes, which can be distinguished based on their size and on their cellular origin. Size and amount of these vesicles makes them challenging to work with, as they are often difficult to obtain as pure preparations. Thus, their proper characterization is still a matter of debate and represent a crucial step prior to any functional study. The International Society for Extracellular Vesicles (ISEV) proposed a set of guidelines to overcome these difficulties, the "Minimal Information for Studies of Extracellular Vesicles ("MISEV") guidelines" to help direct the characterization of exosomes.
To make our data about Ewing Sarcoma-derived exosomes as robust as possible, experiments were performed on different models of IGF2BP3-silencing. Mainly, we worked on two PDX-derived cell lines, EW-PDX #5-C and EW-PDX #2-C, which present respectively high and low levels of IGF2BP3. PDX-derived cell lines, rather than classical cell lines, maintain genotypic and phenotypic properties of the tumors of origin (Shi et al, 2020). The described presence of high or low levels of IGF2BP3 in PDX-derived cell lines, which reflecs those of the originating tumor and of EW-PDX tumor, does not necessarily make the comparison between their phenotype representative of IGF2BP3-directed malignancy. In fact, since IGF2BP3 is constitutively down-modulated in EW-PDX #2-C cell line, the tumor cell has likely activated collateral compensatory pathways in order to maintain the malignant phenotype.
Based on these considerations, we decided to use EW-PDX #5-C cell line to perform an IGF2BP3 knockout via the Crispr/Cas9 system and generate the EW-PDX #5 gIMP3 model.
The total absence of IGF2BP3 protein in gIMP3 cells is a remarkable difference with what is observed in the previously obtained IGF2BP3-knockdown A673 and TC-71 shIMP3 models: while short hairpin directly bind mRNAs (Bot et al, 2005), leading them to disruption, the Crispr/Cas9 system is

designed to specifically cleave the gene of interest at DNA level, de facto disrupting the cellular ability to produce the corresponding mRNA (Doudna and Charpentier, 2014, Shalem et al, 2014). Basal characterization of the newly generated IGF2BP3-knockout model confirmed the role of the RBP in modulating anchorage-independent growth and migration, but not proliferation, as observed in IGF2BP3-knockdown models (Mancarella, 2018).

Extracellular vesicles purified from different models of IGF2BP3 silencing were characterized following MISEV guidelines, in terms of size, concentration, total amount of protein content and marker expression. The observed diameters were consistent with the reported exosomal ones and the expression of protein markers such as HSP90, ALIX and TSG101, accompanied by the total absence of the Endoplasmic Reticulum marker Calnexin, sustained the endosomal origin of the isolated vesicles. Taken together these data allowed us to refer to isolated vesicles as "exosomes". The same set of data did not highlight any association of exosome size nor concetration with IGF2BP3 levels, prompting to exclude a role of the RBP in exosomal biogenesis.

Intercellular communication via the release of key pro-tumorigenic molecules, free or loaded into exosomes, within the scenario of the tumor microenvironment is emerging as a crucial mechanism to explain the progression of many cancer types. IGF2BP3 has been demonstrated to be released both in the serum of patients of renal carcinoma and pancreatic cancer (Szarvas et al, 2014; Tschirdewahn et al, 2019) but, to the best of our knowledge, we reported for the first time that IGF2BP3 is heterogeneously secreted by Ewing Sarcoma cells. We also unveiled for the first time that IGF2BP3 can be effectively loaded into Ewing Sarcoma-derived exosomes, mirroring the cellular levels of the RBP. Statello et al. recently demonstrated that RBPs could serve as key players in the cargo loading of exosomes by forming cellular RBP-RNA complexes which are then transported into exosomes during their biogenesis (Statello e al, 2019) and IGF2BP3 paralogue, IGF2BP1, was indeed described in melanoma-derived exosomes, where it was associated with a signature of differentially expressed RNAs and with a prominent role in influencing the metastatic phenotype of the receiving cells (Ghoshal et al, 2019). The differences we observed between secreted as free protein or exosome-vehicled IGF2BP3 suggest that the release of this protein could be a mechanism used by the cells to extrude excesses of the molecules. In this perspective, we can hypothesize that exosomal IGF2BP3 could be the fraction of released protein that holds a biological significance in terms of intercellular communication.

Recent research demonstrated how the role of two key players of Ewing Sarcoma malignancy, such as EWS/FLI1 and CD99, is exerted not only at cellular level but also through exosome-mediated communication. In the first paper describing Ewing Sarcoma-derived exosomes, Miller et al. demonstrated that EWS/FLI1 is transferred into the cargo of microvesicles and can be selectively

transferred into Ewing Sarcoma receiving cells (Miller et al, 2013). Exosomes produced by cells with different levels of CD99 reportedly mirror the cellular levels of the protein and have a differential influence on the phenotype of recipient cells (Llombart-Bosch 2009, Ventura et al 2016, De Feo et al, 2019).

With our results we hint the relevance of another modulator of Ewing Sarcoma progression such as IGF2BP3 in the exosome-mediated communication between cancer cells. This discovery opens new interesting perspectives to understand Ewing Sarcoma progression, as it lays the basis to demonstrate that the pro-tumorigenic role of IGF2BP3 is not only exerted at the level of the cell itself, but that intercellular communication between tumor cells is particularly crucial in a context of high cellular heterogeneity as the one that can be found in Ewing Sarcoma (Franzetti et al, 2017, Sheffield et al, 2017, Llombart-Bosch et al, 2009).

Exosomes derived from Ewing Sarcoma cells with differential expression of IGF2BP3 are actively up taken by receiving cells but no role in modulating their proliferation was observed. This data is consistent with the described role of cellular IGF2BP3 in Ewing Sarcoma progression, reportedly influencing pro-metastatic properties such as anchorage-independent growth or cellular migration, but not inducing any modulation in cellular proliferation (Mancarella et al, 2018). Data presented in this thesis indicate that IGF2BP3 is able to mediate cell motility through IGF-independent mechanisms, linked to the post-transcriptional regulation of CD164. Moreover, previously published evidence shows that IGF2BP3 supports IGF1R translation thereby promoting motility of Ewing Sarcoma cells (Mancarella et al, 2018). Reportedly, the exosome-mediated transfer of RBP-RNA complexes can actively modulate the phenotype of the receiving cells (Statello et al, 2019). We demonstrated that IGF2BP3 client-mRNAs CD164 and IGF1R are loaded into IGF2BP3+ exosomes. To date, no report for CD164 mRNA exosomal loading is available, while exosomal transfer of IGF1R mRNA had already been reported by Tomasoni et al in the context of mesenchymal stem cells (Tomasoni et al, 2013), although no clear explanation for its mechanism of action in receiving cells was found. The accordance between IGF2BP3 and its client-mRNAs levels in exosomes is consistent with the literature sustaining that cellular RBPs can maintain their ability to bind RNAs also when they are transferred into exosomes, *de facto* exerting their protective role also in the context of vesicular cargo (Koppers-Lalic et al, 2014). Interestingly, also CXCR4 levels were up-regulated in IGF2BP3+ exosomes.

CXCR4 horizontal transfer via exosomes has already been linked to the promotion of the metastatic progression (Li et al, 2018) and acquires major relevance in the context of Ewing Sarcoma when taking into account the IGF2BP3/CD164/CXCR4 axis previously described. Given these premises, we hypothesized a role for Ewing Sarcoma-derived exosomes in regulating cellular migration. We

observed that cells treated with complete medium derived from IGF2BP3+ cell lines showed enhanced migratory abilities when compared to those treated with complete medium derived from IGF2BP3- cell lines, whereas no significant difference was observed in cells receiving exosome-deprived supernatants. This information prompts a role for exosomal IGF2BP3 rather then its soluble form in modulating cell migratory phenotype. In the context of chemo-directed migration towards CXCL12, the administration of IGF2BP3+ exosomes transferring CD164 and CXCR4 mRNAs leads to the increase of both CD164 and CXCR4 protein levels in receiving cells. Interestingly, the marked availability of the elements composing the CXCR4/CD164 receptor is associated to an increased migration rate of cells receiving IGF2BP3+ exosomes when compared to those receiving the IGF2BP3- ones in presence of CXCL12 gradient. The contribution of IGF32BP3+ exosomes on the IGF-dependent migration of Ewing Sarcoma cells was investigated in parallel, as IGF2BP3 exosomal levels had been correlated also with the loading of its client mRNA IGF1R. Its transfer into receiving cells induced an up-regulation of IGF1R protein into receiving cells, which was accompanied by an increase in cellular migration upon administration of IGF1 in cells receiving IGF2BP3+ exosomes when compared to those receiving the IGF2BP3- ones.

Taken together these data demonstrate the fundamental influence exerted by exosomes in the directioning of Ewing Sarcoma metastatic progression, as they actively influence and orchestrate the cellular response to the microenvironmental stimuli. Various reports on the importance for a positive feedback loop of the IGF system in Ewing Sarcoma are present (Scotlandi et al, 2002; Garofalo et al, 2012) and our data confirm that the role of the IGF-dependent migratory response is predominant when compared to the IGF-independent one, when exosomes are taken into account. This preponderance can be observed at least in two points. The administration of IGF2BP3+ exosomes carrying *IGF1R* mRNA in their cargo can induce a dramatic increase of this mRNA in recipient cells. On the contrary, the same administration does not modulate in a comparable way *CD164* mRNA levels, regardless of its presence in IGF2BP3+ exosomes. Moreover, stimulation with IGF1 on cells receiving IGF2BP3+ exosomes induces a more prominent effect on cellular migration rather than what is observed with CXCL12, at least in normoxyc conditions.

The role of these exosomes on the CXCL12-mediated pathway in hypoxic conditions has not been evaluated in the present thesis but certainly deserves to be investigated with further studies.

The signaling pathways triggered by binding of CXCL12 to CXCR4 are multiple. They depend on the cellular context, have pleiotropic effects and include the PI3K pathway, the MAPK pathway and the small GTPase pathway, key regulators of cell remodeling. actin cytoskeleton (Ganju et al, 1998, Gassmann et al, 2009; Amano et al, 2010). Interestingly, activation of IGF1R receptor upon ligand binding reportedly activates the PI3K and the MAPK downstream signaling pathways as well

(Fruman et al, 2017; Liu et al, 2018). Our data show that the administration of IGF2BP3+ exosomes strongly affects both the aforementioned pathways but at different levels. The activation of the PI3K pathway was sustained by an increase in both AKT and mTOR phosphorylation in cells receiving IGF2BP3+ exosomes, while the increased activation of the MAPK pathway in cells receiving IGF2BP3+ exosomes didn't rely on ERK 1/2 phosphorylation, but rather on an increased availability of the total form of the protein.

Interestingly, we observed that the administration of exosomes, independently of their IGF2BP3 content, is actually a minor stressor for the receiving cells. This could be due to exosomal precipitation method, as all functional studies were performed using ExoQuick precipitated exosomes which may still be associated to a small portion of uncleared resin, or, specially in experiments conducted with heterologous exosomes, to the nature of the cell of origin which may slightly affect the complex exosomal cargo independently of IGF2BP3 presence and role. This effect is observed bot at migration and protein expression levels in IGF2BP3pos cells receiving IGF2BP3pos exosomes and prevent us to properly observe their influence, thus we decided to perform in parallel experiments on an IGF2P3neg cells. Further investigation increasing the doses of IGF2BP3pos exosomes could be useful to give stronger relevance to their role in regulating the phenotype of IGF2BP3pos cells.

The importance of exosomal miRNAs is widely assessed troughout different cancer types and a role of RBPs in modulating the loading of miRNAs in exosomal cargos has been described (Villaroya-Beltri et al, 2013; Wozniack et al, 2020). Thus, to gain a wider and more complete perspective on the cargo composition of exosomes with differential expression of IGF2BP3, we evaluated the content of IGF2BP3+ and IGF2BP3- exosomes via miRNA sequencing and observed a modest difference between their miRNA cargos. Moreover, very few miRNAs were commonly deregulated in exosomes derived from the two cellular models. This information, reflecting the intrinsic differences between TC-71 and A673 cells, highlits the relevance of the identification of shared mechanisms.

Gene Set Enrichment analysis of the reported predicted targets of the differentially expressed miRNAs identified showed an enrichment in the regulation of cellular migration, sustaining the proposed role of these vesicles in broadly influencing the migratory phenotype of Ewing Sarcoma receiving cells. We also observed an enrichment in the MAPK pathway: considering the relevance of the MAPK pathway in the metastatization of Ewing Sarcoma, not only in association with the reported CD164/CXCR4 or IGF1R directed pathways (Benini et al, 2004), furhter investigation is needed.

5 CONCLUSIONS

In conclusion, this study demonstrated that the role of IGF2BP3 in the context of Ewing Sarcoma microenvironment is predominantly exerted in the process of metastatization.

We demonstrated, both at clinical and preclinical level, the existence of a functional axis that indirectly connects IGF2BP3 and CXCR4, through the mediation of CD164. This axis modulates the migratory response to the chemo-mediated stimulation carried out by CXCL12, confirming the reported fundamental role of this ligand as a stimulus for Ewing Sarcoma migration. With these results we demonstrate for the first time that the pro-tumorigenic role of IGF2BP3 in mediating cellular migration can be exerted through IGF-independent mechanisms and in stressing microenvironmental conditions, such as hypoxia. These discoveries could open new perspectives from a diagnostic/prognostic and therapeutic point of view.

We reported for the first time that IGF2BP3 is secreted in an exosome-dependent manner by Ewing Sarcoma cells, according to cellular levels. This discovery opens new interesting perspectives to understand this tumor progression, as it lays the basis to demonstrate that the pro-tumorigenic role of IGF2BP3 is not only exerted at the level of the cell itself, but that intercellular communication between tumor cells is particularly crucial in a context of high cellular heterogeneity as the one that can be found in Ewing Sarcoma. In fact, we proved that IGF2BP3+ exosomes maintain the pro-oncogenic properties of the RBP and actively promote the up-regulation and the activation of both IGF-dependent or independent pathways of cellular migration. Taken together these data demonstrate the fundamental influence exerted by exosomes in the directioning of Ewing Sarcoma metastatic progression, as they actively influence and orchestrate the cellular response to the microenvironmental stimuli.

6 MATERIALS AND METHODS

6.1 CLINICAL AND PRECLINICAL MODELS

6.1.1 Clinical Specimens

Snap-frozen tissue samples from Ewing Sarcoma primary localized tumors and metastatic lesions were included in this study. Patients enrolled in prospective studies had been diagnosed and treated at the Rizzoli Institute (Ferrari et al, 2011). Selected patients' diagnosis was made on representative specimens from open or needle biopsies and based on immunohistochemical, histological and cytological features. The molecular presence of the chimeric product derived from EWS-specific chromosomal translocations was also evlauated (Toomey et al, 2010). Local treatment, performed after induction chemotherapy, consisted of surgery, radiation therapy or surgery followed by radiation therapy. Clinical-pathological features of patients, updated to 2018, are summarized in Table 5.

		Primary tumors (N=48)	
Characteristics		No	%
Gender	**Female**	11	22.9
	Male	37	77.1
Age	**≤14 years**	22	45.8
	>14 years	26	54.2
Location	**Extremity**	33	68.7
	Central	4	8.3
	Pelvis	11	23
Surgery	**YES**	38	79.2
	NO	10	20.8
Local Treatment	**RxT**	10	20.8
	RxT+Surgery	11	23
	Surgery	27	56.2
Response to chemotherapy*	**Good**	10	26.3
	Poor	28	73.7

Table 5. Clinical-pathological features of primary localized Ewing Sarcoma patients included in this research

(Data available for 38 out of 48 patients)*

6.1.2 Ethical Statement

The ethical committee of the Rizzoli Institute approved the studies on clinical specimens (0041040/2015) and the establishment of PDX models (0009323/2016). The study was conducted in accordance with the Declaration of Helsinki ethical guidelines, and patient informed consent forms were obtained.

6.1.3 Preclinical models

6.1.3.1 Classical cell lines

Human Ewing Sarcoma A673 lines were provided by the American Type Culture Collection (ATCC), TC-71 were kindly provided by Dr. T.J. Triche (Children's Hospital, Los Angeles, CA).

6.1.3.2 Patient-derived Xenografts and PDX-derived cell lines

The cell lines PDX-EWS#2-C and PDX-EWS#5-C were obtained by the respective Ewing Sarcoma PDX after the first passage in animal. To obtain PDXs, primary patient specimens are implanted into immunodeficient mice shortly after explant. Tumors grown in mice are then harvested and minced to obtain PDX-derived cell lines, which are stabilized under 2D *in vitro* colture conditions. PDX and matching cell lines share elevated genotypic and phenotypic similarity between themselves and with the tumor of origin (Shi et al, 2020, Nanni et al, 2019).

6.1.4 Cell culture conditions

All cell lines were tested for Mycoplasma contamination (Mycoalert Mycoplasma Detection Kit, Lonza Bioscience, Basel, CH) before use and authenticated (last control December 2017 and July 2018) by short tandem repeat (STR) polymerase chain reaction (PCR) analysis using a PowerPlex ESX Fast System kit (Promega, Madison, WI). All cell lines were immediately amplified to constitute liquid nitrogen stocks and were never passaged for more than one month upon thawing.

All cell lines were maintained in Iscove's modified Dulbecco's medium (IMDM) (Euroclone, Milan, IT) supplemented with 10% heat-inactivated fetal bovine serum (FBS) (Euroclone), 20 units/ml penicillin and 100 μg/ml streptomycin (Euroclone) in a 37°C humidified environment at 5% CO2. For hypoxia studies, cells were cultured in 1% O2 using a Galaxy 14S incubator (New Brunswick, Eppendorf, Milan, IT) at 37°C and 5% CO2.

6.1.5 Loss-of-function models

6.1.5.1 Short hairpin RNA (shRNA) mediated knockdown of IGF2BP3

A673 and TC-71 stably silenced models had previously been obtained at the Oncology Research Laboratory of the IRCCS Istituto Ortopedico Rizzoli (Mancarella et al, 2018). Cells were transfected with pLKO.1 vector containing the IGF2BP3-specific short hairpin RNA shRNA (TRCN0000074673) (Open Biosystems, Huntsville, AL) or the empty vector shGFP (Open Biosystems). Subsequently, cells were selected with puromycin (2 μg/ml) (Sigma-Aldrich, St.Louis, MI).

6.1.5.2 Crispr/Cas9 mediated knockout of IGF2BP3

PDX-EWS#5-C was used to establish a novel Crispr/Cas9 IGF2BP3 knockout model. LentiCRISPR v2 plasmids, containing the hSpCas9 locus and the chimeric guide RNA, were employed. Four guide RNAs directed against IGF2BP3 (gIMP3) and a randomly rearranged control (gSCR) were kindly designed and cloned into plasmids by Prof. A.M. Mercurio (University of Massachusetts Medical School, Worchester, MA). Transfer plasmids were co-transfected into HEK293T cells with the packaging plasmids pVSVg (AddGene 8454) and psPAX2 (AddGene 12260). The transfections were performed using Lipofectamine 3000 (Life Technologies, Carlsbad, CA) according to the manufacturer's protocol. After 48h, colture medium containing the assembled lentiviruses was harvested and 10 μg/ml of polybrene were supplemented (Sigma-Aldrich). Lentiviral infection was performed to transfer into PDX-EWS#5-C cells the plasmids containing the specific gRNA sequence. The infection protocol was carried out with the help of dr. Manuela Piazzi (Istituto di Genetica Molecolare, Centro Nazionale per la Ricerca (CNR) and IRCCS Istituto Ortopedico Rizzoli, Bo, IT). Infected cells were selected in puromycin 2μg/ml (Sigma-Aldrich) and subsequently amplified in puromycin 0.5 μg/ml to constitute liquid nitrogen stocks.

6.1.5.3 Small interfering RNA (siRNA) mediated transient CD164 silencing

Short interfering RNA (siRNA)-mediated knockdown of CD164 was performed with siRNA from Dharmacon (Thermo Scientific, Waltham, MA). SMART POOL siGENOME_siRNA (M-016196-00-0020). siGENOME_non targeting_siRNA was used as control (D-001206-13-05). 1.5 x 10^5 TC-71 or A673 cells/well were seeded in 6-well plates coated with fibronectin from bovine plasma (3 μg/cm2; Sigma-Aldrich). 24 h after seeding, cells were transfected with siRNAs (80 nM) using TransIT-X2 (Mirus Bio, Madison, WI), according to the manufacturers' protocols. Evaluation of CD164 levels and functional studies were performed 72 h after transfection.

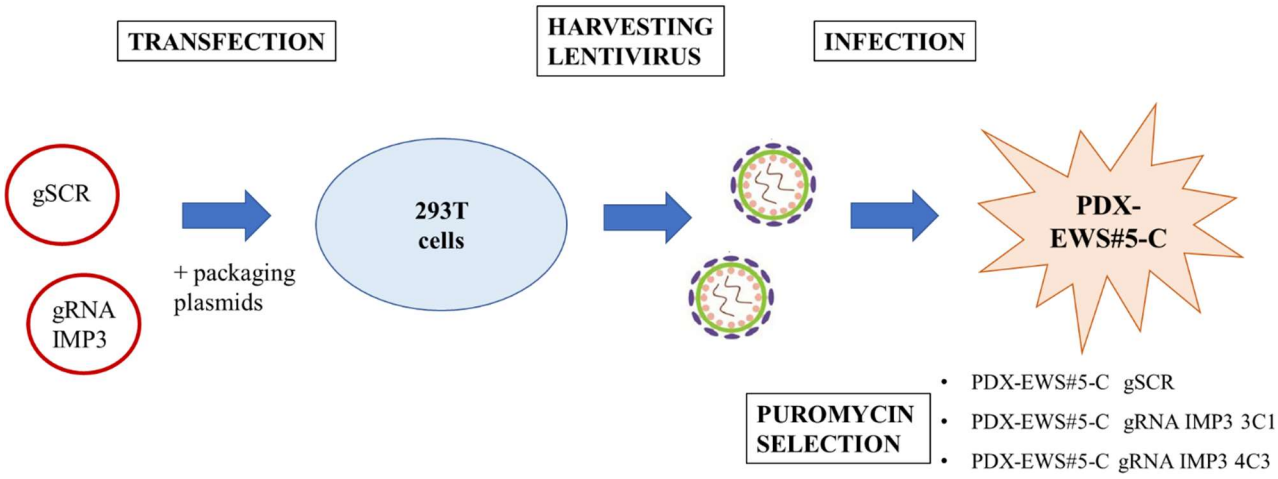

Figure26 *Schematic representation of the Crispr/Cas9 mediated knockout of IGF2BP3 protocol*

6.2 EXOSOME PURIFICATION AND CHARACTERIZATION

Exosomes produced by Ewing Sarcoma cells were isolated from cell culture medium using the ExoQuick (System Biosciences, Mountain View, CA) method or the Ultracentrifugation method. Ultracentrifugation was carried out with the collaboration of dr. Francesca Perut and dr. Laura Roncuzzi (SC Scienze e Tecnologie Biomediche, BST Lab, IRCCS Istituto Ortoperico Rizzoli, Bo, IT). Cells were cultured in IMDM supplemented with exo-depleted FBS. FBS had previously been ultracentrifuged at 100.000 x g for 6h and filtered in order to deplete it of bovine-derived exosomes. After 24h of cell-colture, the conditioned medium was collected and centrifuged at 3000 × g for 15 min to remove cell debris and the supernatant was transferred to a new sterile tube.

From this common preparation, we proceeded to:

1) ExoQuick (EQ) precipitation: the solution was added to the supernatants for an overnight incubation at +4 °C. Exosomes were isolated the following day by centrifugation at 1500 × g for 30 min at +4°C.

2) Ultracentrifugation (U) precipitation: the supernatants were ultracentrifuged at 110,000× g for 1 h at 4 ◦C, then the pellet containing the extracellular vesicles was resuspended in PBS and centrifuged at 110,000× g for 1 h at 4 ◦C (Beckman Coulter, Brea, CA).

The pellets obtained were resuspended in IMDM 0% FBS for in vitro functional studies or in PBS before RNA extraction or protein isolation prior to Western Blots.

Exosomes obtained via ExoQuick or Ultracentrifugation precipitation had previously been characterized in our laboratory to determine whether the two obtained populations were comparable. Indeed they were, thus we decided to use exosomes obtained by Ultracentrifugation precipitation to perform Western Blot analyses as this method guarantees a more efficient isolation of protein.

Yet, our Ultracentrifugation precipitation protocol doesn't guarantee the sterility of the exosomal samples so we decided to use exosomes obtained by ExoQuick precipitation to perform functional studies requiring exosomal administration to cultured cells. Moreover, exosomes obtained via ExoQuick precipitation were used for RNA isolation and characterization since the kit used for exosomal RNA extraction is optimized for EQ-extracted exosomes (see "6.5.1 RNA extraction and Reverse Transcription").

Exosomal labelling was performed using the fluorescent dye PKH67 (Sigma-Aldrich), following manufacturer's instructions. Briefly, 6 µl of PKH67 were added to 120 µg of exosomes for 5' at room temperature, then the reaction was blocked with FBS (1:1), exosomes were precipitated by centrifµgation (3000 rpm 5' RT, 12000 rpm 1' RT) and added to the receiving cells for 3 hours.

The number and size of the exosomes were directly tracked using a NanoSight NS300 system (NanoSight technology, Malvern, UK), configured with a 488 nm laser and a high-sensitivity sCMOS camera. Videos were collected and analyzed using NanoSight NTA software (version 3.0). For each sample, multiple videos 60 s in duration were recorded to generate replicate histograms, which were averaged. Nanosight analysis were conducted with the collaboration of dr.Ymera Pignochino (Division of Medical Oncology, IRCCS Istituto di Candiolo, To, IT).

An indirect quantification of exosomes was performed by evaluating total protein yeald by the Bradford method (See section 5.2 "Western Blotting").

For functional studies, exosomes in equal amounts (15 µg/10.000 cells) were incubated in serum-free conditions with recipient cells at 37 °C before experiments were performed.

6.3 *IN VITRO* ASSAYS

6.3.1 Cell growth

Cell viability and proliferation were assessed either with with Trypan blue dye or with MTT assay. For trypan blue count, a total of 40.000 cells/well were seeded in 12-well plates and cells were counted after 4 and 7 days. MTT assay (Roche, Basel, CH) was used according to manufacturer's instructions. Cells were plated into 96 well-plates (range 2,500-10,000 cells/well). After 24 h, exosomes (15 ug/ 10.000 cells) were added and cell viability was assessed after 24 h.

6.3.2 Anchorage-independent growth

3D anchorage-independent growth was determined in 0.33% SeaPlaque Agarose (Lonza Bioscience) with a 0.5% agarose underlay. To evaluate the effect of IGF2BP3 knockout, 10^4 PDX-EW#5-C gSCR or gRNA transfected cells were plated in semisolid medium (IMDM plus 10% FBS containing 0.33% agarose) in 60 mm Ø dishes, which were incubated at 37°C in a humidified atmosphere containing 5% CO2. Colonies were counted after 10-14 days.

6.3.3 Cell migration

Cellular ability to migrate was tested via or via Wound healing assay. Transwell migration assay was performed using Transwell chambers (Costar, Cambridge, MA). To evaluate the effect of IGF2BP3 knockout, cells (1×10^5/well) were seeded in the upper compartment in IMDM plus 10% FBS and IMDM plus 10% FBS was placed in the lower compartment of the chamber.

For experiments evaluating chemo-mediated migration, cells (1×105/well) were seeded in the upper compartment in IMDM plus 1% FBS and IMDM plus 1% FBS plus CXCL12 (100 ng/ml) (ab9798, Abcam, Cambridge, UK) or IGF1 (50 ng/ml) (Upstate, Waltham, MA) was placed in the lower compartment of the chamber. To assess migration upon exosomal uptake, cells were pretreated with exosomes isolated from IGF2BP3+ or IGF2BP3- cells for 30 min in IMDM 0% FBS prior to seeding. Cells were incubated for 18 h in a humidified 5% CO2 atmosphere at 37°C. The migrated cells were fixed in absolute methanol, counterstained with Giemsa and counted.

Wound healing assay was performed on A673 shIMP3 cells seeded in in 60 mm Ø dishes coated with fibronectin (3 µg/cm2; Sigma-Aldrich) or on TC-71 cells seeded in 12-well plates coated with fibronectin (3 µg/cm2; Sigma-Aldrich). Cells were allowed to grow until 100% confluence was achieved. A pipette tip was used to obtain the cell free lane. For normoxia/hypoxia experiments, A673 shIMP3 cells were placed in 1% O2 or 21% conditions. To assess migration upon exposure to released IGF2BP3 or exosomal uptake, colture medium was renewed with complete/exosome-depleted supernatants or with purified exosomes from IGF2BP3+ or IGF2BP3- cell lines after the scratch was performed. Images were obtained at time 0 and after 24 h, under an inverted microscope (Zeiss, Inc., Thornwood, NY).

6.4 PROTEIN EVALUATION

6.4.1 Immunofluorescence

For colocalization investigations, cells were seeded on fibronectin-coated coverslips (3 μg/cm2; Sigma-Aldrich) and stimulated after 48h with CXCL12 (100ng/ml) (Abcam).

After washing in PBS, cells were fixed in 4% paraformaldehyde and permeabilized in Triton X-100 0.15%-PBS, blocked in 4% BSA and incubated with the following specific antibodies: anti-CXCR4 primary antibody (ab124824, dilution 1:100, Abcam); anti-CD164 (c-271179, dilution 1:50, Santa Cruz Biotechnologies, Dallas, TX). Anti-rabbit rhodamine (#31686, dilution 1:100, Thermo Scientific) and anti-mouse FITC (#31569, dilution 1:100, Thermo Scientific). Nuclei were counterstained with Hoechst 33258. Images were acquired and analyzed with a Nikon A1R confocal microscope with a Plan Apo 60x/NA 1.4 DIC N2. For exosomal uptake evaluation, exosomes were labelled with the green-fluorescent stain PKH67 (See paragraph 2 "Exosome purification, labelling and characterization").

Cells seeded on fibronectin-coated coverslips (3 μg/cm2; Sigma-Aldrich) were treated with labelled exosomes for 3h, then fixed fixed in 4% paraformaldehyde. Nuclei were counterstained with Hoechst 33258. Images were acquired Nikon ECLIPSE 90i microscope. Analyses were performed using the NIS-Elements software (Nikon, Minato JP).

6.4.2 Immunoblotting analysis

Cellular proteins were collected from cells with a sub-confluence status and lysates were prepared on ice with UPSTATE buffer for phophorilated proteins (50mM Tris-HCl pH 7.4, 150mM NaCl, 1% NP-40, 1mM EDTA, 0.25% sodio deossicolato, 1mM NaF) upon addition of proteases inhibitors (1:100): aprotinin (10μg/ml), leupeptin (0.1mM), PMSF (1mM), sodium orhtovanadate (0.2mM), pepstatin (100μg/ml) and phosphatase inhibitor cocktail (Sigma-Aldrich). After 30 minutes incubation, lysates were centrifuged and proteins from solution fraction were collected. Protein concentration was obtained upon dilution in Bradford Protein Assay (1μl in 999μl) (Bio-Rad laboratories, Hercules, CA) and spectrophotometer reading compared to a standard curve.

Exosomal proteins were collected from purified exosomes and directly quantified with Bradford Protein Assay (Bio-Rad laboratories). Equal amounts of proteins were lysed (1:1 ratio) with RIPA buffer (50 mm Tris-HCl, pH 7.4, 150 mm NaCl, 0.1% sodium dodecyl sulfate (SDS), 1% Triton X-100, 5 mm ethylenediaminetetraacetic acid (EDTA), 1% deoxycholate) supplemented with protease inhibitors.

Equal amounts of protein were analyzed by gel electrophoresis with a 4-15% separation SDS gel (Mini-PROTEAN™ TGX Stain-Free™ Protein Gels, Biorad) under denaturing conditions and transferred onto nitrocellulose membranes (Bio-Rad laboratories). Ponceau (Sigma-Aldrich) staining was used to evaluate transfer quality.

Membranes were blocked for 1 hour at room temperature with milk diluted in TBST (10 mM Tris-HCl ph 7.4, 150 mM NaCl e 0.1% Tween20) and incubated overnight with the following primary antibodies: anti-CALNEXIN (2433, dilution 1:1000, Cell Signaling Technology, Danvers, MA), anti-ALIX (3A9, MA1-83977, diultion 1:1000, Thermo Fisher Scientific), anti-TSG101 (4A10, GTX70255, dilution 1:1000, Genetex, Taiwan), anti-HSP90 α/β (AC88, ab13492, dilution 1:1000, Abcam), anti-IGF1-Rβ (F-1, sc-390130, dilution 1:1000, Santa Cruz Biotechnology), anti-CD164 (F5790, dilution 1:1000, R&D Systems, Minneapolis, MN), anti-CXCR4 (ab124824, dilution 1:1000, Abcam), anti-HIF-1α (sc-10790, dilution 1:2000, Santa Cruz Biotechnology), anti-IGF2BP3 (RN009P, dilution 1:20000, MBL International, Woburn, MA), anti-Phospho ERK 1/2 ({Thr202/Tyr204}, 197G2, dilution 1:1000, Cell Signaling Technology), anti-ERK 1/2 p44/42 (9102, dilution 1:1000, Cell Signaling Technology), anti-Phospho-mTOR ({Ser2448}, 2971, dilution 1:1000, Cell Signaling Technology), anti-mTOR (2972, dilution 1:1000, Cell Signaling Technology), anti-Phospho-AKT ({Ser473}, 736E11, dilution 1:1000, Cell Signaling Technology), anti-AKT (9272, dilution 1:1000, Cell Signaling Technology), and anti-GAPDH (sc-25778, dilution 1:10000, Santa Cruz Biotechnology).

Membranes were then incubated with secondary anti-rabbit (NA934) and anti-mouse (NA9310V, GE Healthcare, Little Chalfont, UK) or anti-sheep (HAF016, R&D Systems) antibodies conjugated to horseradish peroxidase. The proteins were visualized with an ECL Western Blotting Detection System (ThermoFisher Scientific).

6.4.3 ELISA

To evaluate secreted IGF2BP3, $4x10^4$ cells were seeded in 12-well plates. After 96 h, cells were counted for futher data normalization and culture medium was harvested. IGF2BP3 levels in cell supernatants were quantified using a sandwich ELISA kit (Cusabio Technology, Houston, TX), according to the manufacturer's instructions. All samples were examined in duplicate, and the mean values were used for statistical analysis.

6.5 GENE EXPRESSION ANALYSIS

6.5.1 RNA extraction and Reverse Transcription

Extraction of total RNA from snap-frozen tissue samples or from cell lines was conducted with TRIzol (Invitrogen, Carlsbad, CA), a monophasic solution of guanidine isothiocynate and phenol, and purified by precipitation with isopropanol. RNA from exosomes was isolated using ExoQuick® Exosome Isolation and RNA Purification kit (System Bioscience).

RNA quality and quantity were assessed by Nano-Spectrophotometric analysis (Implen™ NanoPhotometer™ N60 Micro-Volume UV-VIS Spectrophotometer, ThermoFisher Scientific). RNA with appropriate 260/280 nm and 260/230 nm absorbance ratios (respectively 1.8-2 and 2-2.3) were considered for reverse transcription to cDNA performed using the High Capacity cDNA Reverse Transcription Kit (Applied Biosystems, Waltham, MA) according to the manufacturer's instructions.

6.5.2 Quantitative Real Time PCR

Quantitative Real-Time PCR was performed on ViiA7 (Life Technologies) using TaqMan or SYBR Geen PCR Master Mix (Life Technologies).

The following predesigned TaqMan assays for target gene were used: IGF2BP3 (Hs00559907_g1), IGF-1Rb (Hs00181385_m1). SYBR Green primers for other target genes were designed using PrimerBlast (Ye et al, 2012): CD164 (Forward: 5′-GAGTGCTGTAGGATTAATTGGAAAAT-3′, Reverse: 5′-GGGAGGAATGGAATTCTGC-3′), CXCR4 (Forward:5′-ACGCCACCAACAGTCAG AG-3′, Reverse: 5′-AGTCGGGAATAGTCAGCAG-3′). Primer Express software (Applied Biosystems) was used to design appropriate primer pairs and probe for reference gene GAPDH: Forward 5'-GAAGGTGAAGGTCGGAGTC-3', Reverse 5'-GAAGATGG TGATGGGATTTC-3' and Probe 5'-CAAGCTTCCCGTTCTCAGCC-3'.

Two replicates per gene were considered. Relative quantification analysis was performed on $2^{-\Delta\Delta Ct}$ method (Livak and Schmittgen, 2001) and the expression levels of each gene were normalized to that of GAPDH.

RT2 Profiler Cancer Inflammation and Immunity Crosstalk PCR Array, profiling 84 genes involved in those pathways, was purchased from Qiagen (Hilden, DE). mRNA profiling for the genes reported in table 4 was carried out according to the manufacturers'instructions and results were analyzed using the online tool https://geneglobe.qiagen.com.

6.5.3 Exosomal miRNA Sequencing

Total exosomal RNA was extracted as previously described and QIAseq miRNA kit was used to sequence miRNAs. MiRNA sequencing libraries were prepared using a single-end, 75bp read lenght protocol. Briefly, adapters are ligated sequentially to the 3' and 5' ends of miRNAs.

During reverse transcription (RT), the primer binds to a region of the 3' adapter and facilitates conversion of the 3'/5' ligated miRNAs into cDNA. After reverse transcription, a cleanup of the cDNA is performed using a streamlined magnetic bead-based method (AMPure XP, Beckman Coulter).

Prior to sequencing, the quality of the synthesis product is assessed by a micro-electrophoretic run on Agilent 2100 Bioanalyzer (Agilent technologies, Santa Clara, CA) with DNA1000 chips and the quantity of the product is assessed via a fluorometric quantification system (Qubit, DNA High Sensitivity kit, Invitrogen). Library concentration is normalized to 4 nM following QIAseq miRNA kit instructions. MiRNA libraries were sequenced on NextSeq500 platform (Illumina, San Diego, CA).

6.5.4 Exosomal miRNA Profiling Analysis

Sequencing result files (".bcl" file, binary format and not viewable) are generated for all the samples in a run and consist of a series of fluorescence images captured and subsequently converted into base calls. These files are demultiplexed into Fastq files, using the bcl2fastq tool provided by Illumina Cloud "Basespace". Demultiplexed Fastq files correspond to the individual biological samples that were sequenced. Quality control of Fastq files was performed using Fastqc Version 0.11.9 (http://www.bioinformatics.babraham.ac.uk/projects/fastqc/).

Given that miRNA-sequencing produces very short reads, accurate alignment requires strict parameters to avoid multiple matches across the reference genome database. Reads were aligned using Burrows-Wheeler Transformation (BWA,Version: 0.7.17) (Li and Durbin, 2009) and Homo_sapiens.GRCh38.dna.primary_assembly.fa as reference genome. After this step we obtained aligned ".BAM" files that store in binary format the aligned sequences.

To assembly and annotate the reads mapped we considered featureCounts (Liao et al, 2014) and hsa.gff3 file (General Feature Format) downloaded form Mirbase database (https://www.mirbase.org/ftp.shtml; Kozomara et al, 2019) as a tab-delimited text format storing annotation of all mature miRNAs sequences.

The output resulted in a list with the number of reads mapping to each mature miRNA. Once the reads mapping to each miRNA were counted, we analyzed the miRNA expression levels and their differentially expression using EdgeR package (Chen et al, 2016). Differentially expression miRNAs with logFC > |0.5| and p-value < 0.05 were selected for further analysis.

MiRabel (Quillet et al, 2020) online tool was used to evaluate experimentally validated or in silico predicted target genes of selected miRNAs. Moreover, miRWalk online target-prediction tool (Sticht et al, 2018), which integrates the information by TargetScan, miRDB and miRTarBase databases (McGeary et al, 2019; Chen and Wang, 2020; Huang et al, 2020), was used to perform target prediction and Gene Onthology Enrichment analysis.

6.6 STATISTICAL ANALYSIS

Differences among means were evaluated by one-way analysis of variance (ANOVA) with Tukey's multiple comparisons test, whereas two-tailed Student's t-test was used for comparisons between two groups. Correlation analysis was performed using Spearman correlation test. Data were considered statistically significant at $p < 0.05$. All statistical analyses were performed using Prism version 6.0 (GraphPad Software, La Jolla, CA).

Pathway	Gene symbol
Immune & Inflammatory Responses	
Immunostimulatory Factors	IFNG, IL12A, IL12B, IL15, IL2, TNF
Immunosuppressive Factors	CD274, CSF2, CTLA4, CXCL12, CXCL5, CXCL8, IDO1, IL10, IL13, IL4, MIF, NOS2, PDCD1, PTGS2, TGFB1, VEGFA
Pro-Inflammatory Genes	CCL2, CCL20, IFNG, IL12A, IL12B, IL17A, IL1A, IL1B, IL2, IL23A, IL6, PTGS2, TLR4, TNF, VEGFA
Anti-Inflammatory Genes	IL10, IL13, IL4, TGFB1
Enzymatic Modulators of Inflammation & Immunity	AICDA, GZMA, GZMB, IDO1, NOS2, PTGS2
Antigen Presentation	HLA-A, HLA-B, HLA-C, MICA, MICB
Chemokines	CCL18, CCL2, CCL20, CCL21, CCL22, CCL28, CCL4, CCL5, CXCL1, CXCL10, CXCL11, CXCL12, CXCL2, CXCL5, CXCL9
Chemokine Receptors	ACKR3, CCR1, CCR10, CCR2, CCR4, CCR7, CCR9, CXCR1, CXCR2, CXCR3, CXCR4, CXCR5
Interleukins	CXCL8, IL10, IL12A, IL12B, IL13, IL15, IL17A, IL1A, IL1B, IL2, IL23A, IL4, IL6
Other Cytokines	KITLG, MIF, SPP1, TNF, TNFSF10
Growth Factors & Receptors	CSF1, CSF2, CSF3, EGF, EGFR, IGF1, TGFB1, VEGFA
Signal Transduction	
Interferon Signaling	GBP1, IFNG, IL6, IRF1.
Interferon-Responsive Genes	CCL2, CCL5, CXCL10, CXCL9, GBP1, IRF1, MYD88, STAT1, TLR3, TNFSF10
NFκB Targets	BCL2L1, CCL2, CCL5, CSF1, CSF2, CSF3, CXCL8, IFNG, TNF.
STAT Targets	CCL2, CCL4, CCL5, CSF1, CSF2, CSF3, CXCL10, CXCL11, CXCL12, CXCL8, CXCL9, IL10, IL17A, IL1B, IL23A, IL6, MYC
Tollo-Like Receptor Segnalino	MYD88, TLR2, TLR3, TLR4
Transcription Factors	FOXP3, HIF1A, IRF1, MYC, NFKB1, STAT1, STAT3, TP53
Apoptosis	
Pro-Apoptotic	FASLG, TNF, TNFSF10, TP53
Anti-Apoptotic	BCL2, BCL2L1, MYC, STAT3

Table 6. *Genes profiled by RT2 Profiler Cancer Inflammation and Immunity Crosstalk PCR Array*

7 BIBLIOGRAPHY

1.
Adeshakin FO, Adeshakin AO, Afolabi LO, Yan D, Zhang G, Wan X. Mechanisms for Modulating Anoikis Resistance in Cancer and the Relevance of Metabolic Reprogramming. Frontiers in Oncology [Internet]. 2021 [cited 2022 Jan 23];11. Available from: https://www.frontiersin.org/article/10.3389/fonc.2021.626577
2.
Admyre C, Johansson SM, Qazi KR, Filén J-J, Lahesmaa R, Norman M, et al. Exosomes with immune modulatory features are present in human breast milk. J Immunol. 2007;179:1969–78.
3.
Al-Nedawi K, Meehan B, Micallef J, Lhotak V, May L, Guha A, et al. Intercellular transfer of the oncogenic receptor EGFRvIII by microvesicles derived from tumor cells. Nat Cell Biol. 2008;10:619–24.
4.
Alkasalias T, Moyano-Galceran L, Arsenian-Henriksson M, Lehti K. Fibroblasts in the Tumor Microenvironment: Shield or Spear? Int J Mol Sci. 2018;19:E1532.
5.
Alzahrani FA, El-Magd MA, Abdelfattah-Hassan A, Saleh AA, Saadeldin IM, El-Shetry ES, et al. Potential Effect of Exosomes Derived from Cancer Stem Cells and MSCs on Progression of DEN-Induced HCC in Rats. Stem Cells Int. 2018;2018:8058979.
6.
Ambros IM, Ambros PF, Strehl S, Kovar H, Gadner H, Salzer-Kuntschik M. MIC2 is a specific marker for Ewing's sarcoma and peripheral primitive neuroectodermal tumors. Evidence for a common histogenesis of Ewing's sarcoma and peripheral primitive neuroectodermal tumors from MIC2 expression and specific chromosome aberration. Cancer. 1991;67:1886–93.
7.
Ambros IM, Ambros PF, Strehl S, Kovar H, Gadner H, Salzer-Kuntschik M. MIC2 is a specific marker for Ewing's sarcoma and peripheral primitive neuroectodermal tumors. Evidence for a common histogenesis of Ewing's sarcoma and peripheral primitive neuroectodermal tumors from MIC2 expression and specific chromosome aberration. Cancer. 1991;67:1886–93.
8.
Antonescu CR, Owosho AA, Zhang L, Chen S, Deniz K, Huryn JM, et al. Sarcomas With CIC-rearrangements Are a Distinct Pathologic Entity With Aggressive Outcome: A Clinicopathologic and Molecular Study of 115 Cases. Am J Surg Pathol. 2017;41:941–9.
9.
Arvand A, Denny CT. Biology of EWS/ETS fusions in Ewing's family tumors. Oncogene. 2001;20:5747–54.
10.
Aspord C, Pedroza-Gonzalez A, Gallegos M, Tindle S, Burton EC, Su D, et al. Breast cancer instructs dendritic cells to prime interleukin 13-secreting CD4+ T cells that facilitate tumor development. J Exp Med. 2007;204:1037–47.
11.
Atiya H, Frisbie L, Pressimone C, Coffman L. Mesenchymal Stem Cells in the Tumor Microenvironment. Adv Exp Med Biol. 2020;1234:31–42.
12.
Au Yeung CL, Co N-N, Tsuruga T, Yeung T-L, Kwan S-Y, Leung CS, et al. Exosomal transfer of stroma-derived miR21 confers paclitaxel resistance in ovarian cancer cells through targeting APAF1. Nat Commun. 2016;7:11150.
13.
Baghban R, Roshangar L, Jahanban-Esfahlan R, Seidi K, Ebrahimi-Kalan A, Jaymand M, et al. Tumor microenvironment complexity and therapeutic implications at a glance. Cell Commun Signal. 2020;18:59.

14.
Bailey KM, Airik M, Krook MA, Pedersen EA, Lawlor ER. Micro-Environmental Stress Induces Src-Dependent Activation of Invadopodia and Cell Migration in Ewing Sarcoma. Neoplasia. 2016;18:480–8.
15.
Balaji S, Kim U, Muthukkaruppan V, Vanniarajan A. Emerging role of tumor microenvironment derived exosomes in therapeutic resistance and metastasis through epithelial-to-mesenchymal transition. Life Sci. 2021;280:119750.
16.
Balestra T, Manara MC, Laginestra MA, Pasello M, De Feo A, Bassi C, et al. Targeting CD99 Compromises the Oncogenic Effects of the Chimera EWS-FLI1 by Inducing Reexpression of Zyxin and Inhibition of GLI1 Activity. Mol Cancer Ther. 2022;21:58–69.
17.
Ban J, Jug G, Mestdagh P, Schwentner R, Kauer M, Aryee DNT, et al. Hsa-mir-145 is the top EWS-FLI1-repressed microRNA involved in a positive feedback loop in Ewing's sarcoma. Oncogene. 2011;30:2173–80.
18.
Bao L, You B, Shi S, Shan Y, Zhang Q, Yue H, et al. Metastasis-associated miR-23a from nasopharyngeal carcinoma-derived exosomes mediates angiogenesis by repressing a novel target gene TSGA10. Oncogene. 2018;37:2873–89.
19.
Barghash A, Helms V, Kessler SM. Overexpression of IGF2 mRNA-Binding Protein 2 (IMP2/p62) as a Feature of Basal-like Breast Cancer Correlates with Short Survival. Scand J Immunol. 2015;82:142–3.
20.
Barghash A, Golob-Schwarzl N, Helms V, Haybaeck J, Kessler SM. Elevated expression of the IGF2 mRNA binding protein 2 (IGF2BP2/IMP2) is linked to short survival and metastasis in esophageal adenocarcinoma. Oncotarget. 2016;7:49743–50.
21.
Baroni S, Romero-Cordoba S, Plantamura I, Dugo M, D'Ippolito E, Cataldo A, et al. Exosome-mediated delivery of miR-9 induces cancer-associated fibroblast-like properties in human breast fibroblasts. Cell Death Dis. 2016;7:e2312.
22.
Bastid J, Regairaz A, Bonnefoy N, Déjou C, Giustiniani J, Laheurte C, et al. Inhibition of CD39 enzymatic function at the surface of tumor cells alleviates their immunosuppressive activity. Cancer Immunol Res. 2015;3:254–65.
23.
Batlle E, Clevers H. Cancer stem cells revisited. Nat Med. 2017;23:1124–34.
24.
Bauer AL, Jackson TL, Jiang Y. Topography of extracellular matrix mediates vascular morphogenesis and migration speeds in angiogenesis. PLoS Comput Biol. 2009;5:e1000445.
25.
Beauchamp E, Bulut G, Abaan O, Chen K, Merchant A, Matsui W, et al. GLI1 is a direct transcriptional target of EWS-FLI1 oncoprotein. J Biol Chem. 2009;284:9074–82.
26.
Belgiovine C, D'Incalci M, Allavena P, Frapolli R. Tumor-associated macrophages and anti-tumor therapies: complex links. Cell Mol Life Sci. 2016;73:2411–24.
27.
Bell JL, Turlapati R, Liu T, Schulte JH, Hüttelmaier S. IGF2BP1 harbors prognostic significance by gene gain and diverse expression in neuroblastoma. J Clin Oncol. 2015;33:1285–93.
28.

Bell JL, Wächter K, Mühleck B, Pazaitis N, Köhn M, Lederer M, et al. Insulin-like growth factor 2 mRNA-binding proteins (IGF2BPs): post-transcriptional drivers of cancer progression? Cell Mol Life Sci. 2013;70:2657–75.
29.
Benini S, Manara MC, Baldini N, Cerisano V, Massimo Serra null, Mercuri M, et al. Inhibition of insulin-like growth factor I receptor increases the anti-tumor activity of doxorubicin and vincristine against Ewing's sarcoma cells. Clin Cancer Res. 2001;7:1790–7.
30.
Bennani-Baiti IM, Cooper A, Lawlor ER, Kauer M, Ban J, Aryee DNT, et al. Intercohort gene expression co-analysis reveals chemokine receptors as prognostic indicators in Ewing's sarcoma. Clin Cancer Res. 2010;16:3769–78.
31.
Berghuis D, Santos SJ, Baelde HJ, Taminiau AH, Egeler RM, Schilham MW, et al. Pro-inflammatory chemokine-chemokine receptor interactions within the Ewing sarcoma microenvironment determine CD8(+) T-lymphocyte infiltration and affect tumor progression. J Pathol. 2011;223:347–57.
32.
Bhargava S, Visvanathan A, Patil V, Kumar A, Kesari S, Das S, et al. IGF2 mRNA binding protein 3 (IMP3) promotes glioma cell migration by enhancing the translation of RELA/p65. Oncotarget. 2017;8:40469–85.
33.
Bhattacharya S, Michels CL, Leung M-K, Arany ZP, Kung AL, Livingston DM. Functional role of p35srj, a novel p300/CBP binding protein, during transactivation by HIF-1. Genes Dev. 1999;13:64–75.
34.
Blanc L, Vidal M. New insights into the function of Rab GTPases in the context of exosomal secretion. Small GTPases. 2018;9:95–106.
35.
Bonnans C, Chou J, Werb Z. Remodelling the extracellular matrix in development and disease. Nat Rev Mol Cell Biol. 2014;15:786–801.
36.
Bot I, Guo J, Van Eck M, Van Santbrink PJ, Groot PHE, Hildebrand RB, et al. Lentiviral shRNA silencing of murine bone marrow cell CCR2 leads to persistent knockdown of CCR2 function in vivo. Blood. 2005;106:1147–53.
37.
Boyerinas B, Park S-M, Shomron N, Hedegaard MM, Vinther J, Andersen JS, et al. Identification of let-7-regulated oncofetal genes. Cancer Res. 2008;68:2587–91.
38.
Bradford N, Cashion C, Condon P, Rumble S, Bowers A. Recruitment principles and strategies for supportive care research in pediatric oncology. BMC Med Res Methodol. 2021;21:178.
39.
Brenner JC, Feng FY, Han S, Patel S, Goyal SV, Bou-Maroun LM, et al. PARP-1 inhibition as a targeted strategy to treat Ewing's sarcoma. Cancer Res. 2012;72:1608–13.
40.
Buratta S, Tancini B, Sagini K, Delo F, Chiaradia E, Urbanelli L, et al. Lysosomal Exocytosis, Exosome Release and Secretory Autophagy: The Autophagic- and Endo-Lysosomal Systems Go Extracellular. Int J Mol Sci. 2020;21:E2576.
41.
Bussard KM, Mutkus L, Stumpf K, Gomez-Manzano C, Marini FC. Tumor-associated stromal cells as key contributors to the tumor microenvironment. Breast Cancer Res. 2016;18:84.
42.

Canella A, Cordero Nieves H, Sborov DW, Cascione L, Radomska HS, Smith E, et al. HDAC inhibitor AR-42 decreases CD44 expression and sensitizes myeloma cells to lenalidomide. Oncotarget. 2015;6:31134–50.
43.
Cao J, Mu Q, Huang H. The Roles of Insulin-Like Growth Factor 2 mRNA-Binding Protein 2 in Cancer and Cancer Stem Cells. Stem Cells Int. 2018;2018:4217259.
44.
Cao W, Zeng Z, He Z, Lei S. Hypoxic pancreatic stellate cell-derived exosomal mirnas promote proliferation and invasion of pancreatic cancer through the PTEN/AKT pathway. Aging (Albany NY). 2021;13:7120–32.
45.
Carrabotta M, Laginestra MA, Durante G, Mancarella C, Landuzzi L, Parra A, et al. Integrated molecular characterization of patient-derived models reveals therapeutic strategies for treating CIC-DUX4 sarcoma. Cancer Res. 2021;canres.1222.2021.
46.
Casali PG, Bielack S, Abecassis N, Aro HT, Bauer S, Biagini R, et al. Bone sarcomas: ESMO-PaedCan-EURACAN Clinical Practice Guidelines for diagnosis, treatment and follow-up. Ann Oncol. 2018;29:iv79–95.
47.
Cen W-N, Pang J-S, Huang J-C, Hou J-Y, Bao W-G, He R-Q, et al. The expression and biological information analysis of miR-375-3p in head and neck squamous cell carcinoma based on 1825 samples from GEO, TCGA, and peer-reviewed publications. Pathol Res Pract. 2018;214:1835–47.
48.
Chairoungdua A, Smith DL, Pochard P, Hull M, Caplan MJ. Exosome release of β-catenin: a novel mechanism that antagonizes Wnt signaling. J Cell Biol. 2010;190:1079–91.
49.
Chang C-C, Campoli M, Ferrone S. Classical and nonclassical HLA class I antigen and NK Cell-activating ligand changes in malignant cells: current challenges and future directions. Adv Cancer Res. 2005;93:189–234.
50.
Chansky HA, Barahmand-Pour F, Mei Q, Kahn-Farooqi W, Zielinska-Kwiatkowska A, Blackburn M, et al. Targeting of EWS/FLI-1 by RNA interference attenuates the tumor phenotype of Ewing's sarcoma cells in vitro. J Orthop Res. 2004;22:910–7.
51.
Chao JA, Patskovsky Y, Patel V, Levy M, Almo SC, Singer RH. ZBP1 recognition of beta-actin zipcode induces RNA looping. Genes Dev. 2010;24:148–58.
52.
Chatterjee S, Azad BB, Nimmagadda S. The Intricate Role of CXCR4 in Cancer. Adv Cancer Res. 2014;124:31–82.
53.
Chen C-L, Tsukamoto H, Liu J-C, Kashiwabara C, Feldman D, Sher L, et al. Reciprocal regulation by TLR4 and TGF-β in tumor-initiating stem-like cells. J Clin Invest. 2013;123:2832–49.
54.
Chen G, Huang AC, Zhang W, Zhang G, Wu M, Xu W, et al. Exosomal PD-L1 contributes to immunosuppression and is associated with anti-PD-1 response. Nature. 2018;560:382–6.
55.
Chen G, Kim YH, Li H, Luo H, Liu D-L, Zhang Z-J, et al. PD-L1 inhibits acute and chronic pain by suppressing nociceptive neuron activity via PD-1. Nat Neurosci. 2017;20:917–26.
56.

Chen Q, Li T, Yue W. Drug response to PD-1/PD-L1 blockade: based on biomarkers. Onco Targets Ther. 2018;11:4673–83.
57.
Chen S, Deniz K, Sung Y-S, Zhang L, Dry S, Antonescu CR. Ewing sarcoma with ERG gene rearrangements: A molecular study focusing on the prevalence of FUS-ERG and common pitfalls in detecting EWSR1-ERG fusions by FISH. Genes Chromosomes Cancer. 2016;55:340–9.
58.
Chen W, Chen M, Xu Y, Chen X, Zhou P, Zhao X, et al. Long non-coding RNA THOR promotes human osteosarcoma cell growth in vitro and in vivo. Biochem Biophys Res Commun. 2018;499:913–9.
59.
Chen W-L, Huang A-F, Huang S-M, Ho C-L, Chang Y-L, Chan JY-H. CD164 promotes lung tumor-initiating cells with stem cell activity and determines tumor growth and drug resistance via Akt/mTOR signaling. Oncotarget. 2017;8:54115–35.
60.
Chen Y, Wang X. miRDB: an online database for prediction of functional microRNA targets. Nucleic Acids Res. 2020;48:D127–31.
61.
Chen Y, Lun ATL, Smyth GK. From reads to genes to pathways: differential expression analysis of RNA-Seq experiments using Rsubread and the edgeR quasi-likelihood pipeline. F1000Res. 2016;5:1438.
62.
Cheng KC, Loeb LA. Genomic instability and tumor progression: mechanistic considerations. Adv Cancer Res. 1993;60:121–56.
63.
Cheng Z-H, Luo C, Guo Z-L. MicroRNA-130b-5p accelerates the migration and invasion of osteosarcoma via binding to TIMP2. Eur Rev Med Pharmacol Sci. 2021;25:2461.
64.
Chittezhath M, Dhillon MK, Lim JY, Laoui D, Shalova IN, Teo YL, et al. Molecular profiling reveals a tumor-promoting phenotype of monocytes and macrophages in human cancer progression. Immunity. 2014;41:815–29.
65.
Cho JA, Park H, Lim EH, Lee KW. Exosomes from breast cancer cells can convert adipose tissue-derived mesenchymal stem cells into myofibroblast-like cells. Int J Oncol. 2012;40:130–8.
66.
Chow A, Zhou W, Liu L, Fong MY, Champer J, Van Haute D, et al. Macrophage immunomodulation by breast cancer-derived exosomes requires Toll-like receptor 2-mediated activation of NF-κB. Sci Rep. 2014;4:5750.
67.
Chowdhury R, Webber JP, Gurney M, Mason MD, Tabi Z, Clayton A. Cancer exosomes trigger mesenchymal stem cell differentiation into pro-angiogenic and pro-invasive myofibroblasts. Oncotarget. 2015;6:715–31.
68.
Cipriani P, Di Benedetto P, Ruscitti P, Capece D, Zazzeroni F, Liakouli V, et al. The Endothelial-mesenchymal Transition in Systemic Sclerosis Is Induced by Endothelin-1 and Transforming Growth Factor-β and May Be Blocked by Macitentan, a Dual Endothelin-1 Receptor Antagonist. J Rheumatol. 2015;42:1808–16.
69.
Cirri P, Chiarugi P. Cancer associated fibroblasts: the dark side of the coin. Am J Cancer Res. 2011;1:482–97.
70.
Clancy JW, Schmidtmann M, D'Souza-Schorey C. The ins and outs of microvesicles. FASEB Bioadv. 2021;3:399–406.
71.

Clayton A, Al-Taei S, Webber J, Mason MD, Tabi Z. Cancer exosomes express CD39 and CD73, which suppress T cells through adenosine production. J Immunol. 2011;187:676–83.
72.
Cleynen I, Brants JR, Peeters K, Deckers R, Debiec-Rychter M, Sciot R, et al. HMGA2 regulates transcription of the Imp2 gene via an intronic regulatory element in cooperation with nuclear factor-kappaB. Mol Cancer Res. 2007;5:363–72.
73.
Cleynen I, Brants JR, Peeters K, Deckers R, Debiec-Rychter M, Sciot R, et al. HMGA2 regulates transcription of the Imp2 gene via an intronic regulatory element in cooperation with nuclear factor-kappaB. Mol Cancer Res. 2007;5:363–72.
74.
Conway AE, Van Nostrand EL, Pratt GA, Aigner S, Wilbert ML, Sundararaman B, et al. Enhanced CLIP Uncovers IMP Protein-RNA Targets in Human Pluripotent Stem Cells Important for Cell Adhesion and Survival. Cell Rep. 2016;15:666–79.
75.
Coppin L, Leclerc J, Vincent A, Porchet N, Pigny P. Messenger RNA Life-Cycle in Cancer Cells: Emerging Role of Conventional and Non-Conventional RNA-Binding Proteins? Int J Mol Sci. 2018;19:E650.
76.
Cossetti C, Iraci N, Mercer TR, Leonardi T, Alpi E, Drago D, et al. Extracellular vesicles from neural stem cells transfer IFN-γ via Ifngr1 to activate Stat1 signaling in target cells. Mol Cell. 2014;56:193–204.
77.
Coste C, Neirinckx V, Sharma A, Agirman G, Rogister B, Foguenne J, et al. Human bone marrow harbors cells with neural crest-associated characteristics like human adipose and dermis tissues. PLoS One. 2017;12:e0177962.
78.
Crompton BD, Stewart C, Taylor-Weiner A, Alexe G, Kurek KC, Calicchio ML, et al. The genomic landscape of pediatric Ewing sarcoma. Cancer Discov. 2014;4:1326–41.
79.
Dai N, Christiansen J, Nielsen FC, Avruch J. mTOR complex 2 phosphorylates IMP1 cotranslationally to promote IGF2 production and the proliferation of mouse embryonic fibroblasts. Genes Dev. 2013;27:301–12.
80.
Dai N, Rapley J, Angel M, Yanik MF, Blower MD, Avruch J. mTOR phosphorylates IMP2 to promote IGF2 mRNA translation by internal ribosomal entry. Genes Dev. 2011;25:1159–72.
81.
Dai N, Zhao L, Wrighting D, Krämer D, Majithia A, Wang Y, et al. IGF2BP2/IMP2-Deficient mice resist obesity through enhanced translation of Ucp1 mRNA and Other mRNAs encoding mitochondrial proteins. Cell Metab. 2015;21:609–21.
82.
Das K, Prasad R, Singh A, Bhattacharya A, Roy A, Mallik S, et al. Protease-activated receptor 2 promotes actomyosin dependent transforming microvesicles generation from human breast cancer. Mol Carcinog. 2018;57:1707–22.
83.
Dawson MA, Prinjha RK, Dittmann A, Giotopoulos G, Bantscheff M, Chan W-I, et al. Inhibition of BET recruitment to chromatin as an effective treatment for MLL-fusion leukaemia. Nature. 2011;478:529–33.
84.
de Alava E, Kawai A, Healey JH, Fligman I, Meyers PA, Huvos AG, et al. EWS-FLI1 fusion transcript structure is an independent determinant of prognosis in Ewing's sarcoma. J Clin Oncol. 1998;16:1248–55.
85.

De Feo A, Sciandra M, Ferracin M, Felicetti F, Astolfi A, Pignochino Y, et al. Exosomes from CD99-deprived Ewing sarcoma cells reverse tumor malignancy by inhibiting cell migration and promoting neural differentiation. Cell Death Dis. 2019;10:471.
86.
de Visser KE, Eichten A, Coussens LM. Paradoxical roles of the immune system during cancer development. Nat Rev Cancer. 2006;6:24–37.
87.
De Vito C, Riggi N, Suvà M-L, Janiszewska M, Horlbeck J, Baumer K, et al. Let-7a is a direct EWS-FLI-1 target implicated in Ewing's sarcoma development. PLoS One. 2011;6:e23592.
88.
De Wever O, Demetter P, Mareel M, Bracke M. Stromal myofibroblasts are drivers of invasive cancer growth. Int J Cancer. 2008;123:2229–38.
89.
Degrauwe N, Schlumpf TB, Janiszewska M, Martin P, Cauderay A, Provero P, et al. The RNA Binding Protein IMP2 Preserves Glioblastoma Stem Cells by Preventing let-7 Target Gene Silencing. Cell Rep. 2016;15:1634–47.
90.
Degrauwe N, Suvà M-L, Janiszewska M, Riggi N, Stamenkovic I. IMPs: an RNA-binding protein family that provides a link between stem cell maintenance in normal development and cancer. Genes Dev. 2016;30:2459–74.
91.
Delattre O, Zucman J, Plougastel B, Desmaze C, Melot T, Peter M, et al. Gene fusion with an ETS DNA-binding domain caused by chromosome translocation in human tumors. Nature. 1992;359:162–5.
92.
Delorme-Axford E, Donker RB, Mouillet J-F, Chu T, Bayer A, Ouyang Y, et al. Human placental trophoblasts confer viral resistance to recipient cells. Proc Natl Acad Sci U S A. 2013;110:12048–53.
93.
DeNardo DG, Barreto JB, Andreu P, Vasquez L, Tawfik D, Kolhatkar N, et al. CD4(+) T cells regulate pulmonary metastasis of mammary carcinomas by enhancing pro-tumor properties of macrophages. Cancer Cell. 2009;16:91–102.
94.
Dengler VL, Galbraith M, Espinosa JM. Transcriptional Regulation by Hypoxia Inducible Factors. Crit Rev Biochem Mol Biol. 2014;49:1–15.
95.
Deregibus MC, Cantaluppi V, Calogero R, Lo Iacono M, Tetta C, Biancone L, et al. Endothelial progenitor cell derived microvesicles activate an angiogenic program in endothelial cells by a horizontal transfer of mRNA. Blood. 2007;110:2440–8.
96.
Ding J, Xu Z, Zhang Y, Tan C, Hu W, Wang M, et al. Exosome-mediated miR-222 transferring: An insight into NF-κB-mediated breast cancer metastasis. Exp Cell Res. 2018;369:129–38.
97.
Dirat B, Bochet L, Dabek M, Daviaud D, Dauvillier S, Majed B, et al. Cancer-associated adipocytes exhibit an activated phenotype and contribute to breast cancer invasion. Cancer Res. 2011;71:2455–65.
98.
Direkze NC, Hodivala-Dilke K, Jeffery R, Hunt T, Poulsom R, Oukrif D, et al. Bone marrow contribution to tumor-associated myofibroblasts and fibroblasts. Cancer Res. 2004;64:8492–5.
99.

Donnarumma E, Fiore D, Nappa M, Roscigno G, Adamo A, Iaboni M, et al. Cancer-associated fibroblasts release exosomal microRNAs that dictate an aggressive phenotype in breast cancer. Oncotarget. 2017;8:19592–608.
100.
Doudna JA, Charpentier E. Genome editing. The new frontier of genome engineering with CRISPR-Cas9. Science. 2014;346:1258096.
101.
Doyle GA, Betz NA, Leeds PF, Fleisig AJ, Prokipcak RD, Ross J. The c-myc coding region determinant-binding protein: a member of a family of KH domain RNA-binding proteins. Nucleic Acids Res. 1998;26:5036–44.
102.
Doyle LA. Sarcoma classification: an update based on the 2013 World Health Organization Classification of Tumors of Soft Tissue and Bone. Cancer. 2014;120:1763–74.
103.
Doyle LA. Sarcoma classification: an update based on the 2013 World Health Organization Classification of Tumors of Soft Tissue and Bone. Cancer. 2014;120:1763–74.
104.
Du S, McCall N, Park K, Guan Q, Fontina P, Ertel A, et al. Blockade of Tumor-Expressed PD-1 promotes lung cancer growth. Oncoimmunology. 2018;7:e1408747.
105.
DuBois SG, Krailo MD, Gebhardt MC, Donaldson SS, Marcus KJ, Dormans J, et al. Comparative evaluation of local control strategies in localized Ewing sarcoma of bone: a report from the Children's Oncology Group. Cancer. 2015;121:467–75.
106.
Dvorak HF. Tumors: wounds that do not heal. Similarities between tumor stroma generation and wound healing. N Engl J Med. 1986;315:1650–9.
107.
Dylla L, Moore C, Jedlicka P. MicroRNAs in Ewing Sarcoma. Front Oncol. 2013;3:65.
108.
Eden RE, Coviello JM. Chronic Myelogenous Leukemia. StatPearls [Internet]. Treasure Island (FL): StatPearls Publishing; 2022 [cited 2022 Jan 24]. Available from: http://www.ncbi.nlm.nih.gov/books/NBK531459/
109.
Eden RE, Coviello JM. Chronic Myelogenous Leukemia. StatPearls [Internet]. Treasure Island (FL): StatPearls Publishing; 2022 [cited 2022 Jan 26]. Available from: http://www.ncbi.nlm.nih.gov/books/NBK531459/
110.
El-Naggar AM, Veinotte CJ, Cheng H, Grunewald TGP, Negri GL, Somasekharan SP, et al. Translational Activation of HIF1α by YB-1 Promotes Sarcoma Metastasis. Cancer Cell. 2015;27:682–97.
111.
Elagib KE, Lu C-H, Mosoyan G, Khalil S, Zasadzińska E, Foltz DR, et al. Neonatal expression of RNA-binding protein IGF2BP3 regulates the human fetal-adult megakaryocyte transition. J Clin Invest. 2017;127:2365–77.
112.
Embree LJ, Azuma M, Hickstein DD. Ewing sarcoma fusion protein EWSR1/FLI1 interacts with EWSR1 leading to mitotic defects in zebrafish embryos and human cell lines. Cancer Res. 2009;69:4363–71.
113.
Ennajdaoui H, Howard JM, Sterne-Weiler T, Jahanbani F, Coyne DJ, Uren PJ, et al. IGF2BP3 Modulates the Interaction of Invasion-Associated Transcripts with RISC. Cell Rep. 2016;15:1876–83.
114.

Eom T, Antar LN, Singer RH, Bassell GJ. Localization of a beta-actin messenger ribonucleoprotein complex with zipcode-binding protein modulates the density of dendritic filopodia and filopodial synapses. J Neurosci. 2003;23:10433–44.
115.
Erez N, Truitt M, Olson P, Arron ST, Hanahan D. Cancer-Associated Fibroblasts Are Activated in Incipient Neoplasia to Orchestrate Tumor-Promoting Inflammation in an NF-kappaB-Dependent Manner. Cancer Cell. 2010;17:135–47.
116.
Erkizan HV, Kong Y, Merchant M, Schlottmann S, Barber-Rotenberg JS, Yuan L, et al. A small molecule blocking oncogenic protein EWS-FLI1 interaction with RNA helicase A inhibits growth of Ewing's sarcoma. Nat Med. 2009;15:750–6.
117.
Esiashvili N, Goodman M, Marcus RB. Changes in incidence and survival of Ewing sarcoma patients over the past 3 decades: Surveillance Epidemiology and End Results data. J Pediatr Hematol Oncol. 2008;30:425–30.
118.
Ewing J. Classics in oncology. Diffuse endothelioma of bone. James Ewing. Proceedings of the New York Pathological Society, 1921. CA Cancer J Clin. 1972;22:95–8.
119.
Farina KL, Huttelmaier S, Musunuru K, Darnell R, Singer RH. Two ZBP1 KH domains facilitate beta-actin mRNA localization, granule formation, and cytoskeletal attachment. J Cell Biol. 2003;160:77–87.
120.
Faye MD, Beug ST, Graber TE, Earl N, Xiang X, Wild B, et al. IGF2BP1 controls cell death and drug resistance in rhabdomyosarcomas by regulating translation of cIAP1. Oncogene. 2015;34:1532–41.
121.
Felicetti F, Parolini I, Bottero L, Fecchi K, Errico MC, Raggi C, et al. Caveolin-1 tumor-promoting role in human melanoma. Int J Cancer. 2009;125:1514–22.
122.
Feng Q, Zhang C, Lum D, Druso JE, Blank B, Wilson KF, et al. A class of extracellular vesicles from breast cancer cells activates VEGF receptors and tumor angiogenesis. Nat Commun. 2017;8:14450.
123.
Ferrari A, Dirksen U, Bielack S. Sarcomas of Soft Tissue and Bone. Tumors in Adolescents and Young Adults. Karger Publishers; 2016;43:128–41.
124.
Figueroa JM, Skog J, Akers J, Li H, Komotar R, Jensen R, et al. Detection of wild-type EGFR amplification and EGFRvIII mutation in CSF-derived extracellular vesicles of glioblastoma patients. Neuro Oncol. 2017;19:1494–502.
125.
Filippakopoulos P, Qi J, Picaud S, Shen Y, Smith WB, Fedorov O, et al. Selective inhibition of BET bromodomains. Nature. 2010;468:1067–73.
126.
Folpe AL, Goldblum JR, Rubin BP, Shehata BM, Liu W, Dei Tos AP, et al. Morphologic and immunophenotypic diversity in Ewing family tumors: a study of 66 genetically confirmed cases. Am J Surg Pathol. 2005;29:1025–33.
127.
Forde S, Tye BJ, Newey SE, Roubelakis M, Smythe J, McGuckin CP, et al. Endolyn (CD164) modulates the CXCL12-mediated migration of umbilical cord blood CD133+ cells. Blood. 2007;109:1825–33.
128.
Fouad YA, Aanei C. Revisiting the hallmarks of cancer. Am J Cancer Res. 2017;7:1016–36.

129.
Franzetti G-A, Laud-Duval K, van der Ent W, Brisac A, Irondelle M, Aubert S, et al. Cell-to-cell heterogeneity of EWSR1-FLI1 activity determines proliferation/migration choices in Ewing sarcoma cells. Oncogene. 2017;36:3505–14.
130.
Fridlender ZG, Sun J, Kim S, Kapoor V, Cheng G, Ling L, et al. Polarization of tumor-associated neutrophil phenotype by TGF-beta: "N1" versus "N2" TAN. Cancer Cell. 2009;16:183–94.
131.
Fujiwara T, Fukushi J, Yamamoto S, Matsumoto Y, Setsu N, Oda Y, et al. Macrophage infiltration predicts a poor prognosis for human ewing sarcoma. Am J Pathol. 2011;179:1157–70.
132.
Gaggioli C, Hooper S, Hidalgo-Carcedo C, Grosse R, Marshall JF, Harrington K, et al. Fibroblast-led collective invasion of carcinoma cells with differing roles for RhoGTPases in leading and following cells. Nat Cell Biol. 2007;9:1392–400.
133.
Galindo-Hernandez O, Serna-Marquez N, Castillo-Sanchez R, Salazar EP. Extracellular vesicles from MDA-MB-231 breast cancer cells stimulated with linoleic acid promote an EMT-like process in MCF10A cells. Prostaglandins Leukot Essent Fatty Acids. 2014;91:299–310.
134.
Galon J, Costes A, Sanchez-Cabo F, Kirilovsky A, Mlecnik B, Lagorce-Pagès C, et al. Type, density, and location of immune cells within human colorectal tumors predict clinical outcome. Science. 2006;313:1960–4.
135.
Gambarotti M, Benini S, Gamberi G, Cocchi S, Palmerini E, Sbaraglia M, et al. CIC-DUX4 fusion-positive round-cell sarcomas of soft tissue and bone: a single-institution morphological and molecular analysis of seven cases. Histopathology. 2016;69:624–34.
136.
Gangwal K, Close D, Enriquez CA, Hill CP, Lessnick SL. Emergent Properties of EWS/FLI Regulation via GGAA Microsatellites in Ewing's Sarcoma. Genes Cancer. 2010;1:177–87.
137.
Gao Y, Yang M, Jiang Z, Woda BA, Mercurio AM, Qin J, et al. IMP3 expression is associated with poor outcome and epigenetic deregulation in intrahepatic cholangiocarcinoma. Hum Pathol. 2014;45:1184–91.
138.
Garnier D, Magnus N, Meehan B, Kislinger T, Rak J. Qualitative changes in the proteome of extracellular vesicles accompanying cancer cell transition to mesenchymal state. Exp Cell Res. 2013;319:2747–57.
139.
Gaspar N, Hawkins DS, Dirksen U, Lewis IJ, Ferrari S, Le Deley M-C, et al. Ewing Sarcoma: Current Management and Future Approaches Through Collaboration. J Clin Oncol. 2015;33:3036–46.
140.
Gassmann H, Schneider K, Evdokimova V, Ruzanov P, Schober SJ, Xue B, et al. Ewing Sarcoma-Derived Extracellular Vesicles Impair Dendritic Cell Maturation and Function. Cells. 2021;10:2081.
141.
Ghaemmaghami AB, Mahjoubin-Tehran M, Movahedpour A, Morshedi K, Sheida A, Taghavi SP, et al. Role of exosomes in malignant glioma: microRNAs and proteins in pathogenesis and diagnosis. Cell Commun Signal. 2020;18:120.

142.
Ghoshal A, Rodrigues LC, Gowda CP, Elcheva IA, Liu Z, Abraham T, Spiegelman VS. Extracellular vesicle-dependent effect of RNA-binding protein IGF2BP1 on melanoma metastasis. Oncogene. 2019 May; 38(21):4182-4196.
143.
Ginsberg JP, de Alava E, Ladanyi M, Wexler LH, Kovar H, Paulussen M, et al. EWS-FLI1 and EWS-ERG gene fusions are associated with similar clinical phenotypes in Ewing's sarcoma. J Clin Oncol. 1999;17:1809–14.
144.
Git A, Allison R, Perdiguero E, Nebreda AR, Houliston E, Standart N. Vg1RBP phosphorylation by Erk2 MAP kinase correlates with the cortical release of Vg1 mRNA during meiotic maturation of Xenopus oocytes. RNA. 2009;15:1121–33.
145.
Gong L, Bao Q, Hu C, Wang J, Zhou Q, Wei L, et al. Exosomal miR-675 from metastatic osteosarcoma promotes cell migration and invasion by targeting CALN1. Biochem Biophys Res Commun. 2018;500:170–6.
146.
Gonzalez H, Hagerling C, Werb Z. Roles of the immune system in cancer: from tumor initiation to metastatic progression. Genes Dev. 2018;32:1267–84.
147.
Gorthi A, Romero JC, Loranc E, Cao L, Lawrence LA, Goodale E, et al. EWS-FLI1 increases transcription to cause R-loops and block BRCA1 repair in Ewing sarcoma. Nature. 2018;555:387–91.
148.
Grange C, Brossa A, Bussolati B. Extracellular Vesicles and Carried miRNAs in the Progression of Renal Cell Carcinoma. Int J Mol Sci. 2019;20:E1832.
149.
Grünewald TGP, Cidre-Aranaz F, Surdez D, Tomazou EM, de Álava E, Kovar H, et al. Ewing sarcoma. Nat Rev Dis Primers. 2018;4:5.
150.
Grunewald TGP, Willier S, Janik D, Unland R, Reiss C, Prazeres da Costa O, et al. The Zyxin-related protein thyroid receptor interacting protein 6 (TRIP6) is overexpressed in Ewing's sarcoma and promotes migration, invasion and cell growth. Biol Cell. 2013;105:535–47.
151.
Gu W, Wells AL, Pan F, Singer RH. Feedback regulation between zipcode binding protein 1 and beta-catenin mRNAs in breast cancer cells. Mol Cell Biol. 2008;28:4963–74.
152.
Guerzoni C, Fiori V, Terracciano M, Manara MC, Moricoli D, Pasello M, et al. CD99 triggering in Ewing sarcoma delivers a lethal signal through p53 pathway reactivation and cooperates with doxorubicin. Clin Cancer Res. 2015;21:146–56.
153.
Guillon N, Tirode F, Boeva V, Zynovyev A, Barillot E, Delattre O. The oncogenic EWS-FLI1 protein binds in vivo GGAA microsatellite sequences with potential transcriptional activation function. PLoS One. 2009;4:e4932.
154.
Hafner M, Landthaler M, Burger L, Khorshid M, Hausser J, Berninger P, et al. Transcriptome-wide identification of RNA-binding protein and microRNA target sites by PAR-CLIP. Cell. 2010;141:129–41.

155.
Hammer NA, Hansen T v O, Byskov AG, Rajpert-De Meyts E, Grøndahl ML, Bredkjaer HE, et al. Expression of IGF-II mRNA-binding proteins (IMPs) in gonads and testicular cancer. Reproduction. 2005;130:203–12.
156.
Han F, Pu P, Wang C, Ding X, Zhu Z, Xiang W, et al. Osteosarcoma Cell-Derived Exosomal miR-1307 Promotes Tumorigenesis via Targeting AGAP1. Biomed Res Int. 2021;2021:7358153.
157.
Hanada K, Hino F, Amano H, Fukuda T, Kuroda Y. Current treatment strategies for pancreatic cancer in the elderly. Drugs Aging. 2006;23:403–10.
158.
Hanahan D, Weinberg RA. Hallmarks of cancer: the next generation. Cell. 2011;144:646–74.
159.
Hansen TVO, Hammer NA, Nielsen J, Madsen M, Dalbaeck C, Wewer UM, et al. Dwarfism and impaired gut development in insulin-like growth factor II mRNA-binding protein 1-deficient mice. Mol Cell Biol. 2004;24:4448–64.
160.
Hanson PI, Cashikar A. Multivesicular body morphogenesis. Annu Rev Cell Dev Biol. 2012;28:337–62.
161.
Harding C, Heuser J, Stahl P. Receptor-mediated endocytosis of transferrin and recycling of the transferrin receptor in rat reticulocytes. J Cell Biol. 1983;97:329–39.
162.
Havens AM, Jung Y, Sun YX, Wang J, Shah RB, Bühring HJ, et al. The role of sialomucin CD164 (MGC-24v or endolyn) in prostate cancer metastasis. BMC Cancer. 2006;6:195.
163.
He H, Ni J, Huang J. Molecular mechanisms of chemoresistance in osteosarcoma (Review). Oncol Lett. 2014;7:1352–62.
164.
Heijnen HF, Schiel AE, Fijnheer R, Geuze HJ, Sixma JJ. Activated platelets release two types of membrane vesicles: microvesicles by surface shedding and exosomes derived from exocytosis of multivesicular bodies and alpha-granules. Blood. 1999;94:3791–9.
165.
Henke E, Nandigama R, Ergün S. Extracellular Matrix in the Tumor Microenvironment and Its Impact on Cancer Therapy. Front Mol Biosci. 2019;6:160.
166.
Herrero-Martín D, Osuna D, Ordóñez JL, Sevillano V, Martins AS, Mackintosh C, et al. Stable interference of EWS-FLI1 in an Ewing sarcoma cell line impairs IGF-1/IGF-1R signalling and reveals TOPK as a new target. Br J Cancer. 2009;101:80–90.
167.
Herrero-Martin D, Fourtouna A, Niedan S, Riedmann LT, Schwentner R, Aryee DNT. Factors Affecting EWS-FLI1 Activity in Ewing's Sarcoma. Sarcoma. 2011;2011:352580.
168.
Hessvik NP, Llorente A. Current knowledge on exosome biogenesis and release. Cell Mol Life Sci. 2018;75:193–208.
169.
Hinshaw DC, Shevde LA. The Tumor Microenvironment Innately Modulates Cancer Progression. Cancer Res. 2019;79:4557–66.

170.
Hood JL, San RS, Wickline SA. Exosomes released by melanoma cells prepare sentinel lymph nodes for tumor metastasis. Cancer Res. 2011;71:3792–801.
171.
Hoxhaj G, Manning BD. The PI3K-AKT network at the interface of oncogenic signalling and cancer metabolism. Nat Rev Cancer. 2020;20:74–88.
172.
Hsu K-F, Shen M-R, Huang Y-F, Cheng Y-M, Lin S-H, Chow N-H, et al. Overexpression of the RNA-binding proteins Lin28B and IGF2BP3 (IMP3) is associated with chemoresistance and poor disease outcome in ovarian cancer. Br J Cancer. 2015;113:414–24.
173.
Hsu Y-L, Hung J-Y, Chang W-A, Lin Y-S, Pan Y-C, Tsai P-H, et al. Hypoxic lung cancer-secreted exosomal miR-23a increased angiogenesis and vascular permeability by targeting prolyl hydroxylase and tight junction protein ZO-1. Oncogene. 2017;36:4929–42.
174.
Hu JL, Wang W, Lan XL, Zeng ZC, Liang YS, Yan YR, et al. CAFs secreted exosomes promote metastasis and chemotherapy resistance by enhancing cell stemness and epithelial-mesenchymal transition in colorectal cancer. Mol Cancer. 2019;18:91.
175.
Hu Y, Yan C, Mu L, Huang K, Li X, Tao D, et al. Fibroblast-Derived Exosomes Contribute to Chemoresistance through Priming Cancer Stem Cells in Colorectal Cancer. PLoS One. 2015;10:e0125625.
176.
Huang A-F, Chen M-W, Huang S-M, Kao C-L, Lai H-C, Chan JY-H. CD164 regulates the tumorigenesis of ovarian surface epithelial cells through the SDF-1α/CXCR4 axis. Mol Cancer. 2013;12:115.
177.
Huang H-Y, Lin Y-C-D, Li J, Huang K-Y, Shrestha S, Hong H-C, et al. miRTarBase 2020: updates to the experimentally validated microRNA-target interaction database. Nucleic Acids Res. 2020;48:D148–54.
178.
Huang H-Y, Lin Y-C-D, Li J, Huang K-Y, Shrestha S, Hong H-C, et al. miRTarBase 2020: updates to the experimentally validated microRNA-target interaction database. Nucleic Acids Res. 2020;48:D148–54.
179.
Huang J, Li Y, Tang Y, Tang G, Yang G-Y, Wang Y. CXCR4 antagonist AMD3100 protects blood-brain barrier integrity and reduces inflammatory response after focal ischemia in mice. Stroke. 2013;44:190–7.
180.
Huang S, Apasov S, Koshiba M, Sitkovsky M. Role of A2a extracellular adenosine receptor-mediated signaling in adenosine-mediated inhibition of T-cell activation and expansion. Blood. 1997;90:1600–10.
181.
Huang X, Wu W, Yang W, Qing X, Shao Z. Surface engineering of nanoparticles with ligands for targeted delivery to osteosarcoma. Colloids Surf B Biointerfaces. 2020;190:110891.
182.
Huang X, Zhang H, Guo X, Zhu Z, Cai H, Kong X. Insulin-like growth factor 2 mRNA-binding protein 1 (IGF2BP1) in cancer. J Hematol Oncol. 2018;11:88.
183.
Huang X, Zhang H, Guo X, Zhu Z, Cai H, Kong X. Insulin-like growth factor 2 mRNA-binding protein 1 (IGF2BP1) in cancer. J Hematol Oncol. 2018;11:88.
184.
Hume S, Dianov GL, Ramadan K. A unified model for the G1/S cell cycle transition. Nucleic Acids Res. 2020;48:12483–501.

185.
Hurwitz SN, Conlon MM, Rider MA, Brownstein NC, Meckes DG. Nanoparticle analysis sheds budding insights into genetic drivers of extracellular vesicle biogenesis. J Extracell Vesicles. 2016;5:31295.
186.
Hurwitz SN, Nkosi D, Conlon MM, York SB, Liu X, Tremblay DC, et al. CD63 Regulates Epstein-Barr Virus LMP1 Exosomal Packaging, Enhancement of Vesicle Production, and Noncanonical NF-κB Signaling. J Virol. 2017;91:e02251-16.
187.
Hüttelmaier S, Zenklusen D, Lederer M, Dictenberg J, Lorenz M, Meng X, et al. Spatial regulation of beta-actin translation by Src-dependent phosphorylation of ZBP1. Nature. 2005;438:512–5.
188.
Inagaki Y, Hookway E, Williams KA, Hassan AB, Oppermann U, Tanaka Y, et al. Dendritic and mast cell involvement in the inflammatory response to primary malignant bone tumors. Clin Sarcoma Res. 2016;6:13.
189.
Ioannidis P, Mahaira LG, Perez SA, Gritzapis AD, Sotiropoulou PA, Kavalakis GJ, et al. CRD-BP/IMP1 expression characterizes cord blood CD34+ stem cells and affects c-myc and IGF-II expression in MCF-7 cancer cells. J Biol Chem. 2005;280:20086–93.
190.
Jacques C, Lamoureux F, Baud'huin M, Rodriguez Calleja L, Quillard T, Amiaud J, et al. Targeting the epigenetic readers in Ewing sarcoma inhibits the oncogenic transcription factor EWS/Fli1. Oncotarget. 2016;7:24125–40.
191.
Janeczek Portalska K, Leferink A, Groen N, Fernandes H, Moroni L, van Blitterswijk C, et al. Endothelial differentiation of mesenchymal stromal cells. PLoS One. 2012;7:e46842.
192.
Janiszewska M, Suvà ML, Riggi N, Houtkooper RH, Auwerx J, Clément-Schatlo V, et al. Imp2 controls oxidative phosphorylation and is crucial for preserving glioblastoma cancer stem cells. Genes Dev. 2012;26:1926–44.
193.
Jawad MU, Cheung MC, Min ES, Schneiderbauer MM, Koniaris LG, Scully SP. Ewing sarcoma demonstrates racial disparities in incidence-related and sex-related differences in outcome: an analysis of 1631 cases from the SEER database, 1973-2005. Cancer. 2009;115:3526–36.
194.
Jeon IS, Davis JN, Braun BS, Sublett JE, Roussel MF, Denny CT, et al. A variant Ewing's sarcoma translocation (7;22) fuses the EWS gene to the ETS gene ETV1. Oncogene. 1995;10:1229–34.
195.
Jeppesen DK, Fenix AM, Franklin JL, Higginbotham JN, Zhang Q, Zimmerman LJ, et al. Reassessment of Exosome Composition. Cell. 2019;177:428-445.e18.
196.
Jeppesen DK, Nawrocki A, Jensen SG, Thorsen K, Whitehead B, Howard KA, et al. Quantitative proteomics of fractionated membrane and lumen exosome proteins from isogenic metastatic and nonmetastatic bladder cancer cells reveal differential expression of EMT factors. Proteomics. 2014;14:699–712.
197.
Jerez S, Araya H, Hevia D, Irarrázaval CE, Thaler R, van Wijnen AJ, et al. Extracellular vesicles from osteosarcoma cell lines contain miRNAs associated with cell adhesion and apoptosis. Gene. 2019;710:246–57.

198.
Jetten N, Verbruggen S, Gijbels MJ, Post MJ, De Winther MPJ, Donners MMPC. Anti-inflammatory M2, but not pro-inflammatory M1 macrophages promote angiogenesis in vivo. Angiogenesis. 2014;17:109–18.
199.
Jia M, Gut H, Chao JA. Structural basis of IMP3 RRM12 recognition of RNA. RNA. 2018;24:1659–66.
200.
Jin P, Huang Y, Zhu P, Zou Y, Shao T, Wang O. CircRNA circHIPK3 serves as a prognostic marker to promote glioma progression by regulating miR-654/IGF2BP3 signaling. Biochem Biophys Res Commun. 2018;503:1570–4.
201.
Jing X, Yang F, Shao C, Wei K, Xie M, Shen H, et al. Role of hypoxia in cancer therapy by regulating the tumor microenvironment. Mol Cancer. 2019;18:157.
202.
Johnstone RM, Mathew A, Mason AB, Teng K. Exosome formation during maturation of mammalian and avian reticulocytes: evidence that exosome release is a major route for externalization of obsolete membrane proteins. J Cell Physiol. 1991;147:27–36.
203.
Jønson L, Christiansen J, Hansen TVO, Vikeså J, Yamamoto Y, Nielsen FC. IMP3 RNP safe houses prevent miRNA-directed HMGA2 mRNA decay in cancer and development. Cell Rep. 2014;7:539–51.
204.
Jønson L, Vikesaa J, Krogh A, Nielsen LK, Hansen T vO, Borup R, et al. Molecular composition of IMP1 ribonucleoprotein granules. Mol Cell Proteomics. 2007;6:798–811.
205.
Joo J, Christensen L, Warner K, States L, Kang H-G, Vo K, et al. GLI1 is a central mediator of EWS/FLI1 signaling in Ewing tumors. PLoS One. 2009;4:e7608.
206.
Juergens C, Weston C, Lewis I, Whelan J, Paulussen M, Oberlin O, et al. Safety assessment of intensive induction with vincristine, ifosfamide, doxorubicin, and etoposide (VIDE) in the treatment of Ewing tumors in the EURO-E.W.I.N.G. 99 clinical trial. Pediatr Blood Cancer. 2006;47:22–9.
207.
Juergens H, Daw NC, Geoerger B, Ferrari S, Villarroel M, Aerts I, et al. Preliminary efficacy of the anti-insulin-like growth factor type 1 receptor antibody figitumumab in patients with refractory Ewing sarcoma. J Clin Oncol. 2011;29:4534–40.
208.
Jun JC, Rathore A, Younas H, Gilkes D, Polotsky VY. Hypoxia-Inducible Factors and Cancer. Curr Sleep Med Rep. 2017;3:1–10.
209.
Jung T, Castellana D, Klingbeil P, Cuesta Hernández I, Vitacolonna M, Orlicky DJ, et al. CD44v6 dependence of premetastatic niche preparation by exosomes. Neoplasia. 2009;11:1093–105.
210.
Kailayangiri S, Altvater B, Meltzer J, Pscherer S, Luecke A, Dierkes C, et al. The ganglioside antigen G(D2) is surface-expressed in Ewing sarcoma and allows for MHC-independent immune targeting. Br J Cancer. 2012;106:1123–33.
211.
Kailayangiri S, Altvater B, Lesch S, Balbach S, Göttlich C, Kühnemundt J, et al. EZH2 Inhibition in Ewing Sarcoma Upregulates GD2 Expression for Targeting with Gene-Modified T Cells. Mol Ther. 2019;27:933–46.

212.
Kalluri R, LeBleu VS. The biology, function, and biomedical applications of exosomes. Science. 2020;367:eaau6977.
213.
Karagiannis GS, Poutahidis T, Erdman SE, Kirsch R, Riddell RH, Diamandis EP. Cancer-associated fibroblasts drive the progression of metastasis through both paracrine and mechanical pressure on cancer tissue. Mol Cancer Res. 2012;10:1403–18.
214.
Karamanos NK, Theocharis AD, Piperigkou Z, Manou D, Passi A, Skandalis SS, et al. A guide to the composition and functions of the extracellular matrix. FEBS J. 2021;288:6850–912.
215.
Kato T, Hayama S, Yamabuki T, Ishikawa N, Miyamoto M, Ito T, et al. Increased expression of insulin-like growth factor-II messenger RNA-binding protein 1 is associated with tumor progression in patients with lung cancer. Clin Cancer Res. 2007;13:434–42.
216.
Kendall RT, Feghali-Bostwick CA. Fibroblasts in fibrosis: novel roles and mediators. Front Pharmacol. 2014;5:123.
217.
Kennedy AL, Vallurupalli M, Chen L, Crompton B, Cowley G, Vazquez F, et al. Functional, chemical genomic, and super-enhancer screening identify sensitivity to cyclin D1/CDK4 pathway inhibition in Ewing sarcoma. Oncotarget. 2015;6:30178–93.
218.
Kessler SM, Laggai S, Barghash A, Schultheiss CS, Lederer E, Artl M, et al. IMP2/p62 induces genomic instability and an aggressive hepatocellular carcinoma phenotype. Cell Death Dis. 2015;6:e1894.
219.
Kim D-H, Provenzano PP, Smith CL, Levchenko A. Matrix nanotopography as a regulator of cell function. J Cell Biol. 2012;197:351–60.
220.
Kim H-Y, Ha Thi HT, Hong S. IMP2 and IMP3 cooperate to promote the metastasis of triple-negative breast cancer through destabilization of progesterone receptor. Cancer Lett. 2018;415:30–9.
221.
Kim JR, Moon YJ, Kwon KS, Bae JS, Wagle S, Kim KM, et al. Tumor infiltrating PD1-positive lymphocytes and the expression of PD-L1 predict poor prognosis of soft tissue sarcomas. PLoS One. 2013;8:e82870.
222.
Kim SK, Park Y-K. Ewing sarcoma: a chronicle of molecular pathogenesis. Hum Pathol. 2016;55:91–100.
223.
Kim SY, Toretsky JA, Scher D, Helman LJ. The role of IGF-1R in pediatric malignancies. Oncologist. 2009;14:83–91.
224.
Kleffel S, Posch C, Barthel SR, Mueller H, Schlapbach C, Guenova E, et al. Melanoma Cell-Intrinsic PD-1 Receptor Functions Promote Tumor Growth. Cell. 2015;162:1242–56.
225.
Kling MJ, Chaturvedi NK, Kesherwani V, Coulter DW, McGuire TR, Sharp JG, et al. Exosomes secreted under hypoxia enhance stemness in Ewing's sarcoma through miR-210 delivery. Oncotarget. 2020;11:3633–45.
226.
Knowles HJ, Schaefer K-L, Dirksen U, Athanasou NA. Hypoxia and hypoglycaemia in Ewing's sarcoma and osteosarcoma: regulation and phenotypic effects of Hypoxia-Inducible Factor. BMC Cancer. 2010;10:372.

227.
Kobayashi T, Winslow S, Sunesson L, Hellman U, Larsson C. PKCα binds G3BP2 and regulates stress granule formation following cellular stress. PLoS One. 2012;7:e35820.
228.
Köbel M, Weidensdorfer D, Reinke C, Lederer M, Schmitt WD, Zeng K, et al. Expression of the RNA-binding protein IMP1 correlates with poor prognosis in ovarian carcinoma. Oncogene. 2007;26:7584–9.
229.
Kohrt HE, Nouri N, Nowels K, Johnson D, Holmes S, Lee PP. Profile of immune cells in axillary lymph nodes predicts disease-free survival in breast cancer. PLoS Med. 2005;2:e284.
230.
Koster H, Weintrob M. Diffuse Endothelioma of Bone: Ewing's Sarcoma. Ann Surg. 1931;94:111–6.
231.
Kouhkan F, Mobarra N, Soufi-Zomorrod M, Keramati F, Hosseini Rad SMA, Fathi-Roudsari M, et al. MicroRNA-129-1 acts as tumor suppressor and induces cell cycle arrest of GBM cancer cells through targeting IGF2BP3 and MAPK1. J Med Genet. 2016;53:24–33.
232.
Kovar H. Ewing's sarcoma and peripheral primitive neuroectodermal tumors after their genetic union. Curr Opin Oncol. 1998;10:334–42.
233.
Kowal J, Arras G, Colombo M, Jouve M, Morath JP, Primdal-Bengtson B, et al. Proteomic comparison defines novel markers to characterize heterogeneous populations of extracellular vesicle subtypes. Proc Natl Acad Sci U S A. 2016;113:E968-977.
234.
Kozomara A, Birgaoanu M, Griffiths-Jones S. miRBase: from microRNA sequences to function. Nucleic Acids Res. 2019;47:D155–62.
235.
Krook MA, Nicholls LA, Scannell CA, Chugh R, Thomas DG, Lawlor ER. Stress-induced CXCR4 promotes migration and invasion of ewing sarcoma. Mol Cancer Res. 2014;12:953–64.
236.
Kugeratski FG, Kalluri R. Exosomes as mediators of immune regulation and immunotherapy in cancer. FEBS J. 2021;288:10–35.
237.
Kurzrock R, Patnaik A, Aisner J, Warren T, Leong S, Benjamin R, et al. A phase I study of weekly R1507, a human monoclonal antibody insulin-like growth factor-I receptor antagonist, in patients with advanced solid tumors. Clin Cancer Res. 2010;16:2458–65.
238.
Lagerweij T, Pérez-Lanzón M, Baglio SR. A Preclinical Mouse Model of Osteosarcoma to Define the Extracellular Vesicle-mediated Communication Between Tumor and Mesenchymal Stem Cells. J Vis Exp. 2018;
239.
LaGory EL, Giaccia AJ. The Ever Expanding Role of HIF in Tumor and Stromal Biology. Nat Cell Biol. 2016;18:356–65.
240.
Langemeyer L, Fröhlich F, Ungermann C. Rab GTPase Function in Endosome and Lysosome Biogenesis. Trends Cell Biol. 2018;28:957–70.
241.
Langowski JL, Kastelein RA, Oft M. Swords into plowshares: IL-23 repurposes tumor immune surveillance. Trends Immunol. 2007;28:207–12.

242.
Latifkar A, Hur YH, Sanchez JC, Cerione RA, Antonyak MA. New insights into extracellular vesicle biogenesis and function. J Cell Sci. 2019;132:jcs222406.
243.
Lau YS, Adamopoulos IE, Sabokbar A, Giele H, Gibbons CLMH, Athanasou NA. Cellular and humoral mechanisms of osteoclast formation in Ewing's sarcoma. Br J Cancer. 2007;96:1716–22.
244.
Le Deley M-C, Delattre O, Schaefer K-L, Burchill SA, Koehler G, Hogendoorn PCW, et al. Impact of EWS-ETS fusion type on disease progression in Ewing's sarcoma/peripheral primitive neuroectodermal tumor: prospective results from the cooperative Euro-E.W.I.N.G. 99 trial. J Clin Oncol. 2010;28:1982–8.
245.
Lederer M, Bley N, Schleifer C, Hüttelmaier S. The role of the oncofetal IGF2 mRNA-binding protein 3 (IGF2BP3) in cancer. Semin Cancer Biol. 2014;29:3–12.
246.
Levchenko A, Mehta BM, Niu X, Kang G, Villafania L, Way D, et al. Intercellular transfer of P-glycoprotein mediates acquired multidrug resistance in tumor cells. Proc Natl Acad Sci U S A. 2005;102:1933–8.
247.
Li C, Liu D-R, Li G-G, Wang H-H, Li X-W, Zhang W, et al. CD97 promotes gastric cancer cell proliferation and invasion through exosome-mediated MAPK signaling pathway. World J Gastroenterol. 2015;21:6215–28.
248.
Li H, Durbin R. Fast and accurate short read alignment with Burrows-Wheeler transform. Bioinformatics. 2009;25:1754–60.
249.
Li H, Li F. Exosomes from BM-MSCs increase the population of CSCs via transfer of miR-142-3p. Br J Cancer. 2018;119:744–55.
250.
Li H, Li X, Liu S, Guo L, Zhang B, Zhang J, et al. Programmed cell death-1 (PD-1) checkpoint blockade in combination with a mammalian target of rapamycin inhibitor restrains hepatocellular carcinoma growth induced by hepatoma cell-intrinsic PD-1. Hepatology. 2017;66:1920–33.
251.
Li M, Zhang L, Ge C, Chen L, Fang T, Li H, et al. An isocorydine derivative (d-ICD) inhibits drug resistance by downregulating IGF2BP3 expression in hepatocellular carcinoma. Oncotarget. 2015;6:25149–60.
252.
Li M, Lu Y, Xu Y, Wang J, Zhang C, Du Y, et al. Horizontal transfer of exosomal CXCR4 promotes murine hepatocarcinoma cell migration, invasion and lymphangiogenesis. Gene. 2018;676:101–9.
253.
Li W, Liu D, Chang W, Lu X, Wang Y-L, Wang H, et al. Role of IGF2BP3 in trophoblast cell invasion and migration. Cell Death Dis. 2014;5:e1025.
254.
Li Y, Zhao L, Li X-F. Hypoxia and the Tumor Microenvironment. Technol Cancer Res Treat. 2021;20:15330338211036304.
255.
Liao B, Hu Y, Herrick DJ, Brewer G. The RNA-binding protein IMP-3 is a translational activator of insulin-like growth factor II leader-3 mRNA during proliferation of human K562 leukemia cells. J Biol Chem. 2005;280:18517–24.
256.
Liao Y, Smyth GK, Shi W. featureCounts: an efficient general purpose program for assigning sequence reads to genomic features. Bioinformatics. 2014;30:923–30.

257.
Lin H, Zheng X, Lu T, Gu Y, Zheng C, Yan H. The proliferation and invasion of osteosarcoma are inhibited by miR-101 via targetting ZEB2. Biosci Rep. 2019;39:BSR20181283.
258.
Lin L, Liu D, Liang H, Xue L, Su C, Liu M. MiR-1228 promotes breast cancer cell growth and metastasis through targeting SCAI protein. Int J Clin Exp Pathol. 2015;8:6646–55.
259.
Lin W-W, Karin M. A cytokine-mediated link between innate immunity, inflammation, and cancer. J Clin Invest. 2007;117:1175–83.
260.
Lipinski M, Braham K, Philip I, Wiels J, Philip T, Goridis C, et al. Neuroectoderm-associated antigens on Ewing's sarcoma cell lines. Cancer Res. 1987;47:183–7.
261.
Liu Y, Gu Y, Han Y, Zhang Q, Jiang Z, Zhang X, et al. Tumor Exosomal RNAs Promote Lung Pre-metastatic Niche Formation by Activating Alveolar Epithelial TLR3 to Recruit Neutrophils. Cancer Cell. 2016;30:243–56.
262.
Livak KJ, Schmittgen TD. Analysis of relative gene expression data using real-time quantitative PCR and the 2(-Delta Delta C(T)) Method. Methods. 2001;25:402–8.
263.
Llombart-Bosch A, Machado I, Navarro S, Bertoni F, Bacchini P, Alberghini M, et al. Histological heterogeneity of Ewing's sarcoma/PNET: an immunohistochemical analysis of 415 genetically confirmed cases with clinical support. Virchows Arch. 2009;455:397–411.
264.
Maas SLN, Breakefield XO, Weaver AM. Extracellular Vesicles: Unique Intercellular Delivery Vehicles. Trends Cell Biol. 2017;27:172–88.
265.
Machado I, López-Guerrero JA, Scotlandi K, Picci P, Llombart-Bosch A. Immunohistochemical analysis and prognostic significance of PD-L1, PD-1, and CD8+ tumor-infiltrating lymphocytes in Ewing's sarcoma family of tumors (ESFT). Virchows Arch. 2018;472:815–24.
266.
Machado I, Noguera R, Pellin A, Lopez-Guerrero JA, Piqueras M, Navarro S, et al. Molecular diagnosis of Ewing sarcoma family of tumors: a comparative analysis of 560 cases with FISH and RT-PCR. Diagn Mol Pathol. 2009;18:189–99.
267.
Madison MN, Jones PH, Okeoma CM. Exosomes in human semen restrict HIV-1 transmission by vaginal cells and block intravaginal replication of LP-BM5 murine AIDS virus complex. Virology. 2015;482:189–201.
268.
Maishi N, Hida K. Tumor endothelial cells accelerate tumor metastasis. Cancer Sci. 2017;108:1921–6.
269.
Malla RR, Shailender G, Kamal MA. Exosomes: Critical Mediators of Tumor Microenvironment Reprogramming. Curr Med Chem. 2021;28:8182–202.
270.
Manara MC, Landuzzi L, Nanni P, Nicoletti G, Zambelli D, Lollini PL, et al. Preclinical in vivo study of new insulin-like growth factor-I receptor--specific inhibitor in Ewing's sarcoma. Clin Cancer Res. 2007;13:1322–30.

271.
Mancarella C, Caldoni G, Ribolsi I, Parra A, Manara MC, Mercurio AM, et al. Insulin-Like Growth Factor 2 mRNA-Binding Protein 3 Modulates Aggressiveness of Ewing Sarcoma by Regulating the CD164-CXCR4 Axis. Front Oncol. 2020;10:994.
272.
Mancarella C, Pasello M, Manara MC, Toracchio L, Sciandra EF, Picci P, et al. Insulin-Like Growth Factor 2 mRNA-Binding Protein 3 Influences Sensitivity to Anti-IGF System Agents Through the Translational Regulation of IGF1R. Front Endocrinol (Lausanne). 2018;9:178.
273.
Mancarella C, Pasello M, Ventura S, Grilli A, Calzolari L, Toracchio L, et al. Insulin-Like Growth Factor 2 mRNA-Binding Protein 3 is a Novel Post-Transcriptional Regulator of Ewing Sarcoma Malignancy. Clin Cancer Res. 2018;24:3704–16.
274.
Mancarella C, Scotlandi K. IGF2BP3 From Physiology to Cancer: Novel Discoveries, Unsolved Issues, and Future Perspectives. Front Cell Dev Biol. 2019;7:363.
275.
Manoukian P, Bijlsma M, van Laarhoven H. The Cellular Origins of Cancer-Associated Fibroblasts and Their Opposing Contributions to Pancreatic Cancer Growth. Front Cell Dev Biol. 2021;9:743907.
276.
Mantovani A, Allavena P, Sica A, Balkwill F. Cancer-related inflammation. Nature. 2008;454:436–44.
277.
Mao J, Liang Z, Zhang B, Yang H, Li X, Fu H, et al. UBR2 Enriched in p53 Deficient Mouse Bone Marrow Mesenchymal Stem Cell-Exosome Promoted Gastric Cancer Progression via Wnt/β-Catenin Pathway. Stem Cells. 2017;35:2267–79.
278.
Mashouri L, Yousefi H, Aref AR, Ahadi A mohammad, Molaei F, Alahari SK. Exosomes: composition, biogenesis, and mechanisms in cancer metastasis and drug resistance. Mol Cancer. 2019;18:75.
279.
Maus RLG, Jakub JW, Nevala WK, Christensen TA, Noble-Orcutt K, Sachs Z, et al. Human Melanoma-Derived Extracellular Vesicles Regulate Dendritic Cell Maturation. Front Immunol. 2017;8:358.
280.
May WA, Gishizky ML, Lessnick SL, Lunsford LB, Lewis BC, Delattre O, et al. Ewing sarcoma 11;22 translocation produces a chimeric transcription factor that requires the DNA-binding domain encoded by FLI1 for transformation. Proc Natl Acad Sci U S A. 1993;90:5752–6.
281.
Mazumdar A, Urdinez J, Boro A, Migliavacca J, Arlt MJE, Muff R, et al. Osteosarcoma-Derived Extracellular Vesicles Induce Lung Fibroblast Reprogramming. Int J Mol Sci. 2020;21:E5451.
282.
McGeary SE, Lin KS, Shi CY, Pham TM, Bisaria N, Kelley GM, et al. The biochemical basis of microRNA targeting efficacy. Science. 2019;366:eaav1741.
283.
McKinsey EL, Parrish JK, Irwin AE, Niemeyer BF, Kern HB, Birks DK, et al. A novel oncogenic mechanism in Ewing sarcoma involving IGF pathway targeting by EWS/Fli1-regulated microRNAs. Oncogene. 2011;30:4910–20.
284.
Meehan K, Vella LJ. The contribution of tumor-derived exosomes to the hallmarks of cancer. Crit Rev Clin Lab Sci. 2016;53:121–31.

285.
Melo SA, Luecke LB, Kahlert C, Fernandez AF, Gammon ST, Kaye J, et al. Glypican-1 identifies cancer exosomes and detects early pancreatic cancer. Nature. 2015;523:177–82.
286.
Menck K, Sivaloganathan S, Bleckmann A, Binder C. Microvesicles in Cancer: Small Size, Large Potential. Int J Mol Sci. 2020;21:E5373.
287.
Menon R, Debnath C, Lai A, Guanzon D, Bhatnagar S, Kshetrapal PK, et al. Circulating Exosomal miRNA Profile During Term and Preterm Birth Pregnancies: A Longitudinal Study. Endocrinology. 2019;160:249–75.
288.
Miller IV, Raposo G, Welsch U, Prazeres da Costa O, Thiel U, Lebar M, et al. First identification of Ewing's sarcoma-derived extracellular vesicles and exploration of their biological and potential diagnostic implications. Biol Cell. 2013;105:289–303.
289.
Mitelman F, Johansson B, Mertens F. The impact of translocations and gene fusions on cancer causation. Nat Rev Cancer. 2007;7:233–45.
290.
Miyagawa Y, Okita H, Nakaijima H, Horiuchi Y, Sato B, Taguchi T, et al. Inducible expression of chimeric EWS/ETS proteins confers Ewing's family tumor-like phenotypes to human mesenchymal progenitor cells. Mol Cell Biol. 2008;28:2125–37.
291.
Miyoshi K, Kohashi K, Fushimi F, Yamamoto H, Kishimoto J, Taguchi T, et al. Close correlation between CXCR4 and VEGF expression and frequent CXCR7 expression in rhabdomyosarcoma. Hum Pathol. 2014;45:1900–9.
292.
Mizutani R, Imamachi N, Suzuki Y, Yoshida H, Tochigi N, Oonishi T, et al. Oncofetal protein IGF2BP3 facilitates the activity of proto-oncogene protein eIF4E through the destabilization of EIF4E-BP2 mRNA. Oncogene. 2016;35:3495–502.
293.
Mongroo PS, Noubissi FK, Cuatrecasas M, Kalabis J, King CE, Johnstone CN, et al. IMP-1 displays cross-talk with K-Ras and modulates colon cancer cell survival through the novel proapoptotic protein CYFIP2. Cancer Res. 2011;71:2172–82.
294.
Muralidharan-Chari V, Clancy J, Plou C, Romao M, Chavrier P, Raposo G, et al. ARF6-regulated shedding of tumor cell-derived plasma membrane microvesicles. Curr Biol. 2009;19:1875–85.
295.
Najafi M, Farhood B, Mortezaee K. Extracellular matrix (ECM) stiffness and degradation as cancer drivers. J Cell Biochem. 2019;120:2782–90.
296.
Nakamura K, Sawada K, Kinose Y, Yoshimura A, Toda A, Nakatsuka E, et al. Exosomes Promote Ovarian Cancer Cell Invasion through Transfer of CD44 to Peritoneal Mesothelial Cells. Mol Cancer Res. 2017;15:78–92.
297.
Nakasone ES, Askautrud HA, Kees T, Park J-H, Plaks V, Ewald AJ, et al. Imaging tumor-stroma interactions during chemotherapy reveals contributions of the microenvironment to resistance. Cancer Cell. 2012;21:488–503.

298.
Nazarenko I, Rana S, Baumann A, McAlear J, Hellwig A, Trendelenburg M, et al. Cell surface tetraspanin Tspan8 contributes to molecular pathways of exosome-induced endothelial cell activation. Cancer Res. 2010;70:1668–78.
299.
Nielsen J, Christiansen J, Lykke-Andersen J, Johnsen AH, Wewer UM, Nielsen FC. A family of insulin-like growth factor II mRNA-binding proteins represses translation in late development. Mol Cell Biol. 1999;19:1262–70.
300.
Nielsen J, Adolph SK, Rajpert-De Meyts E, Lykke-Andersen J, Koch G, Christiansen J, et al. Nuclear transit of human zipcode-binding protein IMP1. Biochem J. 2003;376:383–91.
301.
Nielsen J, Kristensen MA, Willemoës M, Nielsen FC, Christiansen J. Sequential dimerization of human zipcode-binding protein IMP1 on RNA: a cooperative mechanism providing RNP stability. Nucleic Acids Res. 2004;32:4368–76.
302.
Nieman KM, Kenny HA, Penicka CV, Ladanyi A, Buell-Gutbrod R, Zillhardt MR, et al. Adipocytes promote ovarian cancer metastasis and provide energy for rapid tumor growth. Nat Med. 2011;17:1498–503.
303.
Ning Y, Shen K, Wu Q, Sun X, Bai Y, Xie Y, et al. Tumor exosomes block dendritic cells maturation to decrease the T cell immune response. Immunol Lett. 2018;199:36–43.
304.
Noubissi FK, Elcheva I, Bhatia N, Shakoori A, Ougolkov A, Liu J, et al. CRD-BP mediates stabilization of betaTrCP1 and c-myc mRNA in response to beta-catenin signalling. Nature. 2006;441:898–901.
305.
Noubissi FK, Nikiforov MA, Colburn N, Spiegelman VS. Transcriptional Regulation of CRD-BP by c-myc: Implications for c-myc Functions. Genes Cancer. 2010;1:1074–82.
306.
O'Connell JT, Sugimoto H, Cooke VG, MacDonald BA, Mehta AI, LeBleu VS, et al. VEGF-A and Tenascin-C produced by S100A4+ stromal cells are important for metastatic colonization. Proc Natl Acad Sci U S A. 2011;108:16002–7.
307.
Odri GA, Dumoucel S, Picarda G, Battaglia S, Lamoureux F, Corradini N, et al. Zoledronic acid as a new adjuvant therapeutic strategy for Ewing's sarcoma patients. Cancer Res. 2010;70:7610–9.
308.
Olmos D, Postel-Vinay S, Molife LR, Okuno SH, Schuetze SM, Paccagnella ML, et al. Safety, pharmacokinetics, and preliminary activity of the anti-IGF-1R antibody figitumumab (CP-751,871) in patients with sarcoma and Ewing's sarcoma: a phase 1 expansion cohort study. Lancet Oncol. 2010;11:129–35.
309.
Ou JY, Spraker-Perlman H, Dietz AC, Smits-Seemann RR, Kaul S, Kirchhoff AC. Conditional survival of pediatric, adolescent, and young adult soft tissue sarcoma and bone tumor patients. Cancer Epidemiol. 2017;50:150–7.
310.
Owen LA, Kowalewski AA, Lessnick SL. EWS/FLI mediates transcriptional repression via NKX2.2 during oncogenic transformation in Ewing's sarcoma. PLoS One. 2008;3:e1965.

311.
Palanichamy JK, Tran TM, Howard JM, Contreras JR, Fernando TR, Sterne-Weiler T, et al. RNA-binding protein IGF2BP3 targeting of oncogenic transcripts promotes hematopoietic progenitor proliferation. J Clin Invest. 2016;126:1495–511.
312.
Palmisano G, Jensen SS, Le Bihan M-C, Lainé J, McGuire JN, Pociot F, et al. Characterization of membrane-shed microvesicles from cytokine-stimulated β-cells using proteomics strategies. Mol Cell Proteomics. 2012;11:230–43.
313.
Pan BT, Johnstone RM. Fate of the transferrin receptor during maturation of sheep reticulocytes in vitro: selective externalization of the receptor. Cell. 1983;33:967–78.
314.
Panebianco F, Kelly LM, Liu P, Zhong S, Dacic S, Wang X, et al. THADA fusion is a mechanism of IGF2BP3 activation and IGF1R signaling in thyroid cancer. Proc Natl Acad Sci U S A. 2017;114:2307–12.
315.
Pappo AS, Patel SR, Crowley J, Reinke DK, Kuenkele K-P, Chawla SP, et al. R1507, a monoclonal antibody to the insulin-like growth factor 1 receptor, in patients with recurrent or refractory Ewing sarcoma family of tumors: results of a phase II Sarcoma Alliance for Research through Collaboration study. J Clin Oncol. 2011;29:4541–7.
316.
Pappo AS, Vassal G, Crowley JJ, Bolejack V, Hogendoorn PCW, Chugh R, et al. A phase 2 trial of R1507, a monoclonal antibody to the insulin-like growth factor-1 receptor (IGF-1R), in patients with recurrent or refractory rhabdomyosarcoma, osteosarcoma, synovial sarcoma, and other soft tissue sarcomas: results of a Sarcoma Alliance for Research Through Collaboration study. Cancer. 2014;120:2448–56.
317.
Parmo-Cabañas M, Molina-Ortiz I, Matías-Román S, García-Bernal D, Carvajal-Vergara X, Valle I, et al. Role of metalloproteinases MMP-9 and MT1-MMP in CXCL12-promoted myeloma cell invasion across basement membranes. J Pathol. 2006;208:108–18.
318.
Paulussen M, Ahrens S, Craft AW, Dunst J, Fröhlich B, Jabar S, et al. Ewing's tumors with primary lung metastases: survival analysis of 114 (European Intergroup) Cooperative Ewing's Sarcoma Studies patients. J Clin Oncol. 1998;16:3044–52.
319.
Peinado H, Alečković M, Lavotshkin S, Matei I, Costa-Silva B, Moreno-Bueno G, et al. Melanoma exosomes educate bone marrow progenitor cells toward a pro-metastatic phenotype through MET. Nat Med. 2012;18:883–91.
320.
Pelon F, Bourachot B, Kieffer Y, Magagna I, Mermet-Meillon F, Bonnet I, et al. Cancer-associated fibroblast heterogeneity in axillary lymph nodes drives metastases in breast cancer through complementary mechanisms. Nat Commun. 2020;11:404.
321.
Peña C, Céspedes MV, Lindh MB, Kiflemariam S, Mezheyeuski A, Edqvist P-H, et al. STC1 expression by cancer-associated fibroblasts drives metastasis of colorectal cancer. Cancer Res. 2013;73:1287–97.
322.
Pereira B, Billaud M, Almeida R. RNA-Binding Proteins in Cancer: Old Players and New Actors. Trends Cancer. 2017;3:506–28.

323.
Perlman EJ, Dickman PS, Askin FB, Grier HE, Miser JS, Link MP. Ewing's sarcoma--routine diagnostic utilization of MIC2 analysis: a Pediatric Oncology Group/Children's Cancer Group Intergroup Study. Hum Pathol. 1994;25:304–7.
324.
Petermann R, Mossier BM, Aryee DN, Khazak V, Golemis EA, Kovar H. Oncogenic EWS-Fli1 interacts with hsRPB7, a subunit of human RNA polymerase II. Oncogene. 1998;17:603–10.
325.
Pickup MW, Mouw JK, Weaver VM. The extracellular matrix modulates the hallmarks of cancer. EMBO Rep. 2014;15:1243–53.
326.
Pinto N, Park JR, Murphy E, Yearley J, McClanahan T, Annamalai L, et al. Patterns of PD-1, PD-L1, and PD-L2 expression in pediatric solid tumors. Pediatr Blood Cancer. 2017;64.
327.
Poggio M, Hu T, Pai C-C, Chu B, Belair CD, Chang A, et al. Suppression of Exosomal PD-L1 Induces Systemic Anti-tumor Immunity and Memory. Cell. 2019;177:414-427.e13.
328.
Polesskaya A, Cuvellier S, Naguibneva I, Duquet A, Moss EG, Harel-Bellan A. Lin-28 binds IGF-2 mRNA and participates in skeletal myogenesis by increasing translation efficiency. Genes Dev. 2007;21:1125–38.
329.
Portela A, Esteller M. Epigenetic modifications and human disease. Nat Biotechnol. 2010;28:1057–68.
330.
Prieur A, Tirode F, Cohen P, Delattre O. EWS/FLI-1 silencing and gene profiling of Ewing cells reveal downstream oncogenic pathways and a crucial role for repression of insulin-like growth factor binding protein 3. Mol Cell Biol. 2004;24:7275–83.
331.
Qi J, Yang Y, Hao P, Xu J. Retraction: Transcription Factor SOX9 Promotes Osteosarcoma Cell Growth by Repressing Claudin-8 Expression. Tohoku J Exp Med. 2017;242:335.
332.
Qiu Y, Pu C, Li Y, Qi B. Construction of a circRNA-miRNA-mRNA network based on competitive endogenous RNA reveals the function of circRNAs in osteosarcoma. Cancer Cell Int. 2020;20:48.
333.
Quail DF, Joyce JA. Microenvironmental regulation of tumor progression and metastasis. Nat Med. 2013;19:1423–37.
334.
Quillet A, Saad C, Ferry G, Anouar Y, Vergne N, Lecroq T, et al. Improving Bioinformatics Prediction of microRNA Targets by Ranks Aggregation. Front Genet. 2019;10:1330.
335.
Rajagopal C, Harikumar KB. The Origin and Functions of Exosomes in Cancer. Front Oncol. 2018;8:66.
336.
Raposo G, Nijman HW, Stoorvogel W, Liejendekker R, Harding CV, Melief CJ, et al. B lymphocytes secrete antigen-presenting vesicles. J Exp Med. 1996;183:1161–72.
337.
Ratajczak J, Miekus K, Kucia M, Zhang J, Reca R, Dvorak P, et al. Embryonic stem cell-derived microvesicles reprogram hematopoietic progenitors: evidence for horizontal transfer of mRNA and protein delivery. Leukemia. 2006;20:847–56.

338.
Read J, Ingram A, Al Saleh HA, Platko K, Gabriel K, Kapoor A, et al. Nuclear transportation of exogenous epidermal growth factor receptor and androgen receptor via extracellular vesicles. Eur J Cancer. 2017;70:62–74.
339.
Ribatti D, Tamma R, Annese T. Epithelial-Mesenchymal Transition in Cancer: A Historical Overview. Transl Oncol. 2020;13:100773.
340.
Ricklefs FL, Alayo Q, Krenzlin H, Mahmoud AB, Speranza MC, Nakashima H, et al. Immune evasion mediated by PD-L1 on glioblastoma-derived extracellular vesicles. Sci Adv. 2018;4:eaar2766.
341.
Riggi N, Suvà ML, Stamenkovic I. Ewing's Sarcoma. N Engl J Med. 2021;384:154–64.
342.
Riggi N, Suva M-L, Stamenkovic I. Ewing's sarcoma origin: from duel to duality. Expert Rev Anticancer Ther. 2009;9:1025–30.
343.
Riggi N, Suvà M-L, Suvà D, Cironi L, Provero P, Tercier S, et al. EWS-FLI-1 expression triggers a Ewing's sarcoma initiation program in primary human mesenchymal stem cells. Cancer Res. 2008;68:2176–85.
344.
Rivera Vargas T, Boudoukha S, Simon A, Souidi M, Cuvellier S, Pinna G, et al. Post-transcriptional regulation of cyclins D1, D3 and G1 and proliferation of human cancer cells depend on IMP-3 nuclear localization. Oncogene. 2014;33:2866–75.
345.
Robainas M, Otano R, Bueno S, Ait-Oudhia S. Understanding the role of PD-L1/PD1 pathway blockade and autophagy in cancer therapy. Onco Targets Ther. 2017;10:1803–7.
346.
Rochefort P, Italiano A, Laurence V, Penel N, Lardy-Cleaud A, Mir O, et al. A Retrospective Multicentric Study of Ewing Sarcoma Family of Tumors in Patients Older Than 50: Management and Outcome. Sci Rep. 2017;7:17917.
347.
Rodrigues CFD, Serrano E, Patrício MI, Val MM, Albuquerque P, Fonseca J, et al. Stroma-derived IL-6, G-CSF and Activin-A mediated dedifferentiation of lung carcinoma cells into cancer stem cells. Sci Rep. 2018;8:11573.
348.
Rowley JD. Letter: A new consistent chromosomal abnormality in chronic myelogenous leukaemia identified by quinacrine fluorescence and Giemsa staining. Nature. 1973;243:290–3.
349.
Ruffell B, Affara NI, Coussens LM. Differential macrophage programming in the tumor microenvironment. Trends Immunol. 2012;33:119–26.
350.
Samanta S, Sharma VM, Khan A, Mercurio AM. Regulation of IMP3 by EGFR signaling and repression by ERβ: implications for triple-negative breast cancer. Oncogene. 2012;31:4689–97.
351.
Samanta S, Sun H, Goel HL, Pursell B, Chang C, Khan A, et al. IMP3 promotes stem-like properties in triple-negative breast cancer by regulating SLUG. Oncogene. 2016;35:1111–21.
352.
Samanta S, Guru S, Elaimy AL, Amante JJ, Ou J, Yu J, et al. IMP3 Stabilization of WNT5B mRNA Facilitates TAZ Activation in Breast Cancer. Cell Rep. 2018;23:2559–67.

353.
Samanta S, Pursell B, Mercurio AM. IMP3 protein promotes chemoresistance in breast cancer cells by regulating breast cancer resistance protein (ABCG2) expression. J Biol Chem. 2013;288:12569–73.
354.
Sankar S, Lessnick SL. Promiscuous partnerships in Ewing's sarcoma. Cancer Genet. 2011;204:351–65.
355.
Sarvaria A, Madrigal JA, Saudemont A. B cell regulation in cancer and anti-tumor immunity. Cell Mol Immunol. 2017;14:662–74.
356.
Savina A, Fader CM, Damiani MT, Colombo MI. Rab11 promotes docking and fusion of multivesicular bodies in a calcium-dependent manner. Traffic. 2005;6:131–43.
357.
Sbaraglia M, Righi A, Gambarotti M, Dei Tos AP. Ewing sarcoma and Ewing-like tumors. Virchows Arch. 2020;476:109–19.
358.
Schmittgen TD, Livak KJ. Analyzing real-time PCR data by the comparative C(T) method. Nat Protoc. 2008;3:1101–8.
359.
Schneider T, Hung L-H, Aziz M, Wilmen A, Thaum S, Wagner J, et al. Combinatorial recognition of clustered RNA elements by the multidomain RNA-binding protein IMP3. Nat Commun. 2019;10:2266.
360.
Schuck A, Ahrens S, Paulussen M, Kuhlen M, Könemann S, Rübe C, et al. Local therapy in localized Ewing tumors: results of 1058 patients treated in the CESS 81, CESS 86, and EICESS 92 trials. Int J Radiat Oncol Biol Phys. 2003;55:168–77.
361.
Scotlandi K, Baldini N, Cerisano V, Manara MC, Benini S, Serra M, et al. CD99 engagement: an effective therapeutic strategy for Ewing tumors. Cancer Res. 2000;60:5134–42.
362.
Scotlandi K, Benini S, Nanni P, Lollini PL, Nicoletti G, Landuzzi L, et al. Blockage of insulin-like growth factor-I receptor inhibits the growth of Ewing's sarcoma in athymic mice. Cancer Res. 1998;58:4127–31.
363.
Scotlandi K, Benini S, Sarti M, Serra M, Lollini PL, Maurici D, et al. Insulin-like growth factor I receptor-mediated circuit in Ewing's sarcoma/peripheral neuroectodermal tumor: a possible therapeutic target. Cancer Res. 1996;56:4570–4.
364.
Scotlandi K, Avnet S, Benini S, Manara MC, Serra M, Cerisano V, et al. Expression of an IGF-I receptor dominant negative mutant induces apoptosis, inhibits tumorigenesis and enhances chemosensitivity in Ewing's sarcoma cells. Int J Cancer. 2002;101:11–6.
365.
Scotlandi K, Remondini D, Castellani G, Manara MC, Nardi F, Cantiani L, et al. Overcoming resistance to conventional drugs in Ewing sarcoma and identification of molecular predictors of outcome. J Clin Oncol. 2009;27:2209–16.
366.
Scott LJ, Mohlke KL, Bonnycastle LL, Willer CJ, Li Y, Duren WL, et al. A genome-wide association study of type 2 diabetes in Finns detects multiple susceptibility variants. Science. 2007;316:1341–5.
367.
Shalem O, Sanjana NE, Hartenian E, Shi X, Scott DA, Mikkelson T, et al. Genome-scale CRISPR-Cas9 knockout screening in human cells. Science. 2014;343:84–7.

368.
Shapouri-Moghaddam A, Mohammadian S, Vazini H, Taghadosi M, Esmaeili S-A, Mardani F, et al. Macrophage plasticity, polarization, and function in health and disease. J Cell Physiol. 2018;233:6425–40.
369.
Sharma A, Boise LH, Shanmugam M. Cancer Metabolism and the Evasion of Apoptotic Cell Death. Cancers (Basel). 2019;11:1144.
370.
Sharpe AH, Pauken KE. The diverse functions of the PD1 inhibitory pathway. Nat Rev Immunol. 2018;18:153–67.
371.
Sheen Y-S, Liao Y-H, Lin M-H, Chu C-Y, Ho B-Y, Hsieh M-C, et al. IMP-3 promotes migration and invasion of melanoma cells by modulating the expression of HMGA2 and predicts poor prognosis in melanoma. J Invest Dermatol. 2015;135:1065–73.
372.
Sheffield NC, Pierron G, Klughammer J, Datlinger P, Schönegger A, Schuster M, et al. DNA methylation heterogeneity defines a disease spectrum in Ewing sarcoma. Nat Med. 2017;23:386–95.
373.
Shi J, Li Y, Jia R, Fan X. The fidelity of cancer cells in PDX models: Characteristics, mechanism and clinical significance. Int J Cancer. 2020;146:2078–88.
374.
Shiga K, Hara M, Nagasaki T, Sato T, Takahashi H, Takeyama H. Cancer-Associated Fibroblasts: Their Characteristics and Their Roles in Tumor Growth. Cancers (Basel). 2015;7:2443–58.
375.
Shimbo K, Miyaki S, Ishitobi H, Kato Y, Kubo T, Shimose S, et al. Exosome-formed synthetic microRNA-143 is transferred to osteosarcoma cells and inhibits their migration. Biochem Biophys Res Commun. 2014;445:381–7.
376.
Shimoda M, Principe S, Jackson HW, Luga V, Fang H, Molyneux SD, et al. Loss of the Timp gene family is sufficient for the acquisition of the CAF-like cell state. Nat Cell Biol. 2014;16:889–901.
377.
Shing DC, McMullan DJ, Roberts P, Smith K, Chin S-F, Nicholson J, et al. FUS/ERG gene fusions in Ewing's tumors. Cancer Res. 2003;63:4568–76.
378.
Sica A, Larghi P, Mancino A, Rubino L, Porta C, Totaro MG, et al. Macrophage polarization in tumor progression. Semin Cancer Biol. 2008;18:349–55.
379.
Skog J, Würdinger T, van Rijn S, Meijer DH, Gainche L, Sena-Esteves M, et al. Glioblastoma microvesicles transport RNA and proteins that promote tumor growth and provide diagnostic biomarkers. Nat Cell Biol. 2008;10:1470–6.
380.
Sobierajska K, Ciszewski WM, Sacewicz-Hofman I, Niewiarowska J. Endothelial Cells in the Tumor Microenvironment. Adv Exp Med Biol. 2020;1234:71–86.
381.
Sonnemann J, Dreyer L, Hartwig M, Palani CD, Hong LTT, Klier U, et al. Histone deacetylase inhibitors induce cell death and enhance the apoptosis-inducing activity of TRAIL in Ewing's sarcoma cells. J Cancer Res Clin Oncol. 2007;133:847–58.

382.
Sorensen PH, Lessnick SL, Lopez-Terrada D, Liu XF, Triche TJ, Denny CT. A second Ewing's sarcoma translocation, t(21;22), fuses the EWS gene to another ETS-family transcription factor, ERG. Nat Genet. 1994;6:146–51.
383.
Sorensen PH, Liu XF, Delattre O, Rowland JM, Biggs CA, Thomas G, et al. Reverse transcriptase PCR amplification of EWS/FLI-1 fusion transcripts as a diagnostic test for peripheral primitive neuroectodermal tumors of childhood. Diagn Mol Pathol. 1993;2:147–57.
384.
Spagnoli FM, Brivanlou AH. The RNA-binding protein, Vg1RBP, is required for pancreatic fate specification. Dev Biol. 2006;292:442–56.
385.
Spurny C, Kailayangiri S, Jamitzky S, Altvater B, Wardelmann E, Dirksen U, et al. Programmed cell death ligand 1 (PD-L1) expression is not a predominant feature in Ewing sarcomas. Pediatr Blood Cancer. 2018;65.
386.
Squadrito ML, De Palma M. Macrophage regulation of tumor angiogenesis: implications for cancer therapy. Mol Aspects Med. 2011;32:123–45.
387.
Staege MS, Hutter C, Neumann I, Foja S, Hattenhorst UE, Hansen G, et al. DNA microarrays reveal relationship of Ewing family tumors to both endothelial and fetal neural crest-derived cells and define novel targets. Cancer Res. 2004;64:8213–21.
388.
Stahl M, Ranft A, Paulussen M, Bölling T, Vieth V, Bielack S, et al. Risk of recurrence and survival after relapse in patients with Ewing sarcoma. Pediatr Blood Cancer. 2011;57:549–53.
389.
Stefanius K, Servage K, de Souza Santos M, Gray HF, Toombs JE, Chimalapati S, et al. Human pancreatic cancer cell exosomes, but not human normal cell exosomes, act as an initiator in cell transformation. Elife. 2019;8:e40226.
390.
Steinbichler TB, Dudás J, Riechelmann H, Skvortsova I-I. The role of exosomes in cancer metastasis. Semin Cancer Biol. 2017;44:170–81.
391.
Stiller CA, Craft AW, Corazziari I, EUROCARE Working Group. Survival of children with bone sarcoma in Europe since 1978: results from the EUROCARE study. Eur J Cancer. 2001;37:760–6.
392.
Strauss SJ, Whelan JS. Current questions in bone sarcomas. Curr Opin Oncol. 2018;30:252–9.
393.
Stuffers S, Sem Wegner C, Stenmark H, Brech A. Multivesicular endosome biogenesis in the absence of ESCRTs. Traffic. 2009;10:925–37.
394.
Su E, Han X, Jiang G. The transforming growth factor beta 1/SMAD signaling pathway involved in human chronic myeloid leukemia. Tumori. 2010;96:659–66.
395.
Su Y, Xiong J, Hu J, Wei X, Zhang X, Rao L. MicroRNA-140-5p targets insulin like growth factor 2 mRNA binding protein 1 (IGF2BP1) to suppress cervical cancer growth and metastasis. Oncotarget. 2016;7:68397–411.

396.
Sullivan R, Saez F, Girouard J, Frenette G. Role of exosomes in sperm maturation during the transit along the male reproductive tract. Blood Cells Mol Dis. 2005;35:1–10.
397.
Sun W, Ren Y, Lu Z, Zhao X. The potential roles of exosomes in pancreatic cancer initiation and metastasis. Mol Cancer. 2020;19:135.
398.
Sutton A, Friand V, Brulé-Donneger S, Chaigneau T, Ziol M, Sainte-Catherine O, et al. Stromal cell-derived factor-1/chemokine (C-X-C motif) ligand 12 stimulates human hepatoma cell growth, migration, and invasion. Mol Cancer Res. 2007;5:21–33.
399.
Suvasini R, Shruti B, Thota B, Shinde SV, Friedmann-Morvinski D, Nawaz Z, et al. Insulin growth factor-2 binding protein 3 (IGF2BP3) is a glioblastoma-specific marker that activates phosphatidylinositol 3-kinase/mitogen-activated protein kinase (PI3K/MAPK) pathways by modulating IGF-2. J Biol Chem. 2011;286:25882–90.
400.
Swann JB, Smyth MJ. Immune surveillance of tumors. J Clin Invest. 2007;117:1137–46.
401.
Szarvas T, Tschirdewahn S, Niedworok C, Kramer G, Sevcenco S, Reis H, et al. Prognostic value of tissue and circulating levels of IMP3 in prostate cancer. Int J Cancer. 2014;135:1596–604.
402.
Tang J, Luo Z, Zhou G, Song C, Yu F, Xiang J, et al. Cis-regulatory functions of overlapping HIF-1alpha/E-box/AP-1-like sequences of CD164. BMC Mol Biol. 2011;12:44.
403.
Tang J, Zhang L, She X, Zhou G, Yu F, Xiang J, et al. Inhibiting CD164 expression in colon cancer cell line HCT116 leads to reduced cancer cell proliferation, mobility, and metastasis in vitro and in vivo. Cancer Invest. 2012;30:380–9.
404.
Tang J, Zhang L, She X, Zhou G, Yu F, Xiang J, et al. Inhibiting CD164 expression in colon cancer cell line HCT116 leads to reduced cancer cell proliferation, mobility, and metastasis in vitro and in vivo. Cancer Invest. 2012;30:380–9.
405.
Taniuchi K, Furihata M, Hanazaki K, Saito M, Saibara T. IGF2BP3-mediated translation in cell protrusions promotes cell invasiveness and metastasis of pancreatic cancer. Oncotarget. 2014;5:6832–45.
406.
Taniuchi K, Furihata M, Saibara T. KIF20A-mediated RNA granule transport system promotes the invasiveness of pancreatic cancer cells. Neoplasia. 2014;16:1082–93.
407.
Tauro BJ, Mathias RA, Greening DW, Gopal SK, Ji H, Kapp EA, et al. Oncogenic H-ras reprograms Madin-Darby canine kidney (MDCK) cell-derived exosomal proteins following epithelial-mesenchymal transition. Mol Cell Proteomics. 2013;12:2148–59.
408.
Theisen ER, Pishas KI, Saund RS, Lessnick SL. Therapeutic opportunities in Ewing sarcoma: EWS-FLI inhibition via LSD1 targeting. Oncotarget. 2016;7:17616–30.
409.
Theocharis AD, Skandalis SS, Gialeli C, Karamanos NK. Extracellular matrix structure. Adv Drug Deliv Rev. 2016;97:4–27.

410.
Theodoraki M-N, Yerneni SS, Hoffmann TK, Gooding WE, Whiteside TL. Clinical Significance of PD-L1+ Exosomes in Plasma of Head and Neck Cancer Patients. Clin Cancer Res. 2018;24:896–905.
411.
Théry C, Witwer KW, Aikawa E, Alcaraz MJ, Anderson JD, Andriantsitohaina R, et al. Minimal information for studies of extracellular vesicles 2018 (MISEV2018): a position statement of the International Society for Extracellular Vesicles and update of the MISEV2014 guidelines. J Extracell Vesicles. 2018;7:1535750.
412.
Théry C, Zitvogel L, Amigorena S. Exosomes: composition, biogenesis and function. Nat Rev Immunol. 2002;2:569–79.
413.
Thiel U, Schober SJ, Einspieler I, Kirschner A, Thiede M, Schirmer D, et al. Ewing sarcoma partial regression without GvHD by chondromodulin-I/HLA-A*02:01-specific allorestricted T cell receptor transgenic T cells. Oncoimmunology. 2017;6:e1312239.
414.
Thorsson V, Gibbs DL, Brown SD, Wolf D, Bortone DS, Ou Yang T-H, et al. The Immune Landscape of Cancer. Immunity. 2018;48:812-830.e14.
415.
Tirode F, Laud-Duval K, Prieur A, Delorme B, Charbord P, Delattre O. Mesenchymal stem cell features of Ewing tumors. Cancer Cell. 2007;11:421–9.
416.
Tirode F, Surdez D, Ma X, Parker M, Le Deley MC, Bahrami A, et al. Genomic landscape of Ewing sarcoma defines an aggressive subtype with co-association of STAG2 and TP53 mutations. Cancer Discov. 2014;4:1342–53.
417.
Todorova R. In vitro interaction between the N-terminus of the Ewing's sarcoma protein and the subunit of RNA polymerase II hsRPB7. Mol Biol Rep. 2009;36:1269–74.
418.
Torreggiani E, Roncuzzi L, Perut F, Zini N, Baldini N. Multimodal transfer of MDR by exosomes in human osteosarcoma. Int J Oncol. 2016;49:189–96.
419.
Trajkovic K, Hsu C, Chiantia S, Rajendran L, Wenzel D, Wieland F, et al. Ceramide triggers budding of exosome vesicles into multivesicular endosomes. Science. 2008;319:1244–7.
420.
Treps L, Perret R, Edmond S, Ricard D, Gavard J. Glioblastoma stem-like cells secrete the pro-angiogenic VEGF-A factor in extracellular vesicles. J Extracell Vesicles. 2017;6:1359479.
421.
Tschirdewahn S, Panic A, Püllen L, Harke NN, Hadaschik B, Riesz P, et al. Circulating and tissue IMP3 levels are correlated with poor survival in renal cell carcinoma. Int J Cancer. 2019;145:531–9.
422.
Tsugita M, Yamada N, Noguchi S, Yamada K, Moritake H, Shimizu K, et al. Ewing sarcoma cells secrete EWS/Fli-1 fusion mRNA via microvesicles. PLoS One. 2013;8:e77416.
423.
Tubbs A, Nussenzweig A. Endogenous DNA Damage as a Source of Genomic Instability in Cancer. Cell. 2017;168:644–56.
424.
Ueki A, Shimizu T, Masuda K, Yamaguchi SI, Ishikawa T, Sugihara E, et al. Up-regulation of Imp3 confers in vivo tumorigenicity on murine osteosarcoma cells. PLoS One. 2012;7:e50621.

425.
Umezu T, Tadokoro H, Azuma K, Yoshizawa S, Ohyashiki K, Ohyashiki JH. Exosomal miR-135b shed from hypoxic multiple myeloma cells enhances angiogenesis by targeting factor-inhibiting HIF-1. Blood. 2014;124:3748–57.
426.
Urano F, Umezawa A, Yabe H, Hong W, Yoshida K, Fujinaga K, et al. Molecular analysis of Ewing's sarcoma: another fusion gene, EWS-E1AF, available for diagnosis. Jpn J Cancer Res. 1998;89:703–11.
427.
Urciuoli E, Giorda E, Scarsella M, Petrini S, Peruzzi B. Osteosarcoma-derived extracellular vesicles induce a tumor-like phenotype in normal recipient cells. J Cell Physiol. 2018;233:6158–72.
428.
Valadi H, Ekström K, Bossios A, Sjöstrand M, Lee JJ, Lötvall JO. Exosome-mediated transfer of mRNAs and microRNAs is a novel mechanism of genetic exchange between cells. Nat Cell Biol. 2007;9:654–9.
429.
van Calker D, Müller M, Hamprecht B. Adenosine regulates via two different types of receptors, the accumulation of cyclic AMP in cultured brain cells. J Neurochem. 1979;33:999–1005.
430.
van der Lelij P, Lieb S, Jude J, Wutz G, Santos CP, Falkenberg K, et al. Synthetic lethality between the cohesin subunits STAG1 and STAG2 in diverse cancer contexts. Elife. 2017;6:e26980.
431.
van Erp AEM, Versleijen-Jonkers YMH, Hillebrandt-Roeffen MHS, van Houdt L, Gorris MAJ, van Dam LS, et al. Expression and clinical association of programmed cell death-1, programmed death-ligand-1 and CD8+ lymphocytes in primary sarcomas is subtype dependent. Oncotarget. 2017;8:71371–84.
432.
van Niel G, D'Angelo G, Raposo G. Shedding light on the cell biology of extracellular vesicles. Nat Rev Mol Cell Biol. 2018;19:213–28.
433.
Vedeld HM, Goel A, Lind GE. Epigenetic biomarkers in gastrointestinal cancers: The current state and clinical perspectives. Semin Cancer Biol. 2018;51:36–49.
434.
Ventura S, Aryee DNT, Felicetti F, De Feo A, Mancarella C, Manara MC, et al. CD99 regulates neural differentiation of Ewing sarcoma cells through miR-34a-Notch-mediated control of NF-κB signaling. Oncogene. 2016;35:3944–54.
435.
Verweij FJ, van Eijndhoven MAJ, Hopmans ES, Vendrig T, Wurdinger T, Cahir-McFarland E, et al. LMP1 association with CD63 in endosomes and secretion via exosomes limits constitutive NF-κB activation. EMBO J. 2011;30:2115–29.
436.
Vietri M, Radulovic M, Stenmark H. The many functions of ESCRTs. Nat Rev Mol Cell Biol. 2020;21:25–42.
437.
Villasante A, Marturano-Kruik A, Ambati SR, Liu Z, Godier-Furnemont A, Parsa H, et al. Recapitulating the Size and Cargo of Tumor Exosomes in a Tissue-Engineered Model. Theranostics. 2016;6:1119–30.
438.
Vojtech L, Woo S, Hughes S, Levy C, Ballweber L, Sauteraud RP, et al. Exosomes in human semen carry a distinctive repertoire of small non-coding RNAs with potential regulatory functions. Nucleic Acids Res. 2014;42:7290–304.

439.
Wang B, Mao J-H, Wang B-Y, Wang L-X, Wen H-Y, Xu L-J, et al. Exosomal miR-1910-3p promotes proliferation, metastasis, and autophagy of breast cancer cells by targeting MTMR3 and activating the NF-κB signaling pathway. Cancer Lett. 2020;489:87–99.
440.
Wang C, Gao C, Meng K, Qiao H, Wang Y. Human adipocytes stimulate invasion of breast cancer MCF-7 cells by secreting IGFBP-2. PLoS One. 2015;10:e0119348.
441.
Wang C-C, Hueng D-Y, Huang A-F, Chen W-L, Huang S-M, Yi-Hsin Chan J. CD164 regulates proliferation, progression, and invasion of human glioblastoma cells. Oncotarget. 2019;10:2041–54.
442.
Wang D, Wang X, Si M, Yang J, Sun S, Wu H, et al. Exosome-encapsulated miRNAs contribute to CXCL12/CXCR4-induced liver metastasis of colorectal cancer by enhancing M2 polarization of macrophages. Cancer Lett. 2020;474:36–52.
443.
Wang J-W, Wu X-F, Gu X-J, Jiang X-H. Exosomal miR-1228 From Cancer-Associated Fibroblasts Promotes Cell Migration and Invasion of Osteosarcoma by Directly Targeting SCAI. Oncol Res. 2019;27:979–86.
444.
Wang L, Aireti A, Aihaiti A, Li K. Expression of microRNA-150 and its Target Gene IGF2BP1 in Human Osteosarcoma and their Clinical Implications. Pathol Oncol Res. 2019;25:527–33.
445.
Wang W, Li Q, Yamada T, Matsumoto K, Matsumoto I, Oda M, et al. Crosstalk to stromal fibroblasts induces resistance of lung cancer to epidermal growth factor receptor tyrosine kinase inhibitors. Clin Cancer Res. 2009;15:6630–8.
446.
Wang X, Luo G, Zhang K, Cao J, Huang C, Jiang T, et al. Hypoxic Tumor-Derived Exosomal miR-301a Mediates M2 Macrophage Polarization via PTEN/PI3Kγ to Promote Pancreatic Cancer Metastasis. Cancer Res. 2018;78:4586–98.
447.
Wang Y, Yi J, Chen X, Zhang Y, Xu M, Yang Z. The regulation of cancer cell migration by lung cancer cell-derived exosomes through TGF-β and IL-10. Oncol Lett. 2016;11:1527–30.
448.
Wang Z, Tong D, Han C, Zhao Z, Wang X, Jiang T, et al. Blockade of miR-3614 maturation by IGF2BP3 increases TRIM25 expression and promotes breast cancer cell proliferation. EBioMedicine. 2019;41:357–69.
449.
Watson S, Perrin V, Guillemot D, Reynaud S, Coindre J-M, Karanian M, et al. Transcriptomic definition of molecular subgroups of small round cell sarcomas. J Pathol. 2018;245:29–40.
450.
Webber JP, Spary LK, Sanders AJ, Chowdhury R, Jiang WG, Steadman R, et al. Differentiation of tumor-promoting stromal myofibroblasts by cancer exosomes. Oncogene. 2015;34:290–302.
451.
Webber J, Steadman R, Mason MD, Tabi Z, Clayton A. Cancer exosomes trigger fibroblast to myofibroblast differentiation. Cancer Res. 2010;70:9621–30.
452.
Wei F, Ma C, Zhou T, Dong X, Luo Q, Geng L, et al. Exosomes derived from gemcitabine-resistant cells transfer malignant phenotypic traits via delivery of miRNA-222-3p. Mol Cancer. 2017;16:132.

453.
Wei T, Cheng S, Fu XN, Feng LJ. miR-219a-5p enhances the radiosensitivity of non-small cell lung cancer cells through targeting CD164. Biosci Rep. 2020;40:BSR20192795.
454.
Weidensdorfer D, Stöhr N, Baude A, Lederer M, Köhn M, Schierhorn A, et al. Control of c-myc mRNA stability by IGF2BP1-associated cytoplasmic RNPs. RNA. 2009;15:104–15.
455.
Whelan J, McTiernan A, Cooper N, Wong YK, Francis M, Vernon S, et al. Incidence and survival of malignant bone sarcomas in England 1979-2007. Int J Cancer. 2012;131:E508-517.
456.
Whiteside TL. The role of tumor-derived exosomes in epithelial mesenchymal transition (EMT). Transl Cancer Res. 2017;6:S90–2.
457.
Wiles ET, Lui-Sargent B, Bell R, Lessnick SL. BCL11B is up-regulated by EWS/FLI and contributes to the transformed phenotype in Ewing sarcoma. PLoS One. 2013;8:e59369.
458.
Wittrant Y, Théoleyre S, Chipoy C, Padrines M, Blanchard F, Heymann D, et al. RANKL/RANK/OPG: new therapeutic targets in bone tumors and associated osteolysis. Biochim Biophys Acta. 2004;1704:49–57.
459.
Wolf P. The nature and significance of platelet products in human plasma. Br J Haematol. 1967;13:269–88.
460.
Wolf-Dennen K, Kleinerman ES. Exosomes: Dynamic Mediators of Extracellular Communication in the Tumor Microenvironment. Adv Exp Med Biol. 2020;1258:189–97.
461.
Worch J, Cyrus J, Goldsby R, Matthay KK, Neuhaus J, DuBois SG. Racial differences in the incidence of mesenchymal tumors associated with EWSR1 translocation. Cancer Epidemiol Biomarkers Prev. 2011;20:449–53.
462.
Wu L, Zhang X, Zhang B, Shi H, Yuan X, Sun Y, et al. Exosomes derived from gastric cancer cells activate NF-κB pathway in macrophages to promote cancer progression. Tumor Biol. 2016;37:12169–80.
463.
Wu L, Saxena S, Singh RK. Neutrophils in the Tumor Microenvironment. Adv Exp Med Biol. 2020;1224:1–20.
464.
Xiong Y, McDonald LT, Russell DL, Kelly RR, Wilson KR, Mehrotra M, et al. Hematopoietic stem cell-derived adipocytes and fibroblasts in the tumor microenvironment. World J Stem Cells. 2015;7:253–65.
465.
Xu B, Huang Y. Histone H2a mRNA interacts with Lin28 and contains a Lin28-dependent posttranscriptional regulatory element. Nucleic Acids Res. 2009;37:4256–63.
466.
Xu J-F, Wang Y-P, Zhang S-J, Chen Y, Gu H-F, Dou X-F, et al. Exosomes containing differential expression of microRNA and mRNA in osteosarcoma that can predict response to chemotherapy. Oncotarget. 2017;8:75968–78.
467.
Xue M, Chen W, Xiang A, Wang R, Chen H, Pan J, et al. Hypoxic exosomes facilitate bladder tumorgrowth and development through transferring long non-coding RNA-UCA1. Mol Cancer. 2017;16:143.

468.
Yáñez-Mó M, Siljander PR-M, Andreu Z, Zavec AB, Borràs FE, Buzas EI, et al. Biological properties of extracellular vesicles and their physiological functions. J Extracell Vesicles. 2015;4:27066.
469.
Yang H, Zhang H, Ge S, Ning T, Bai M, Li J, et al. Exosome-Derived miR-130a Activates Angiogenesis in Gastric Cancer by Targeting C-MYB in Vascular Endothelial Cells. Mol Ther. 2018;26:2466–75.
470.
Yang L, Wu X-H, Wang D, Luo C-L, Chen L-X. Bladder cancer cell-derived exosomes inhibit tumor cell apoptosis and induce cell proliferation in vitro. Mol Med Rep. 2013;8:1272–8.
471.
Yang M, McKay D, Pollard JW, Lewis CE. Diverse Functions of Macrophages in Different Tumor Microenvironments. Cancer Res. 2018;78:5492–503.
472.
Yaniv K, Fainsod A, Kalcheim C, Yisraeli JK. The RNA-binding protein Vg1 RBP is required for cell migration during early neural development. Development. 2003;130:5649–61.
473.
Yao H, Wang H, Li C, Fang J-Y, Xu J. Cancer Cell-Intrinsic PD-1 and Implications in Combinatorial Immunotherapy. Front Immunol. 2018;9:1774.
474.
Ye J, Coulouris G, Zaretskaya I, Cutcutache I, Rozen S, Madden TL. Primer-BLAST: a tool to design target-specific primers for polymerase chain reaction. BMC Bioinformatics. 2012;13:134.
475.
Ye Z, Zheng Z, Peng L. MicroRNA profiling of serum exosomes in patients with osteosarcoma by high-throughput sequencing. J Investig Med. 2020;68:893–901.
476.
Ying X, Wu Q, Wu X, Zhu Q, Wang X, Jiang L, et al. Epithelial ovarian cancer-secreted exosomal miR-222-3p induces polarization of tumor-associated macrophages. Oncotarget. 2016;7:43076–87.
477.
Yock TI, Krailo M, Fryer CJ, Donaldson SS, Miser JS, Chen Z, et al. Local control in pelvic Ewing sarcoma: analysis from INT-0091--a report from the Children's Oncology Group. J Clin Oncol. 2006;24:3838–43.
478.
Yoshizaki T, Kondo S, Wakisaka N, Murono S, Endo K, Sugimoto H, et al. Pathogenic role of Epstein-Barr virus latent membrane protein-1 in the development of nasopharyngeal carcinoma. Cancer Lett. 2013;337:1–7.
479.
You Y, Shan Y, Chen J, Yue H, You B, Shi S, et al. Matrix metalloproteinase 13-containing exosomes promote nasopharyngeal carcinoma metastasis. Cancer Sci. 2015;106:1669–77.
480.
Zhang HL, Eom T, Oleynikov Y, Shenoy SM, Liebelt DA, Dictenberg JB, et al. Neurotrophin-induced transport of a beta-actin mRNP complex increases beta-actin levels and stimulates growth cone motility. Neuron. 2001;31:261–75.
481.
Zhang H, Wang J, Ren T, Huang Y, Liang X, Yu Y, et al. Bone marrow mesenchymal stem cell-derived exosomal miR-206 inhibits osteosarcoma progression by targeting TRA2B. Cancer Lett. 2020;490:54–65.
482.
Zhang H, Yu Y, Wang J, Han Y, Ren T, Huang Y, et al. Macrophages-derived exosomal lncRNA LIFR-AS1 promotes osteosarcoma cell progression via miR-29a/NFIA axis. Cancer Cell Int. 2021;21:192.

483.
Zhang J, Wang T, Zhang Y, Wang H, Wu Y, Liu K, et al. Upregulation of serum miR-494 predicts poor prognosis in non-small cell lung cancer patients. Cancer Biomark. 2018;21:763–8.
484.
Zhang L, Liu Y, Hao S, Woda BA, Lu D. IMP2 expression distinguishes endometrioid from serous endometrial adenocarcinomas. Am J Surg Pathol. 2011;35:868–72.
485.
Zhang X-G, Zhang T, Li C-Y, Zhang M-H, Chen F-M. CD164 promotes tumor progression and predicts the poor prognosis of bladder cancer. Cancer Med. 2018;7:3763–72.
486.
Zhao W, Lu D, Liu L, Cai J, Zhou Y, Yang Y, et al. Insulin-like growth factor 2 mRNA binding protein 3 (IGF2BP3) promotes lung tumorigenesis via attenuating p53 stability. Oncotarget. 2017;8:93672–87.
487.
Zhou J, Tang Z, Gao S, Li C, Feng Y, Zhou X. Tumor-Associated Macrophages: Recent Insights and Therapies. Front Oncol. 2020;10:188.
488.
Zhou Y, Huang T, Siu HL, Wong CC, Dong Y, Wu F, et al. IGF2BP3 functions as a potential oncogene and is a crucial target of miR-34a in gastric carcinogenesis. Mol Cancer. 2017;16:77.